NUREG/CR-0362
CE 78-09

DYNAMIC EXCITATION OF A SINGLE-DEGREE-OF-FREEDOM HYSTERETIC SYSTEM

S.J. Stott and S.F. Masri

University of Southern California

Prepared for
U.S. Nuclear Regulatory Commission

Available from
National Technical Information Service
Springfield, Virginia 22161
Price: Printed Copy $6.50; Microfiche $3.00

The price of this document for requesters outside of the North American Continent can be obtained from the National Technical Information Service.

NUREG/CR-0362
CE 78-09
R5, RA

DYNAMIC EXCITATION OF A SINGLE-DEGREE-OF-FREEDOM HYSTERETIC SYSTEM

S.J. Stott and S.F. Masri

Manuscript Completed: May 1978
Date Published: September 1978

Department of Civil Engineering
University of Southern California
Los Angeles, CA 90007

Division of Reactor Safety Research
Office of Nuclear Regulatory Research
U.S. Nuclear Regulatory Commission
Under Contract No. NRC-04-76-262
FIN No. B-5976

ABSTRACT

An analytical investigation is made of the dynamic response of two special classes of nonlinear hysteretic oscillators that model some of the basic phenomena involved in the response of complex nuclear power plant systems which are subjected to dynamic environments.

Numerical studies as well as approximate analytical solutions for the response of the nonlinear oscillators under (a) harmonic and (b) random excitation are presented. The effects of various system parameters are evaluated and the range of validity of the approximate solutions is determined.

SUMMARY

One of the more serious design problems associated with the coolant loop of a nuclear power plant is the postulated rupture of the piping and the subsequent blowdown of the steam supply system. The occurrence of this type of accident has received increasing attention in the development of protective systems, such as those for emergency core cooling and redundant instrumentation, that effect a safe shutdown of the nuclear reactor. Concern for the functional integrity of these safety systems during the faulted condition has led to the installation of a variety of rupture supports that are intended to restrict gross movements of the piping system and to preclude a chain of failures. Since these restraints must not interfere with normal operation of the steam supply system, they are constructed with initial gaps that allow the piping to expand and contract in the operating condition. However, when a pipe breaks, it rapidly moves across the gap and is restrained by the support. Under the high blowdown loads that develop, inelastic behavior of the pipe material is also inevitable. Additionally, pumps and valves that are part of the primary coolant loop will experience nonlinearities because of gaps, friction, and nonproportional damping.

In order to analyze these complicated systems, it is necessary to use relatively simple models that are readily amenable to mathematical analysis or numerical solution techniques. A single-degree-of-freedom model that exhibits characteristics of hysteretic force vs. displacement would allow assessment of the displacement response of a nonlinear piping system. Such a model would be valuable in determining

(a) Whether rupture supports are required.

(b) System displacement response without rupture supports.

(c) Optimum gap distance for rupture support (i.e., yield value for a "hardening type" of hysteretic system).

In the first problem class studied, two solutions are presented. One uses iterative techniques, and the other an exact evaluation of the system equations of motion, to determine the displacement response of a harmonically excited single-degree-of-freedom (SDOF) hysteretic oscillator. Both of these solutions represent a system model that has a nonlinear hysteretic spring-restoring force with a "softening"-type skeleton curve that is described by arbitrary node points. The theoretical logic of both of these solutions is also incorporated in two computer methodologies. These methodologies idealize the system model as a piecewise linear SDOF oscillatory system whose parameters are a function of absolute displacement.

In the second problem class studied, two analytic solutions are presented for the determination of the displacement response of an SDOF-damped bilinear hysteretic oscillator when subjected to stationary random excitation. The first of these solutions generates experimental data by numerically integrating a piecewise linear system model, and the second solution is an hypothesized approximate analytical method. Data values numerically obtained for these two solutions are compared to demonstrate that, under certain conditions, the approximate method provides a satisfactory estimate for displacement response.

For both classes of problems, numerically generated data values are compared, whenever possible, with those existing in the literature in order to verify the analytic logic used for each selection method and to demonstrate accuracy. The effects of various system parameters are evaluated and the range of validity of the approximate solution is determined.

CONTENTS

CONTENTS (continued)

LIST OF FIGURES

LIST OF TABLES

ACKNOWLEDGEMENTS

This study was supported in part by a contract with the U.S. Nuclear Regulatory Commission.

LIST OF SYMBOLS

CHAPTER 1

C_{ci}	Critical damping i-th segment, $2\sqrt{K_i M}$
C_i	Viscous damping i-th segment
$F(T)$	Harmonic forcing function
F_o	Amplitude of harmonic forcing function $F(T)$
K_i	Spring stiffness i-th segment, $(P_{i+1}-P_i)/(y_{i+1}-y_i)$
M	Mass of SDOF system
P_M, y_M	Spring restoring force and deflection corresponding to the maximum values in a steady state hysteresis loop, respectively
P_i, y_i	Spring restoring force and deflection for the i-th node point, respectively
P_y, y_y	Spring restoring force and deflection for the yield point node (i.e., all successive motion will be in the plastic range), respectively
$P(y)$	Static spring restoring force versus deflection function, often referred to as the "skeleton curve"
Q_i	Generalized i-th node force, $\frac{1}{My_N}(-P_i + x_i K_i y_N)$
SDOF	Single degree of freedom
T	Total response time
t	Time within a given segment, set equal to zero at the start of motion in a new segment
x_M	Normalized maximum deflection, y_M/y_N
$x(T)$	Normalized displacement function, $y(T)/y_N$
$\dot{x}(T)$	Normalized velocity function, $\dot{y}(T)/y_N$

$\ddot{x}(T)$ Normalized acceleration function, $\ddot{y}(T)/y_N$

x_{io}, $\dot{x}_{io}$ Initial condition displacement and velocity, respectively, for the start of motion in the i-th segment

y_N Arbitrary normalization factor, often set equal to y_y

$y(T)$ Displacement function

$\dot{y}(T)$ Velocity function

$\ddot{y}(T)$ Acceleration function

Ψ_i i-th segment total phase angle, $\phi_o + \phi_i$

Ω Excitation frequency of harmonic forcing function $F(T)$

ζ_i Critical damping ratio i-th segment, C_i/C_{ci}

ϕ_i i-th segment phase angle for harmonic forcing function, equal to ΩT_i, where T_i is the time when motion in the i-th segment begins

ϕ_o Initial condition (T = 0) phase angle for harmonic forcing function $F(T)$

ω_{di} Damped natural frequency, $\sqrt{1 - \zeta_i^2}\ \omega_i$

ω_i Natural frequency i-th segment, $\sqrt{K_i/M}$

$|\ |$ Absolute value

CHAPTER 2

C_1	Viscous damping in linear elastic range
C_2	Viscous damping in plastic range
$E[\ ]$	Expectation operator
F_o	Amplitude of harmonic excitation force
$F(t)$	Random excitation forcing function
$\lvert H_d(\omega)\rvert$	Amplification factor ("transfer function") corresponging to a discrete harmonic frequency (ω), $x_{max}/(F_o/K_1)$
K_1	Spring constant elastic range
K_2	Spring constant plastic range
M	Mass of SDOF system
P_M, Y_M	Respective spring restoring force and deflection corresponding to the maximum value in a hysteresis loop
PSD	Power spectral density
P_Y, Y	Respective spring restoring force and deflection for the yield point (i.e., all successive motion will be in the plastic range)
$P(y)$	Static spring restoring force versus deflection function, often referred to as "skeleton curve"
RMS	Root mean squared
SDOF	Single degree of freedom
$S_f(\omega)$	Spectral density of excitation force
S_o	Uniform spectral density (one-sided function), $F(t)/(MY)$
$S_x(\omega)$	Displacement spectral density
$f(t)$	$F(t)/(MY)$

$\mathrm{sgn}(\dot{y})$	Sign (+ or -) of the velocity $\dot{y}$
x_M	Normalized maximum deflection, y_M/Y
$x(t)$	Normalized displacement function, $y(t)/Y$
$\dot{x}(t)$	Normalized velocity function, $\dot{y}(t)/Y$
$\ddot{x}(t)$	Normalized acceleration function, $\ddot{y}(t)/Y$
$y(t)$	Displacement function
$\dot{y}(t)$	Velocity function
$\ddot{y}(t)$	Acceleration function
α	K_2/K_1
ζ_1	Fraction of critical damping, $C_1/2\sqrt{K_1M}$
ζ_2	Fraction of critical damping, $C_2/2\sqrt{K_2M}$
σ_x	RMS displacement of M, σ_y/Y
ω	Excitation frequency (harmonic)
ω_1	Frequency, $\sqrt{K_1/M}$
ω_2	Frequency, $\sqrt{K_2/M}$
$\lvert\ \rvert$	Absolute value

DYNAMIC EXCITATION OF A SINGLE-DEGREE-OF-FREEDOM HYSTERETIC SYSTEM

CHAPTER I

HARMONIC EXCITATION OF A SINGLE-DEGREE-OF-FREEDOM HYSTERETIC OSCILLATOR

1.1 BACKGROUND INFORMATION

The damping properties of solid materials and their engineering significance has been studied for almost 200 years. In 1784, Coulomb in his Memoir on Torsion speculated on the microstructural mechanism of damping and described experiments proving that the damping observed under torsional oscillations was not caused by air friction but by internal losses in the material.(1)* Coulomb also observed that the damping mechanism operative at low stresses may be different from those at high stresses. Numerous physical systems, such as piping systems under sudden rupture forces, exhibit damping properties (i.e., energy absorption and dissipation) that are nonlinear.

All systems that dissipate internal energy when under cyclic load display one phenomenon in common: the cyclic load-deformation curve is not a single-valued function, but forms what is called a "hysteresis loop." Since energy is absorbed by the system under these cyclic loading conditions, the unloading branch of the loop must lie below the loading branch. The area between these two branches (i.e., the area enclosed by the hysteresis loop) is proportional to the energy absorbed.

---

*Numbers in parentheses designate references at the end of the chapter.

Figure 1.1* displays several examples of commonly observed hysteresis loops.

1.2 INTRODUCTION

The system model, which will be used to represent piping under sudden rupture forces, is an SDOF oscillator, such as that shown in Figure 1.2, with a "skeleton curve" of the softening type shown in Figure 1.3(B). A "skeleton curve" is defined as the relationship of the static spring-restoring force versus the deflection, and is assumed to be approximated by a piecewise linear nodal construction. Figure 1.4(A) shows this curve for a general hysteretic system and Figure 1.4(B) for a bilinear hysteretic system. The model has additional flexibility in that the critical damping ratio (ζ) can assume a different value for each i-th segment during the system displacement response.

An SDOF oscillator with a linear elastic "skeleton curve" (i.e., $\ddot{P}(y)$ = constant+) has a displacement response that has been discussed and analyzed in detail by numerous authors.(2-5) The typical nonlinear elastic system (i.e., no hysteresis), with an equation of motion of the form

$$\ddot{y}(T) + J(y,\dot{y}) = F(T) \tag{1.1}$$

where $J(y,\dot{y})$ is a nonlinear elastic restoring force function, has no general analytic closed form solutions except for a few special cases such as Duffing's equation. However, several approximate analytical

*The figures, which are grouped together at the end of the text, begin on page 19.

+See List of Symbols, page xiii.

procedures such as the perturbation methods of Poincare or the asymptotic theories of Krylov, Bogoliubov, and Mitropoloky, which approximate the problem as a linear one that can be solved by standard techniques, are available for the solution of the nonlinear elastic system.

For the nonlinear elastic problem it is necessary to verify the stability of a particular displacement solution, since it has been shown by Lazan(6) and others(7) that such systems have frequency response functions displaying an unstable region, as shown in Figure 1.5. This instability is associated with what is commonly referred to as the "jump phenomenon," which occurs when the system is unable to maintain steady state motion and, instead, "jumps" to various response values. Fortunately for the study of nonlinear hysteretic systems, Jennings(8) has shown that the "jump phenomenon" does not occur and the displacement response is bounded in all instances except for the case of elastoplastic hysteresis. Figure 1.6 displays typical examples of hysteretic frequency response functions.

Although steady-state harmonic excitation does not always resemble the excitation encountered in nature, it can be used to gain considerable insight into the dynamic behavior of the system model in response to arbitrary types of excitation. Harmonic analysis is advantageous since it is the most easily analyzed form of excitation; and for even nonlinear systems, periodic solutions can still be assumed.

1.3 DESCRIPTION OF THE PROBLEM

The actual difficulty encountered in the solution of the general hysteretic problem is an *a priori* knowledge of the hysteresis loop geometry based upon defined "skeleton curve" parameters. Figure 1.7 displays the following examples of hysteretic system motion:

a. Figure 1.7(A) is the response to an alternating load of increasing magnitude.

b. Figure 1.7(B) is the response to a load that is increased then decreased to less than zero and then increased beyond its first maximum.

c. Figure 1.7(C) is the response to periodic (i.e., harmonic) excitation.

d. Figure 1.7(D) is the response to general (i.e., random) excitation.

Several authors[9-12] have studied the hysteresis phenomena in detail and have obtained disappointing results in the theoretical predetermination of hysteresis loops. However, Masing[13] proposed a hysteresis-loop hypothesis that has proved successful for softening types of systems. This hypothesis is best described by Jhansale:[11] "The hysteresis curve is geometrically similar to the stress-strain curve (originally meant to be 'monotonic') but magnified by a factor of two." Using the "skeleton curve" segment AEBCD shown in Figure 1.7(C) as an example, the hysteresis loop defined by Masing's Hypothesis is constructed as follows:

a. Motion starts along the skeleton-curve segment BCD until the system velocity becomes zero (i.e., point C). If the displacement point C is in the linear elastic range of the system or the skeleton curve is nonlinear elastic, the restoring force function will next follow the curve segment CBEA in the direction of point A. However, when point C (i.e., $+y_M$) is in the plastic range, the segment BEA is magnified by a factor of two and this magnified curve segment is translated such that point B corresponds with point C. Motion is now down the segment CEA, which forms the lower portion of the hysteresis loop. Because of symmetry and the softening nature of the skeleton curve, the constructed segment CEA will eventually merge into the original skeleton curve. After this merging occurs, further deflections are defined by the original skeleton curve.

b. When the zero velocity position point E (i.e., $-y_M$) is reached, the segment BCD is magnified by a factor of two and translated such that point B now corresponds to point E. Motion is now along the segment ECD, which will now represent the upper portion of the hysteresis loop.

It is important to note that the basic limitations to Masing's Hypothesis are these:

a. The skeleton curve must be softening (i.e., each successive i-th segment in the plastic range must have a stiffness K_i less than the preceding value).

b. The skeleton curve must be symmetric.

Neither of these limitations causes severe restrictions by comparison with those of previously published mathematical models. Caughey[14-15] performed the initial analysis of bilinear hysteretic systems with Iwan,[16-17] extending his work to obtain a general solution for an undamped bilinear hysteretic oscillator and an approximate solution for the same problem with viscous damping in both segments. Masri[18] later refined Iwan's work and obtained an exact solution for the bilinear hysteretic system with viscous damping allowed to vary for each segment region. Jennings[8] presented the solution for hysteretic systems having a softening skeleton curve defined by the relationship

$$\frac{y}{y_y} = \frac{P(y)}{P_y} + \alpha \left(\frac{P(y)}{P_y}\right)^r \tag{1.2}$$

where r is equal to a positive odd integer greater than one and α is an arbitrary positive constant. The special case solutions are α equal to zero, which is the linear elastic system, and r equal to ∞, which is the elasto-plastic system.

The proposed system model that will allow the damping to assume any specified value for each segment in a general prescribed skeleton curve is, even with its aforementioned limitations, a substantial improvement over those presently existing. Jennings[8] made the following observation:

> To obtain agreement with test results, it may be necessary to extend the theory to include non-integer values of r. It may also be necessary to include a viscous damping coefficient in the steady state calculations in order to account for observed energy dissipation at relatively low amplitudes.

Hanson[19] conducted laboratory experiments that he correlated with the Jennings[8] data, and found that theoretically the resonant vibration amplitude would be predicted within 20% and the resonant natural frequency within 3% on the basis of the static virgin force-deflection ("skeleton") curve. Thus, it is reasonable to assume that our improved model will yield even greater agreement between theoretical and experimental data.

For the comparison of data, the Masri[18] model is displayed in Figure 1.4(B) and the Jennings[8] model is defined in Figure 1.8 and Tables 1.1 through 1.3.*

1.4 SCOPE OF RESEARCH

Two separate analytic solutions are derived for the displacement response of a viscously damped, harmonically excited SDOF system with a hysteretic spring stiffness of the softening type defined by Masing's Hypothesis. To determine the accuracy as well as the inherent limitations of these analytic solutions, two computer methodologies, obtained by using algorithms derived for both methods, are evaluated by comparing their generated numerical data with data published by Iwan,[16] Jennings,[8] Hanson,[19] and Masri.[18] The analytic solutions and their associated computer methodologies are appraised to determine future research applications.

This study was conducted under the following assumptions:

a. Analytical solutions for the model in the region of its fundamental elastic response were primary; thus, questions about subharmonic or ultraharmonic responses as discussed by Caughey[20] for the nonlinear elastic system were neglected.

b. Energy transfer devices such as dynamic absorbers were not considered.

c. The effects of energy absorbed by internal structural changes that raise the energy level of the entire system were

*Tables, grouped after figures at the end of the text, begin on page 42.

neglected. Only systems that dissipate energy internally via the hysteresis loop phenomena and viscous damping are discussed.

1.5 SOLUTION OF THE PROBLEM

The equation of motion for the SDOF system shown in Figure 1.2 with a nonlinear hysteretic spring-restoring force relation, such as that shown in Figure 1.4(A), can be written for motion in the i-th segment as

$$M\ddot{y} + C_i\dot{y} + P_i(y) = F(t) \tag{1.3}$$

where $P_i(y)$ is the spring-restoring force function for the multinode system and is defined as

$$P_i(y) = P_i + (y - y_i)\ K_i \tag{1.4}$$

Let x be a normalized dimensionless parameter defined as follows:

$$x = y/y_N \tag{1.5}$$

$$\dot{x} = \dot{y}/y_N \tag{1.6}$$

$$\ddot{x} = \ddot{y}/y_N \tag{1.7}$$

where y_N is an arbitrary normalization parameter often chosen to be equal to the yield displacement (i.e., y_y). Rewriting Definition 1.4, one obtains

$$P_i(x) = P_i + (x - x_i)\ y_N\ K_i \tag{1.8}$$

Using Definitions 1.5 through 1.8, Equation 1.3 can be rewritten in dimensionless form as

$$\ddot{x} + \left(\frac{C_i}{M}\right)\dot{x} + (x - x_i)\frac{K_i}{M} = \frac{1}{My_N}\left[F(t) - P_i\right] \tag{1.9}$$

$$\ddot{x} + 2\zeta_i\omega_i\dot{x} + \omega_i^2 x = \frac{1}{My_N}\left[F(t) - P_i + x_i K_i y_N\right] \tag{1.10}$$

If the generalized i-th node force is defined as

$$Q_i = \frac{1}{My_N}(-P_i + x_i K_i y_N) \tag{1.11}$$

then Equation 1.10 can be written in its final form as

$$\ddot{x} + 2\zeta_i\omega_i\dot{x} + \omega_i^2 x = \frac{F(t)}{My_N} + Q_i \tag{1.12}$$

The solution of Equation 1.12 consists of the sum of the homogenous (that is, $x_h[t]$) and particular (that is, $x_p[t]$) solutions:

$$x(t) = x_h(t) + x_p(t) \tag{1.13}$$

The homogenous solution of Equation 1.12 for the case of subcritical damping is well defined:[2-4]

$$x_h(t) = \exp(-\zeta_i\omega_i t)\left(A_i \sin \omega_{di} t + B_i \cos \omega_{di} t\right) \tag{1.14}$$

For the particular solution of Equation 1.12, one uses the following definition:

$$x_p(t) = x_{p1}(t) + x_{p2}(t) \tag{1.15}$$

where

$$\ddot{x}_{p1} + 2\zeta_i\omega_i\dot{x}_{p1} + \omega_i^2 x_{p1} = \frac{F(t)}{My_N} \tag{1.16}$$

$$\ddot{x}_{p2} + 2\zeta_i\omega_i\dot{x}_{p2} + \omega_i^2 x_{p2} = Q_i \tag{1.17}$$

The solution for $x_{p1}(t)$ is as follows:

$$\ddot{x}_{p1} + 2\zeta_i\omega_i\dot{x}_{p1} + \omega_i^2 x_{p1} = \frac{F_o}{My_N}\cos(\Omega t + \psi_i) \tag{1.18}$$

where

$$F(T) = F_o \cos(\Omega T + \phi_o) \tag{1.19}$$

$$F(t) = F_o \cos(\Omega t + \psi_i) \tag{1.20}$$

$$\psi_i = \phi_o + \phi_i \tag{1.21}$$

Assume the following solution for Equation 1.18:

$$x_{p1}(t) = M_i \sin \Omega t + N_i \cos \Omega t \tag{1.22}$$

Substituting Equation 1.22 into Equation 1.18, one obtains

$$-\Omega^2 (M_i \sin \Omega t + N_i \cos \Omega t) + 2\zeta_i \omega_i \Omega (M_i \cos \Omega t - N_i \sin \Omega t)$$

$$+ \omega_i^2 (M_i \sin \Omega t + N_i \cos \Omega t) = \frac{F_o}{My_N} \cos(\Omega t + \psi_i) \qquad (1.23)$$

Using the double-angle formula[21]

$$\cos(\Omega t + \psi_i) = \cos \Omega t \cos \psi_i - \sin \Omega t \sin \psi_i \qquad (1.24)$$

and equating the terms of Equation 1.23, the following relationships are obtained:

$$(\omega_i^2 - \Omega^2) M_i - (2\zeta_i \omega_i \Omega) N_i = - \frac{F_o}{My_N} \sin \psi_i \qquad (1.25)$$

$$(2\zeta_i \omega_i \Omega) M_i + (\omega_i^2 - \Omega^2) N_i = \frac{F_o}{My_N} \cos \psi_i \qquad (1.26)$$

If Cramer's rule is used to solve Equations 1.25 and 1.26 for M_i and N_i, one obtains

$$D_i = \left(\omega_i^2 - \Omega^2\right)^2 + \left(2\zeta_i \omega_i \Omega\right)^2 \qquad (1.27)$$

$$M_i = \frac{F_o}{My_N D_i} \left[-(\omega_i^2 - \Omega^2) \sin \psi_i + (2\zeta_i \omega_i \Omega) \cos \psi_i\right] \qquad (1.28)$$

$$N_i = \frac{F_o}{My_N D_i} \left[(\omega_i^2 - \Omega^2) \cos \psi_i + (2\zeta_i \omega_i \Omega) \sin \psi_i\right] \qquad (1.29)$$

Thus the solution for $x_{p1}(t)$ is given by Equation 1.22 with M_i and N_i defined respectively by Equations 1.28 and 1.29.

The solution for $x_{p2}(t)$ is obviously obtained by inspection to be

$$x_{p2}(t) = \frac{Q_i}{\omega_i^2} \tag{1.30}$$

Combining Equations 1.14, 1.22, and 1.30, the total solution of Equation 1.3 is written as

$$x(t) = \exp(-\zeta_i\omega_i t)(A_i \sin \omega_{di}t + B_i \cos \omega_{di}t) + M_i \sin \Omega t$$

$$+ N_i \cos \Omega t + Q_i/\omega_i^2 \tag{1.31}$$

where A_i and B_i are dependent upon the initial conditions at the start of motion in the i-th segment. Let the initial conditions be defined as

$$x_i(t = o) = x_{io} \tag{1.32}$$

$$\dot{x}_i(t = o) = \dot{x}_{io} \tag{1.33}$$

Using Equation 1.31 and Definitions 1.32 and 1.33, the constants A_i and B_i are defined as

$$B_i = (x_{io} - N_i - Q_i/\omega_i^2) \tag{1.34}$$

$$A_i = (\dot{x}_{io} - M_i\Omega + \zeta_i\omega_i B_i) /\omega_{di} \tag{1.35}$$

where t is the time within a segment and T is total time.

In the same manner, the velocity within the i-th segment can be expressed as

$$x(t) = -\zeta_i \omega_i \exp(-\zeta_i \omega_i t)(A_i \sin \omega_{di} t + B_i \cos \omega_{di} t) + \exp(-\zeta_i \omega_i t)$$

$$(A_i \omega_{di} \cos \omega_{di} t - B_i \omega_{di} \sin \omega_{di} t) + M_i \Omega \cos \Omega t - N_i \Omega \sin \Omega t \tag{1.36}$$

Masri[18] derived a solution for a system equation similar to Equation 1.12, which for motion in the i-th segment can be expressed in the form

$$\ddot{x} + 2\zeta_i \omega_i \dot{x} + \omega_i^2 x = Q_i + F_o \sin(\Omega t + \psi_i) \tag{1.37}$$

with the forcing function defined as

$$F(T) = F_o \sin(\Omega T + \phi_o) \tag{1.38}$$

The solution of Equation 1.37 can be written in terms of total time (i.e., T), where T_i is equal to the time that motion starts in the i-th segment as follows:

$$x(T) = \exp\left[\frac{-\zeta_i}{R_i}(\Omega T - \psi_i)\right] \left[a_i \sin \frac{\eta_i}{R_i}(\Omega T - \psi_i)\right.$$

$$\left. + b_i \cos \frac{\eta_i}{R_i}(\Omega T - \psi_i)\right] + C_i \sin(\Omega T + \tau_i)$$

$$+ Q_i/\omega_i^2 \tag{1.39}$$

$$\dot{x}(T) = \omega_i \left[\exp \frac{-\zeta_i}{R_i} (\Omega T - \psi_i) \right] \left[-(\zeta_i a_i + \eta_i b_i) \sin \frac{\eta_i}{R_i} (\Omega T - \psi_i) \right.$$

$$\left. + (\eta_i a_i - \zeta_i b_i) \cos \frac{\eta_i}{R_i} (\Omega T - \psi_i) \right] + \Omega C_i \cos (\Omega T - \tau_i) \tag{1.40}$$

The parameters used in Equations 1.39 and 1.40 are defined as:

$$R_i = \Omega / \omega_i \tag{1.41}$$

$$\beta_i = \tan^{-1} \left(\frac{2\zeta_i R_i}{1 - R_i^2} \right) \tag{1.42}$$

$$\eta_i = \sqrt{1 - \zeta_i^2} \tag{1.43}$$

$$\Theta_i = \phi_i + \tau_i \tag{1.44}$$

$$\tau_i = \phi_o - \beta_i \tag{1.45}$$

$$C_i = \frac{F_o / \omega_i^2}{\sqrt{(1 - R_i^2)^2 + (2\zeta_i R_i)^2}} \tag{1.46}$$

$$b_i = x_{io} - C_i \sin \Theta_i - Q_i / \omega_i^2 \tag{1.47}$$

$$a_i = \frac{1}{\eta_i} \left[\frac{1}{\omega_i} \dot{x}_{io} - C_i R_i \cos \Theta_i + \zeta_i (b_i) \right] \tag{1.48}$$

$$\phi_i = \Omega T_i \tag{1.49}$$

1.6 COMPUTER SOLUTION

This section briefly describes the two digital computer logics (i.e., ID501 and ID1000) created to obtain numerical data for the analytic solutions of the system model proposed in Section 1.5.

1.6.1 Computer Logic ID501

This computer method used Equations 1.31 and 1.36, which are the exact solution of the equations of motion within an i-th segment, and the defined system "skeleton curve" to determine the displacement (x) and velocity ($\dot{x}$) at a fixed delta time (Δt) step. The program logic is designed to modify the Δt step when the system passes from the i to the $i + 1$ segment so that the crossover time can be determined exactly. When the modified step is known, the initial numerical conditions can be derived for the $i + 1$ segment. This procedure continues until a system velocity ($\dot{x}$) of zero is reached, thus defining the maximum displacement ($x_M = y_M/y_N$). Then using Masing's Hypothesis, the lower segment of the hysteresis loop is constructed and the procedure is repeated until a negative maximum displacement ($-x_M$) is determined. The upper segment of the hysteresis loop is now constructed, and the entire procedure is repeated for as many cycles as necessary, until the absolute value of the maximum displacement ($|x_M|$) reaches a steady-state value.

1.6.2 Computer Logic ID1000

This computer method uses iteration techniques to determine the hysteresis loop parameters corresponding to a user-supplied forcing function F(T) and system "skeleton curve." Basically, two fundamental facts are known about hysteresis loops corresponding to the steady state motion of an SDOF system subjected to harmonic excitation:

a. The starting and ending loop displacement points that lie on the skeleton curve must correspond to each other.

b. The initial phase angle (ψ) at the start of each loop must be a 2π multiple of the previous starting-loop value.

An error function can thus be defined using facts (a) and (b) to determine the accuracy of a proposed hysteresis loop. For a specific forcing function, there are two possible hysteresis loop parameters that can be iterated: one is the start position ($-x_M$) on the skeleton curve and the other is the initial phase angle (ψ) at the start of motion. This program logic uses Masing's Hypothesis in conjunction with Equations 1.39 and 1.40 to generate hypothetical hysteresis loops for these iteration parameters. The specific set of values (ψ and $-x_M$) that yield a minimum error function value correspond to the steady state problem solution.

1.7 CONCLUSIONS

Two analytic solutions and their digital computer methodologies (ID501 and ID1000) have been presented for determining the dynamic response of a viscously damped, harmonically excited SDOF general hysteresis system. Both computer logics approximate the general hysteresis skeleton curve as a multisegmented, piecewise linear curve. Computer method ID501 solves the problem in the time domain, whereas ID1000 uses iterative techniques. The only limitation on these analytic solutions is that the skeleton curves must be of a softening type defined by Masing's Hypothesis. However, if the hysteresis loop geometry is defined for systems other than softening types, both of these computer programs could be modified to produce satisfactory results, since once the hysteresis loop is defined, the numerical solution for the response is trivial. In Figures 1.9 through 1.24, the computer-generated results are shown to be in good agreement, both qualitatively and quantitatively, with existing published data. Since both of these computer versions can match an arbitrary skeleton curve and also allow for the variation of damping in each i-th segment, they are a substantial improvement over solution methodologies presently available for this class of problem.

1.8 ILLUSTRATIONS

Included in this section are all the figures and tables associated with Chapter 1. They are numbered and displayed in the sequential order in which they are referenced in the text. The following parameters are used only for the included figures and tables (all other parameters are defined in the List of Symbols preceding Chapter 1.

$|A|$ Displacement amplification factor

K1 Spring stiffness in elastic range of a bilinear hysteresis system

K2 Spring stiffness in plastic range of a bilinear hysteresis system

K_y Normalization factor, which is equal to P_y/Y_y, used for the Jennings models presented in Tables 1.1 through 1.3

T2 Hysteresis loop time corresponding to x2, if loop time is set equal to zero at point A (see Figure 1.4[B])

r, α Parameters used for Jennings model, defined by Equation 1.2

x2 Position of $y2/y_N$ in the steady state, dynamic bilinear hysteresis loop (See Figure 1.4[B].)

ζ1 Critical damping ratio in the elastic range of a bilinear hysteresis system

ζ2 Critical damping ratio in the plastic range of bilinear hysteresis system

ω1 Natural frequency in the primary elastic range

The following special notes apply to the included figures and tables:

a. For all plots presented, y_N was set equal to y_y.

b. For Figures 1.20 through 1.24, ω_1 is equal to K_y/M.

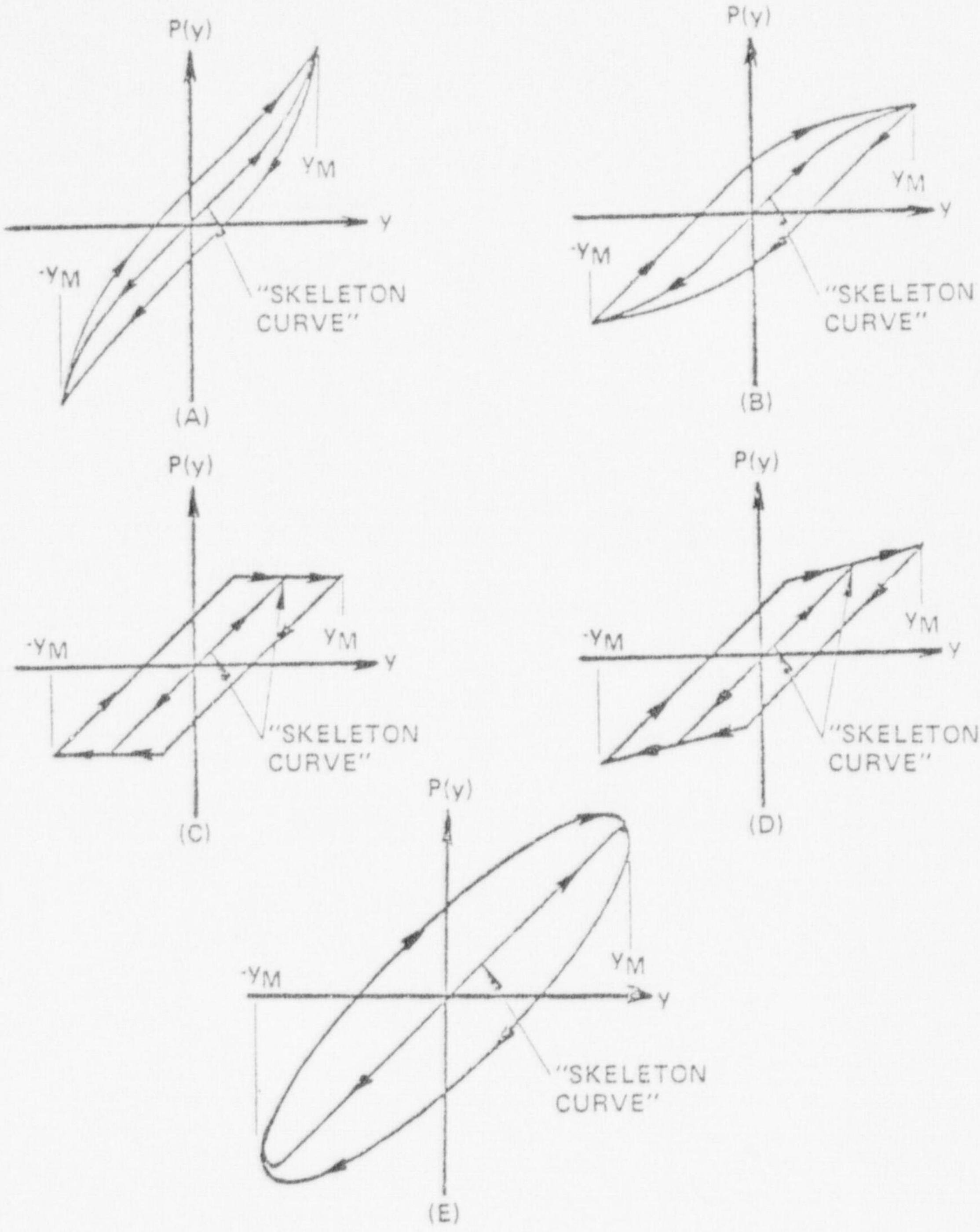

FIGURE 1.1 VARIOUS EXAMPLES OF COMMONLY OBSERVED HYSTERESIS LOOPS; (A) HARDENING; (B) SOFTENING; (C) ELASTO-PLASTIC; (D) BILINEAR; (E) LINEAR SYSTEM WITH VISCOUS DAMPING

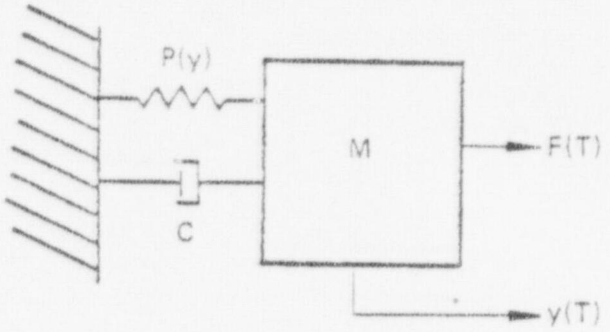

FIGURE 1.2 SYSTEM MODEL

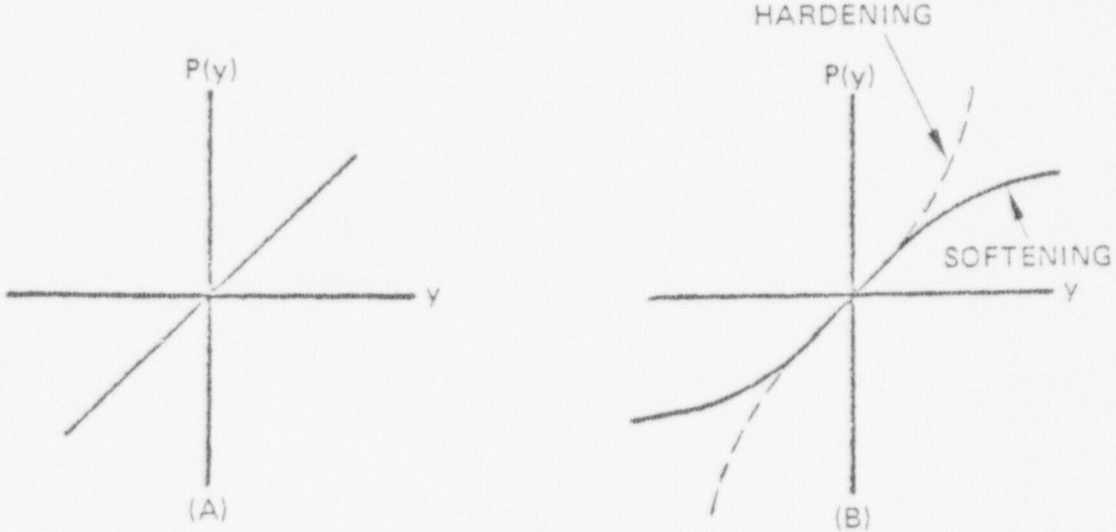

FIGURE 1.3 TYPICAL FORCE – DEFLECTION "SKELETON CURVES"; (A) LINEAR ELASTIC; (B) NONLINEAR

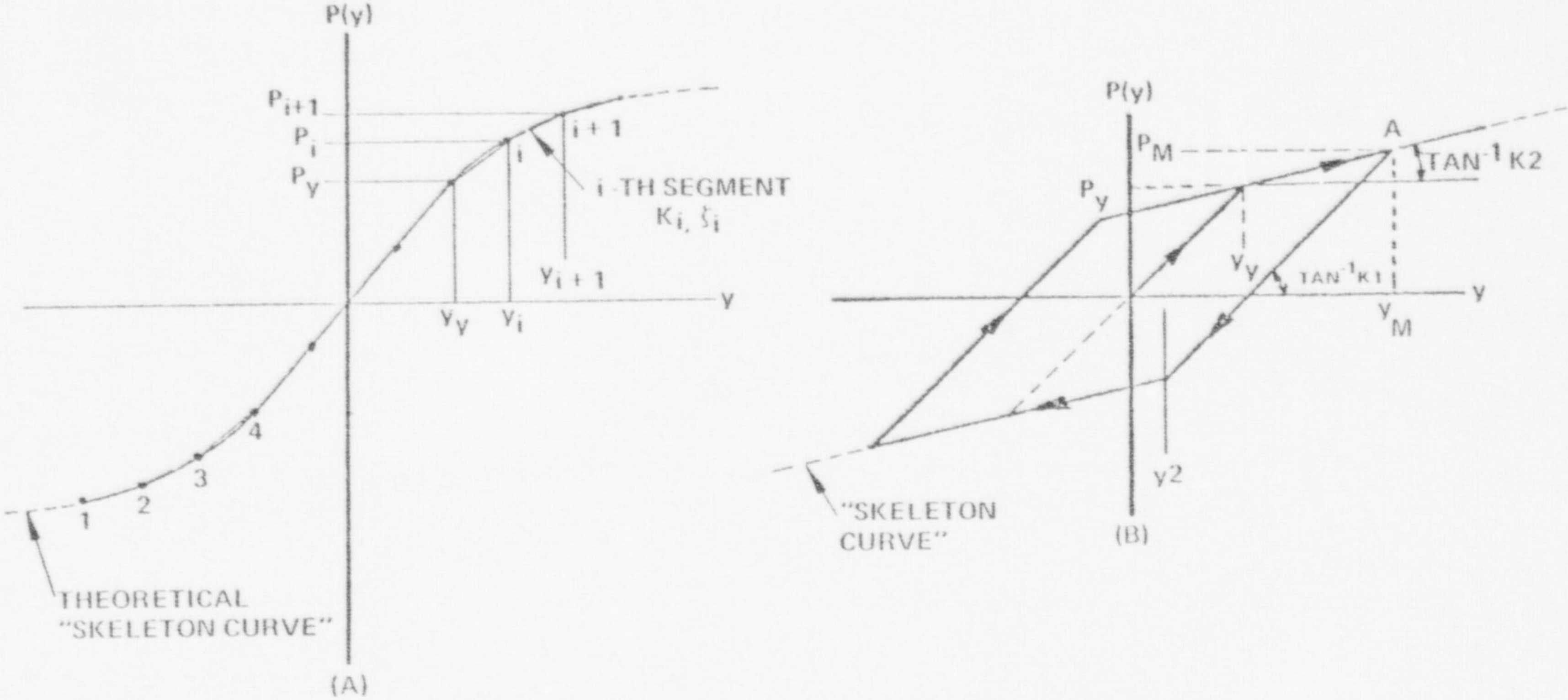

FIGURE 1.4 COMPUTER APPROXIMATION FOR SYSTEM "SKELETON CURVE";
(A) PIECEWISE LINEAR, NODE APPROXIMATION FOR GENERAL HYSTERESIS;
(B) BILINEAR HYSTERESIS "SKELETON CURVE" AND LOOP.

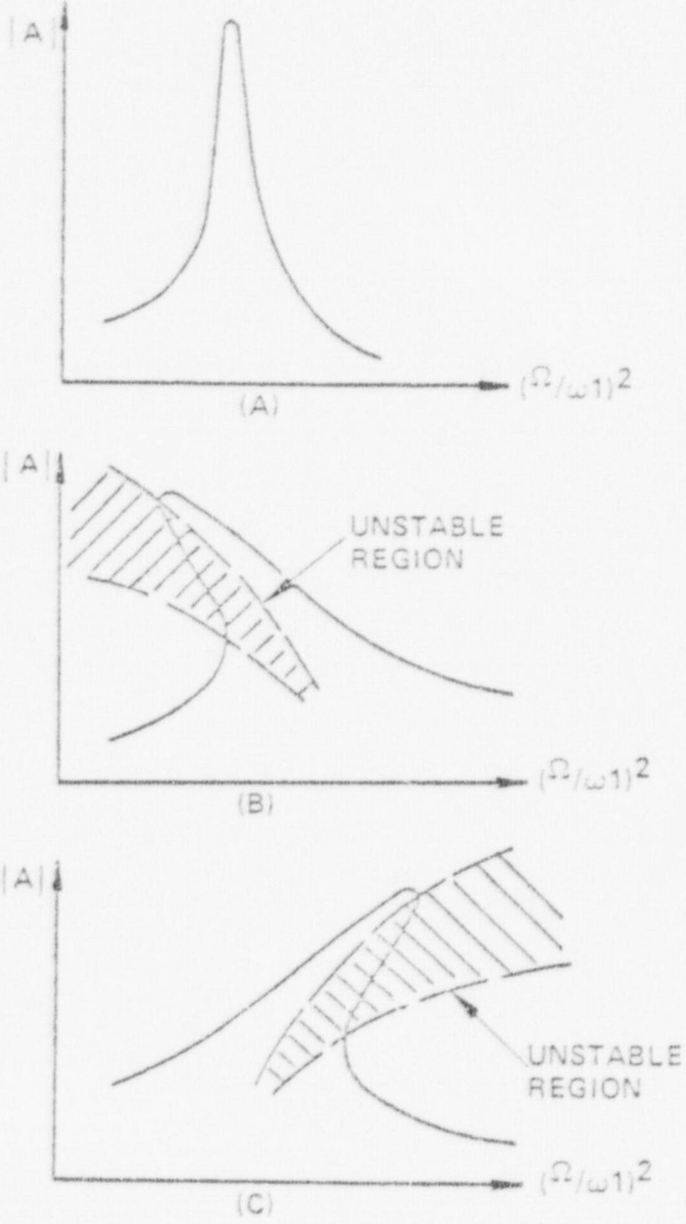

FIGURE 1.5 FREQUENCY RESPONSE CURVES FOR NONHYSTERETIC SYSTEMS; (A) LINEAR; (B) SOFTENING NONLINEAR SPRING; (C) HARDENING NONLINEAR SPRING

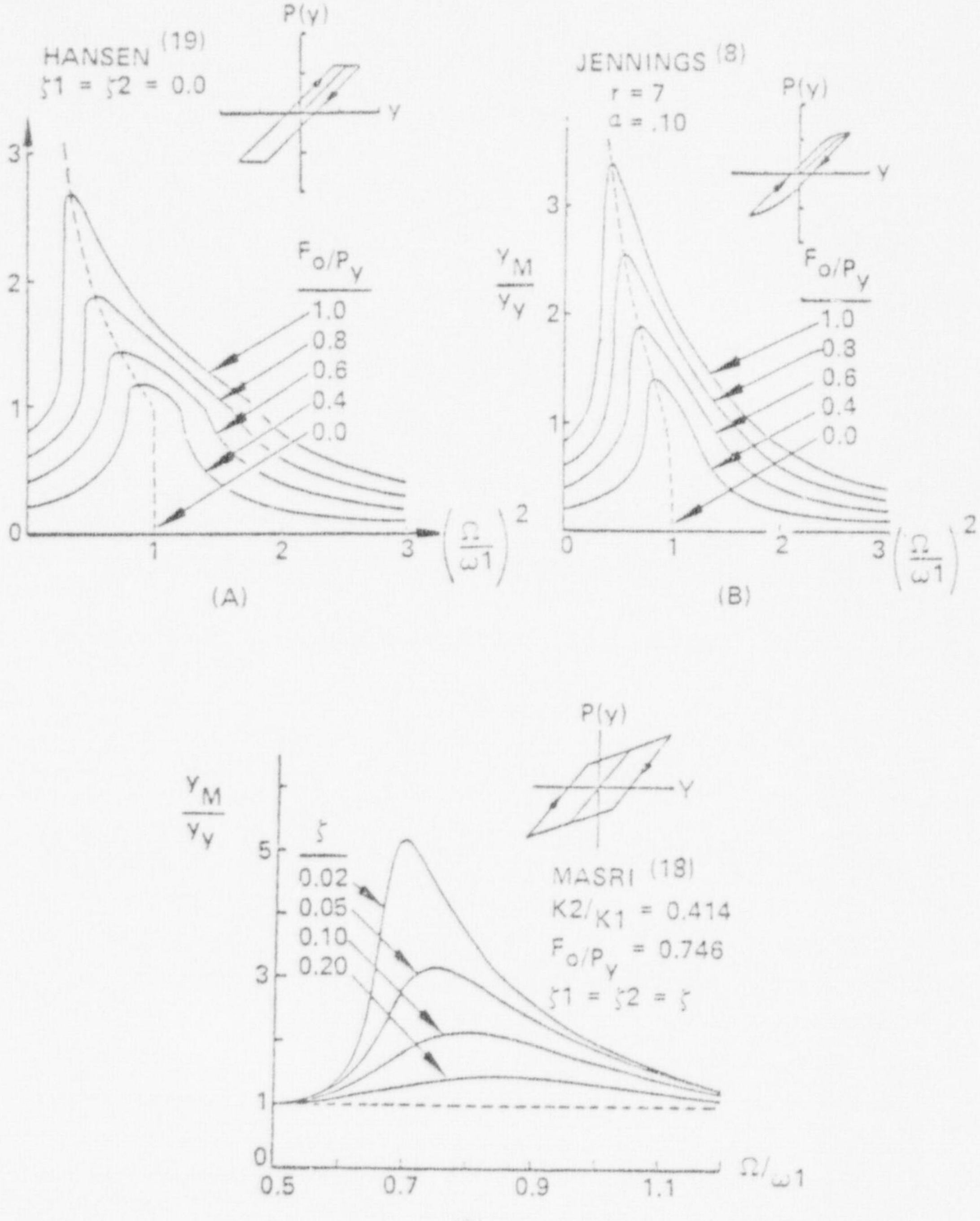

FIGURE 1.6 HYSTERESIS TYPE FREQUENCY RESPONSE CURVES; (A) ELASTO-PLASTIC; (B) GENERAL HYSTERESIS; (C) BILINEAR

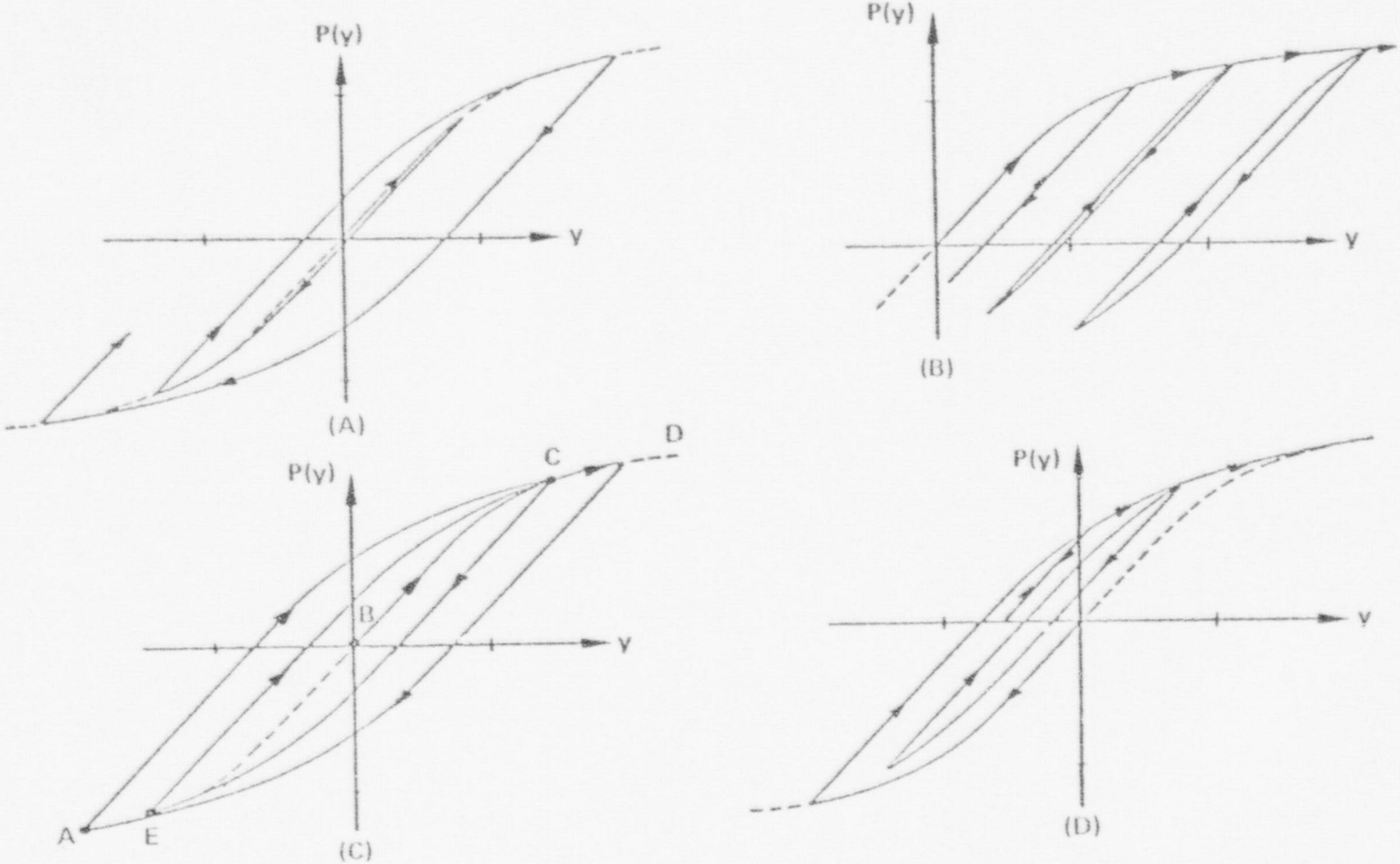

FIGURE 1.7 EXAMPLES OF HYSTERETIC BEHAVIOR

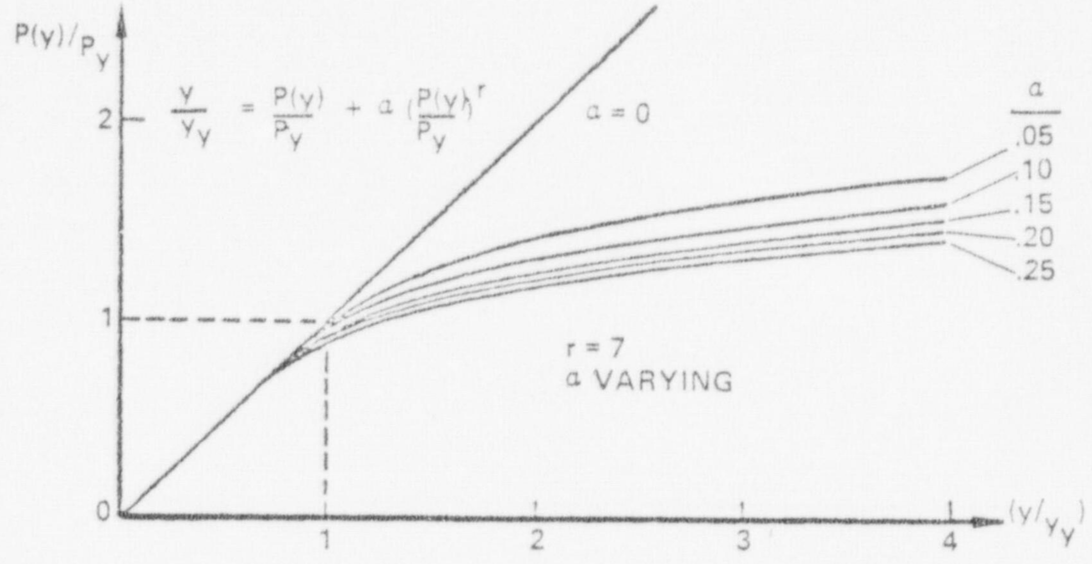

(A)

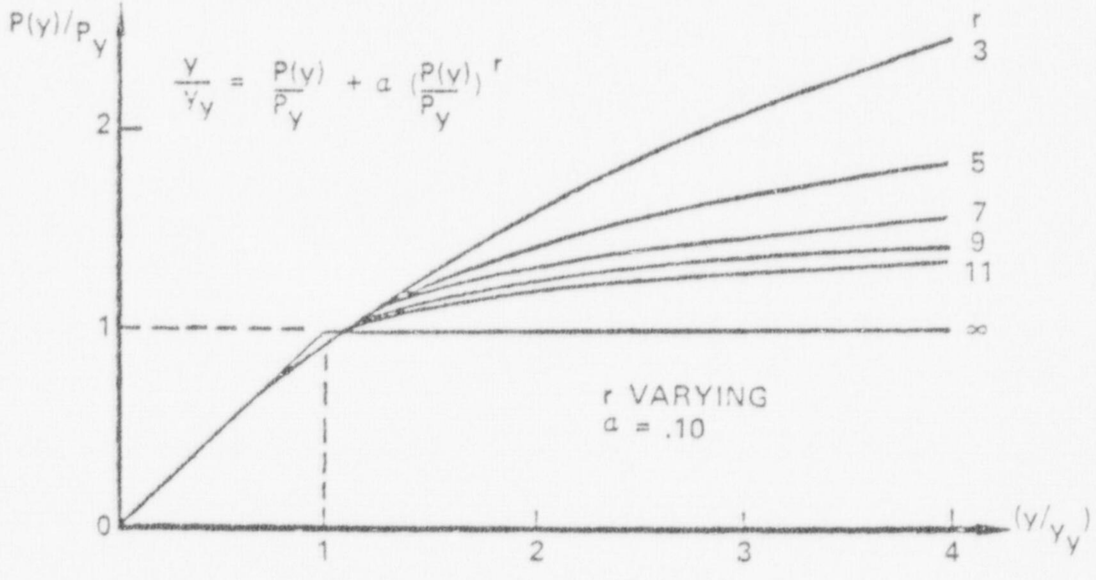

(B)

FIGURE 1.3 EXAMPLES OF JENNINGS SKELETON CURVES DESCRIBED BY VARIOUS r AND a PARAMETER VALUES

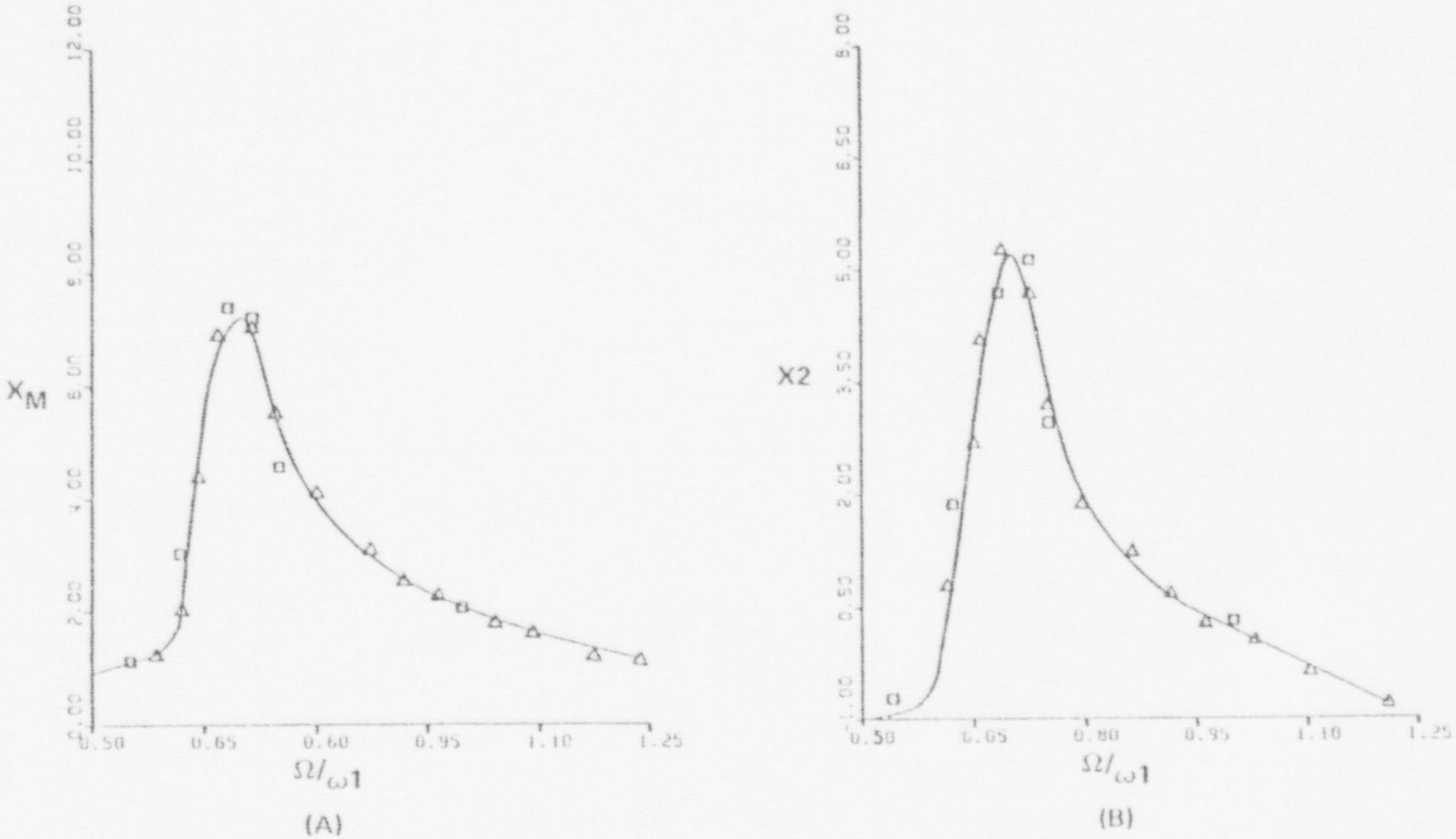

FIGURE 1.9 COMPARISON OF THEORETICAL AND EXPERIMENTAL DATA; $\zeta 1 = \zeta 2 = 0.01$, $K2/_{K1} = 0.414$, $F_o/_{P_y} = .746$

DATA POINTS

— THEORY, MASRI (18)

△ EXPERIMENT (ID501)

□ EXPERIMENT (ID1000)

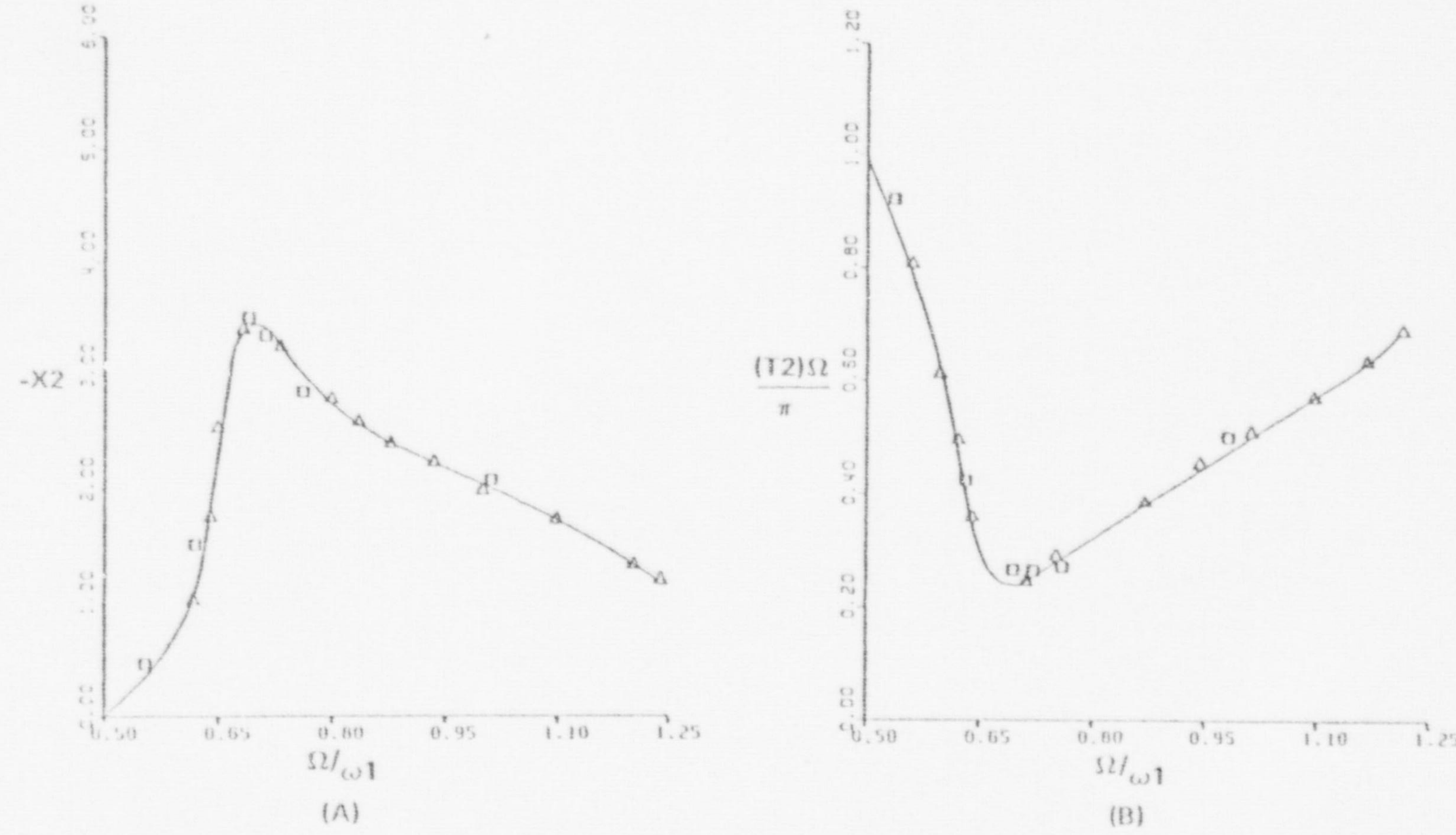

FIGURE 1.10 COMPARISON OF THEORETICAL AND EXPERIMENTAL DATA; $\zeta 1 = \zeta 2 = 0.01$, $K2/_{K1} = 0.414$, $F_o/_{P_y} = 0.746$

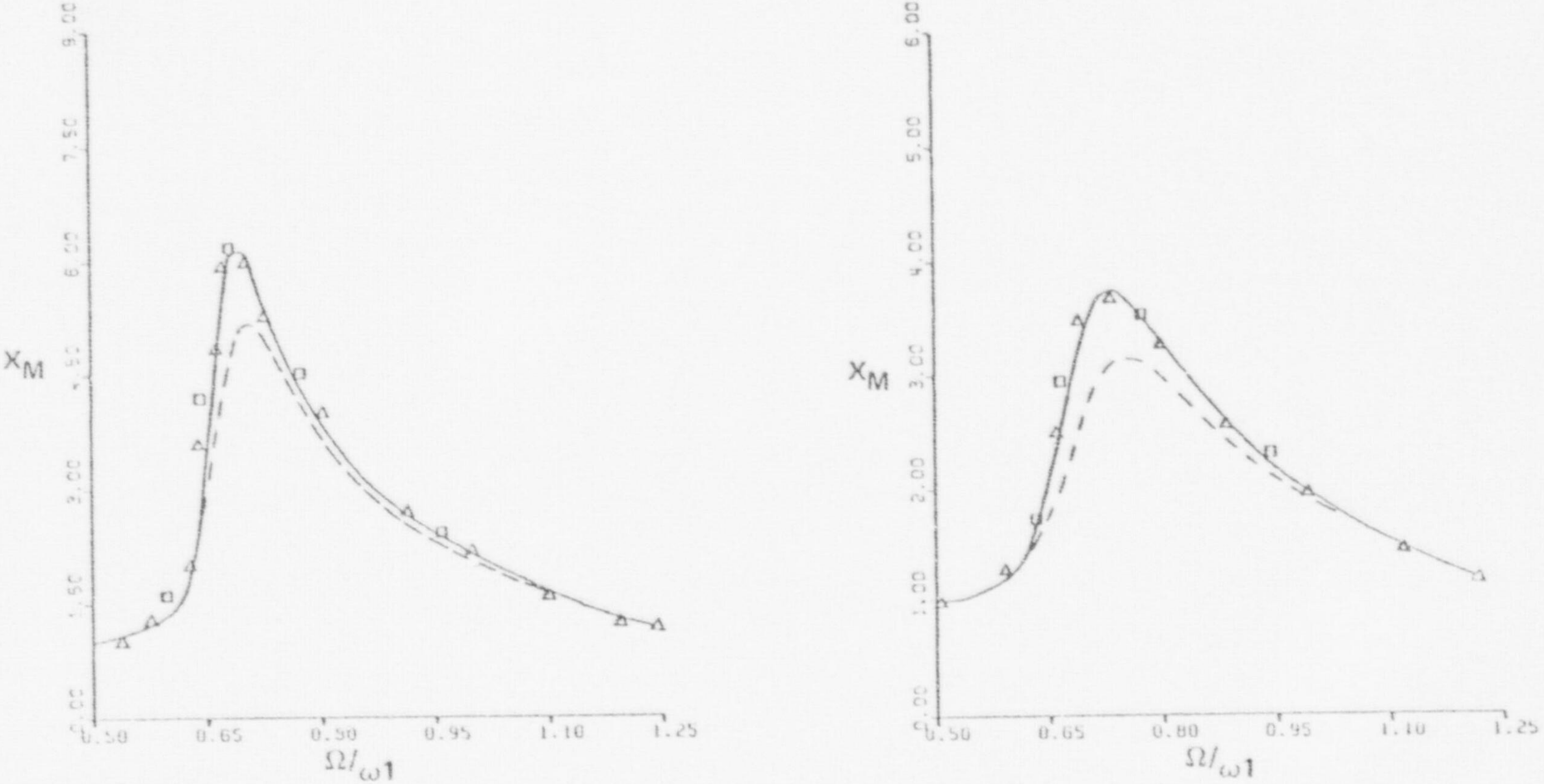

(A) (B)

FIGURE 1.11 COMPARISON OF THEORETICAL AND EXPERIMENTAL DATA; $K2/_{K1} = 0.414$, $^{F}o/_{P_y} = 0.746$; (A) $\zeta 1 = \zeta 2 = 0.02$; (B) $\zeta 1 = \zeta 2 = 0.05$

DATA POINTS

—— THEORY, MASRI (18)

- - - THEORY, IWAN (16)

△ EXPERIMENT (ID501)

□ EXPERIMENT (ID1000)

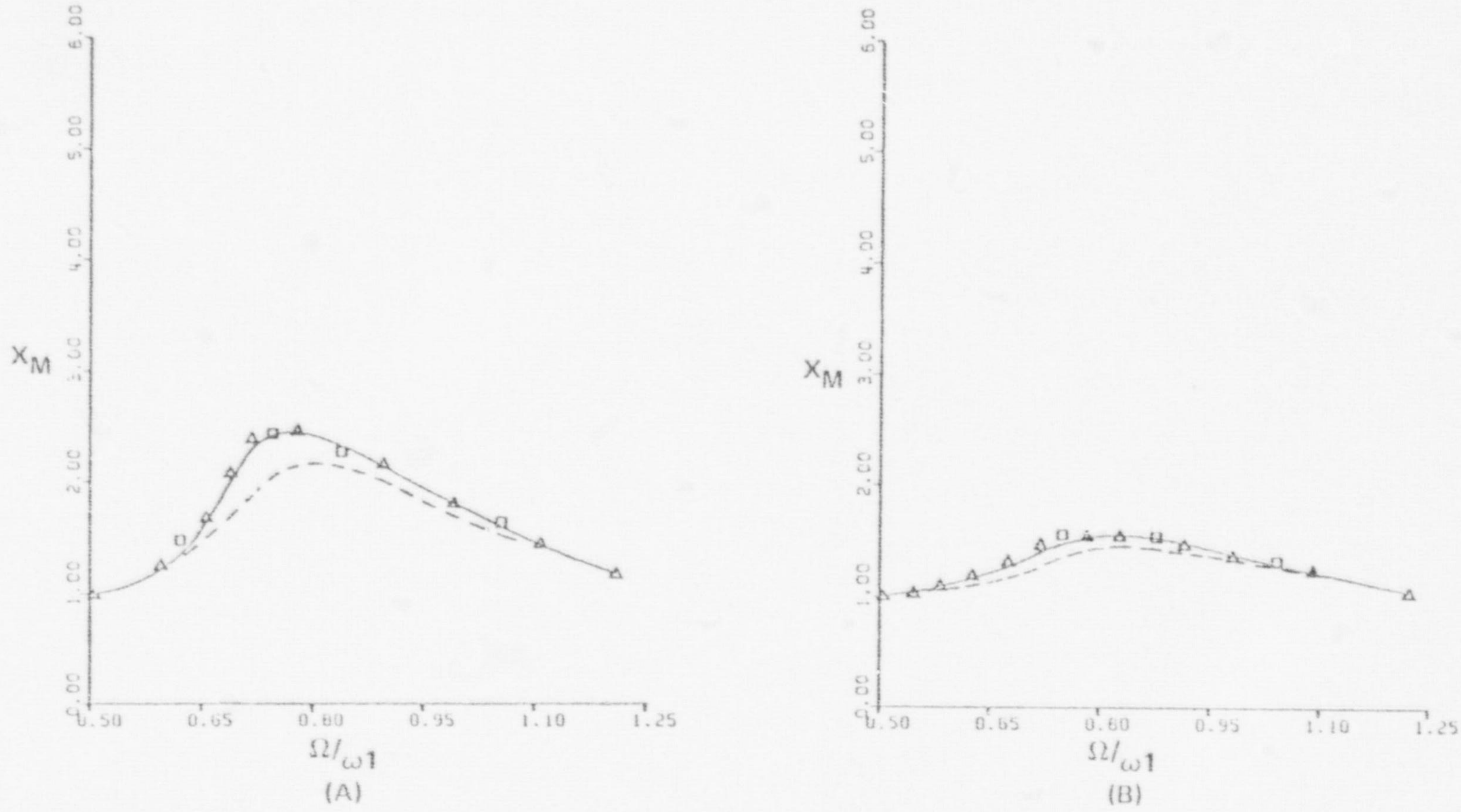

FIGURE 1.12 COMPARISON OF THEORETICAL AND EXPERIMENTAL DATA; $K2/K1 = 0.414$, $F_o/P_y = 0.746$; (A) $\zeta 1 = \zeta 2 = 0.10$; (B) $\zeta 1 = \zeta 2 = 0.20$

DATA POINTS

——— THEORY, MASRI (18)

– – – THEORY, IWAN (16)

△ EXPERIMENT (ID501)

□ EXPERIMENT (ID100C)

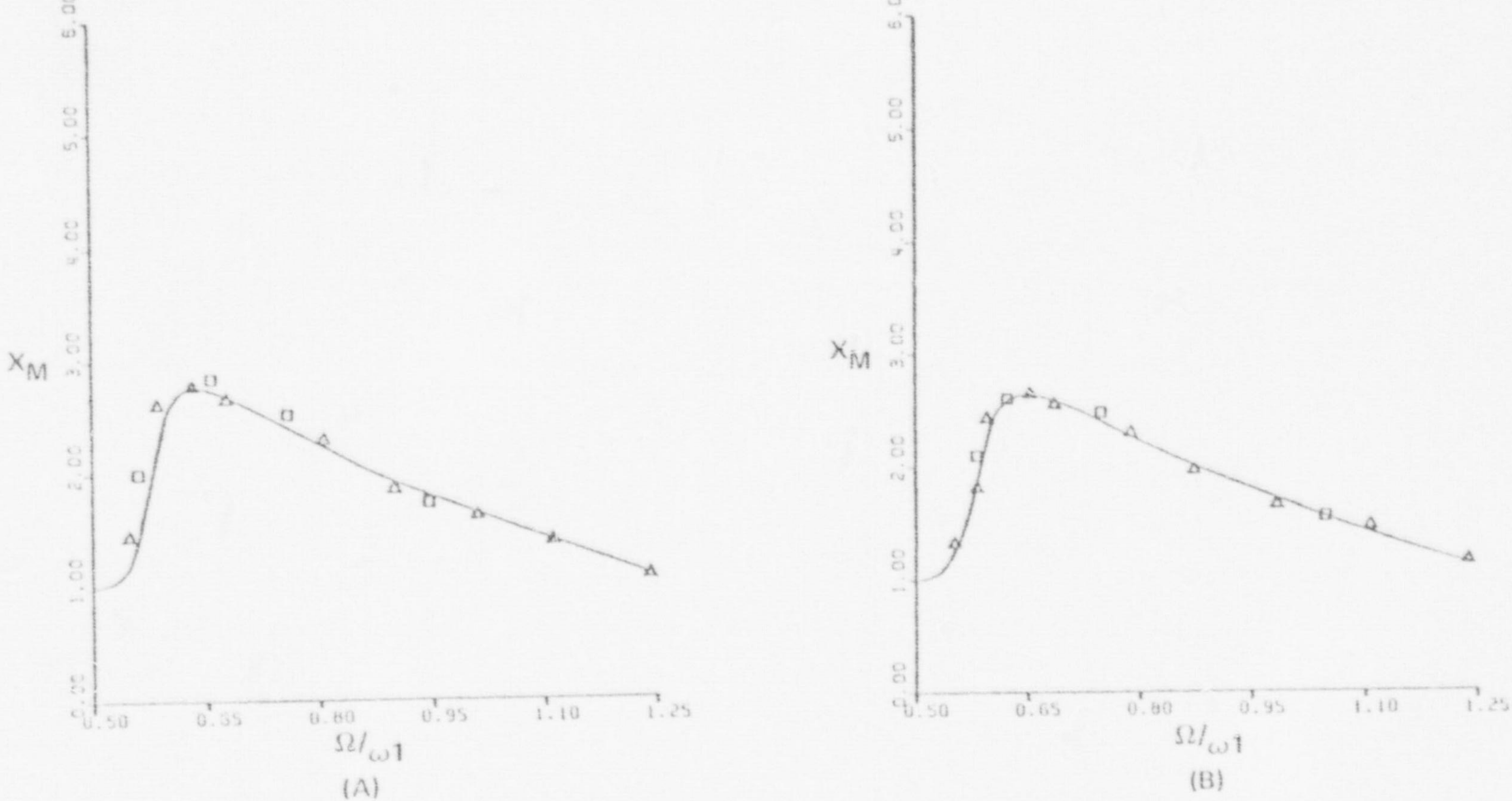

FIGURE 1.13 COMPARISON OF THEORETICAL AND EXPERIMENTAL DATA; $K2/K1 = 0.10$, $\zeta 1 = 0.01$, $F_o/P_y = 0.75$; (A) $\zeta 2 = 0.0$; (B) $\zeta 2 = 0.01$

DATA POINTS

— THEORY, MASRI (18)

△ EXPERIMENT (ID501)

□ EXPERIMENT (ID1000)

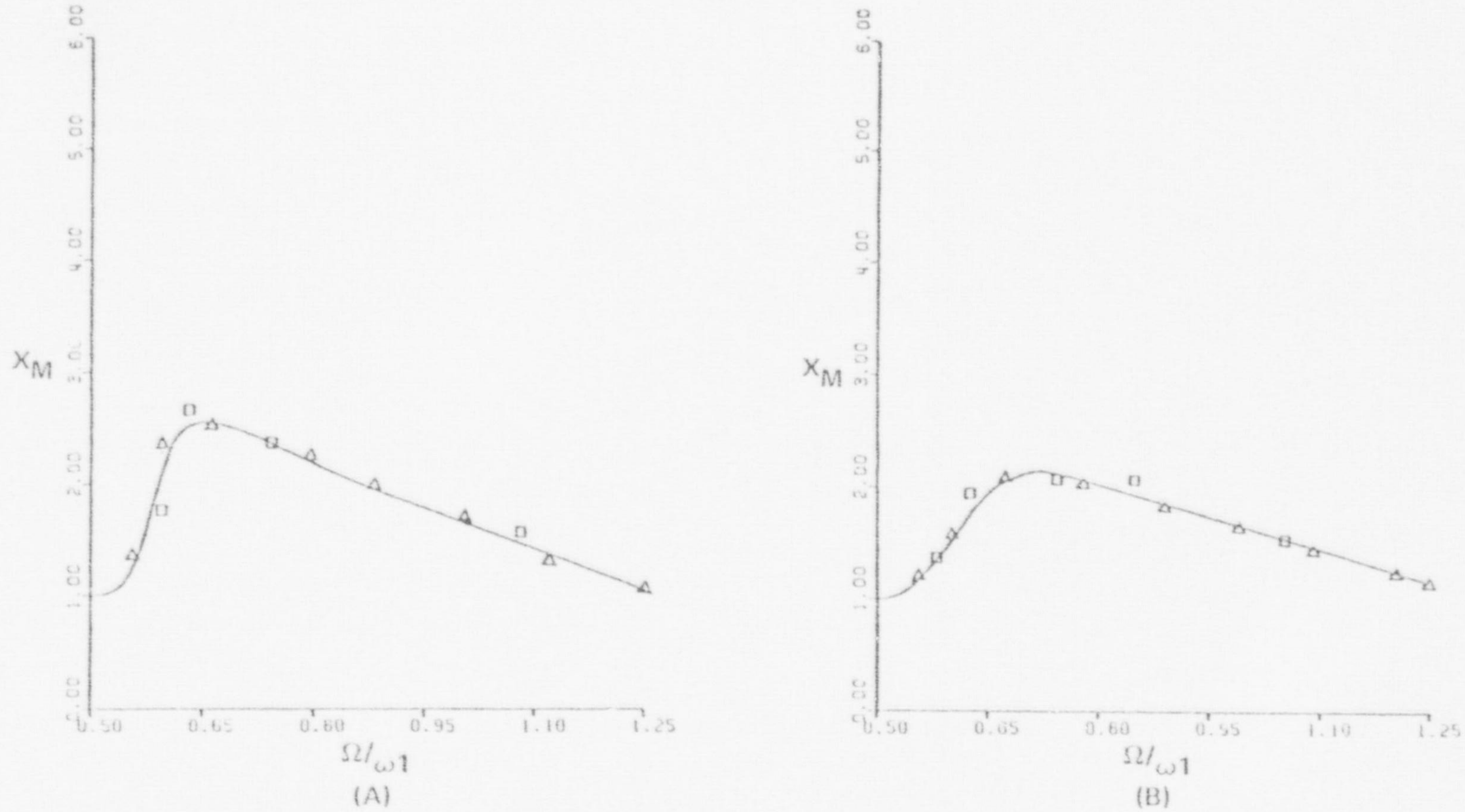

FIGURE 1.14 COMPARISON OF THEORETICAL AND EXPERIMENTAL DATA; $K2/K1 = 0.10$, $\zeta 1 = 0.01$, $F_o/P_y = 0.75$; (A) $\zeta 2 = 0.05$; (B) $\zeta 2 = 0.25$

DATA POINTS

—— THEORY, MASRI (18)

△ EXPERIMENT (ID501)

□ EXPERIMENT (ID1000)

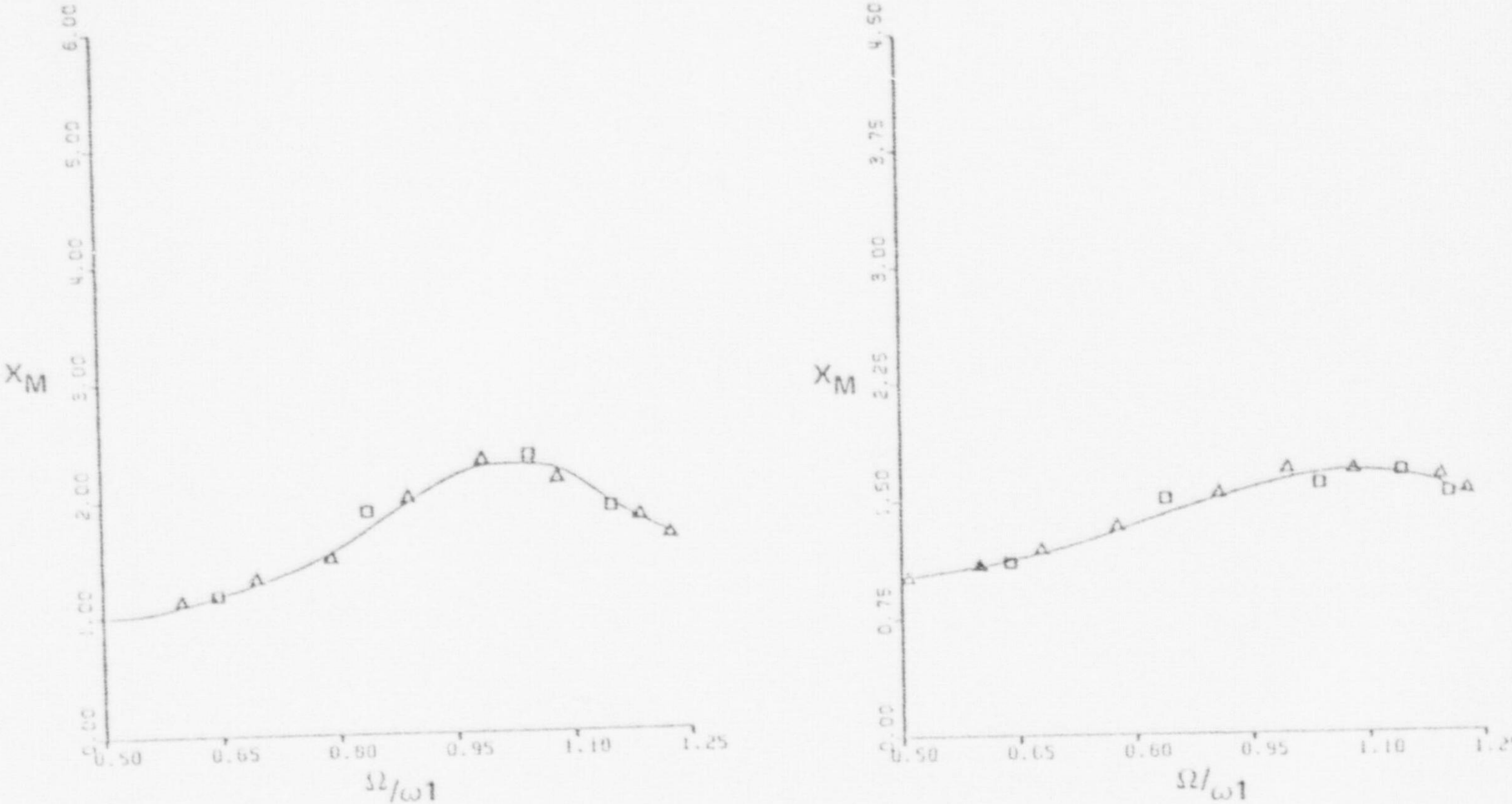

(A) (B)

FIGURE 1.15 COMPARISON OF THEORETICAL AND EXPERIMENTAL DATA; $K2/_{K1} = 0.9$, $\zeta 1 = 0.01$, $F_o/_{P_Y} = 0.75$, (A) $\zeta 2 = 0.25$; (B) $\zeta 2 = 0.50$

DATA POINTS

—— THEORY, MASRI (18)

△ EXPERIMENT (ID501)

□ EXPERIMENT (ID1000)

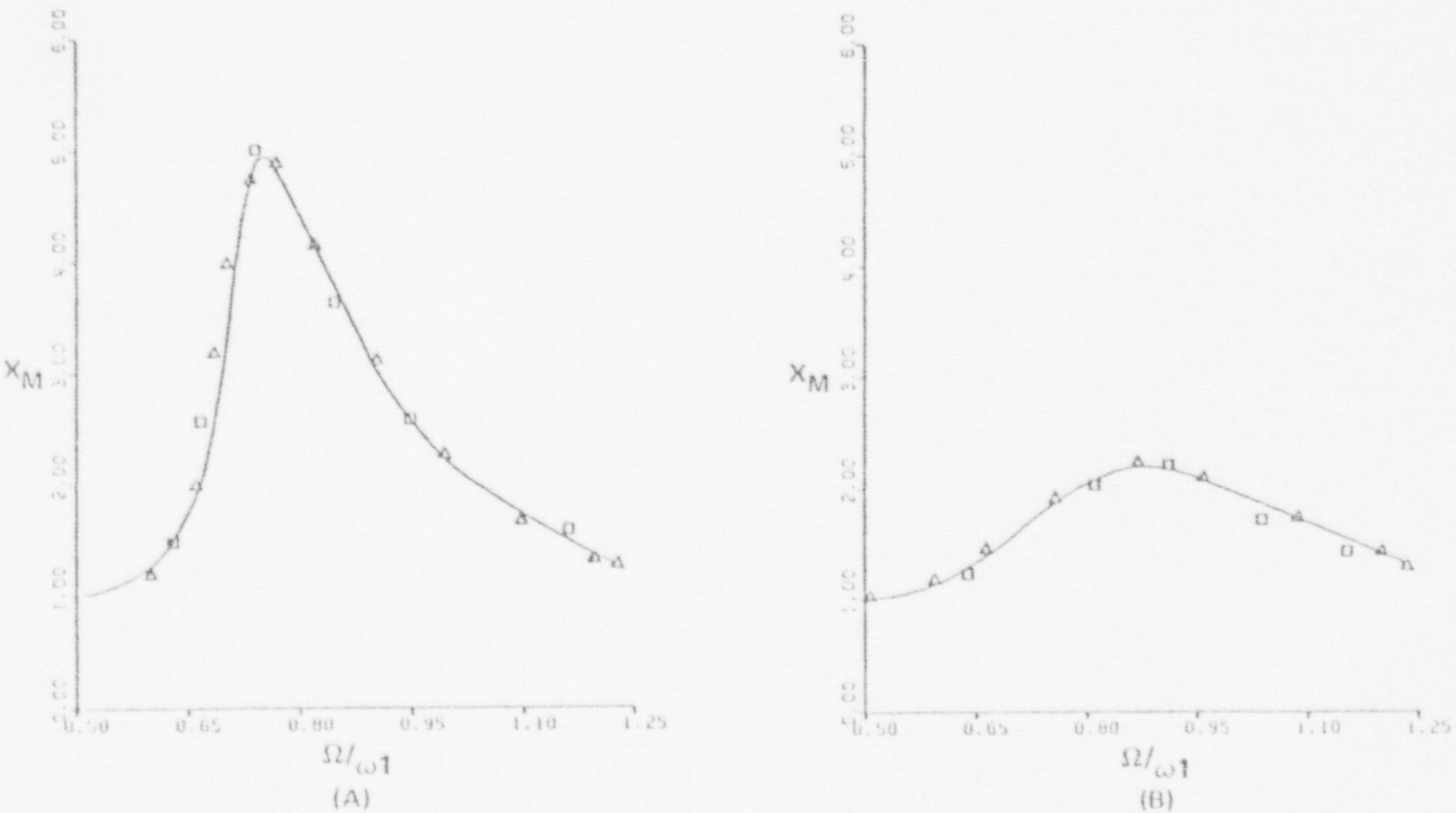

FIGURE 1.16 COMPARISON OF THEORETICAL AND EXPERIMENTAL DATA; $K2/K1 = 0.5$, $\zeta 1 = 0.01$, $F_o/P_Y = 0.75$; (A) $\zeta 2 = 0.05$; (B) $\zeta 2 = 0.25$

DATA POINTS

— THEORY, MASRI (18)

Δ EXPERIMENT (ID501)

$\square$ EXPERIMENT (ID1000)

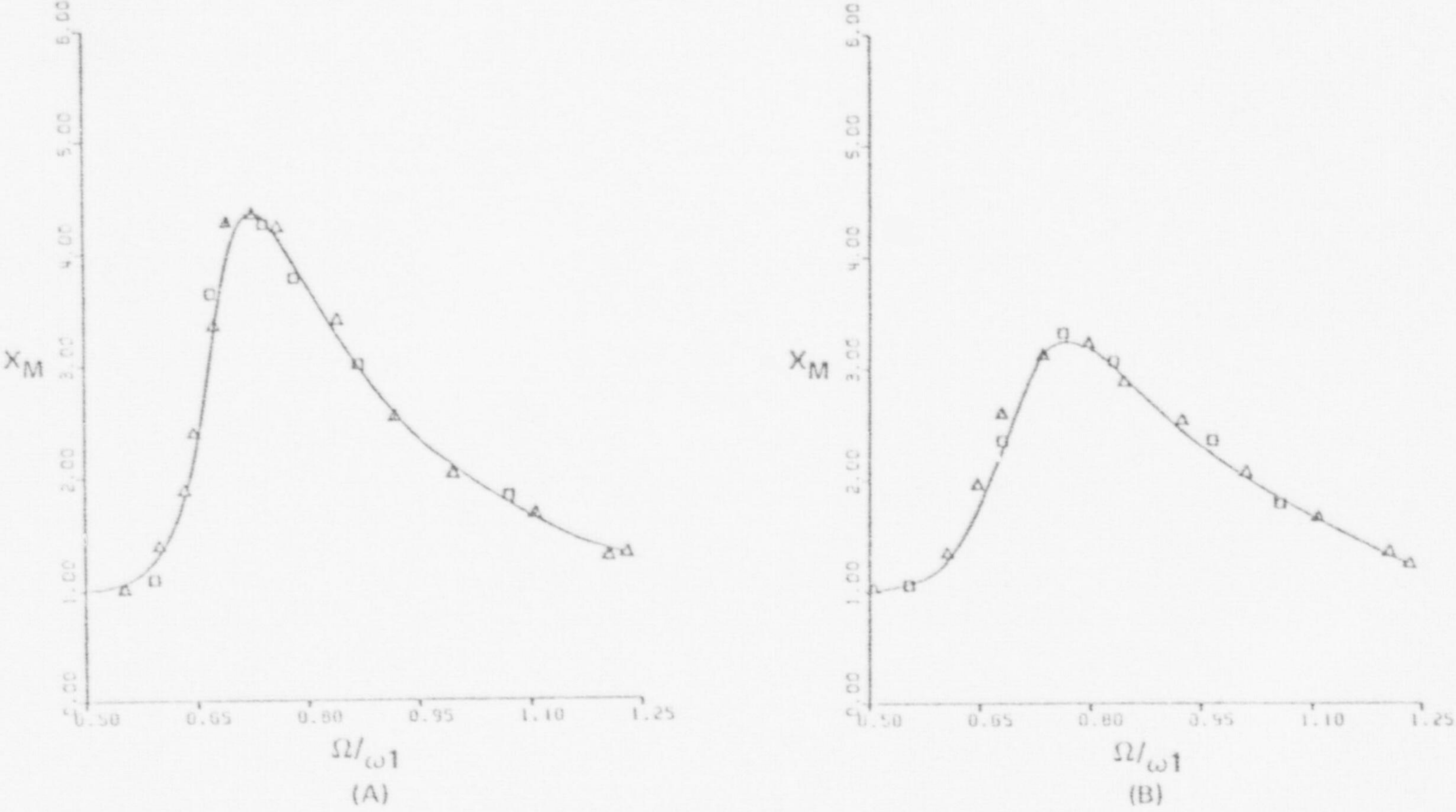

FIGURE 1.17 COMPARISON OF THEORETICAL AND EXPERIMENTAL DATA; $K2/K1$ = 0.414, $\zeta 1$ = 0.0, F_o/P_y = 0.746; (A) $\zeta 2$ = 0.05; (B) $\zeta 2$ = 0.10

DATA POINTS

— THEORY, MASRI [18]

△ EXPERIMENT (ID501)

□ EXPERIMENT (ID1000)

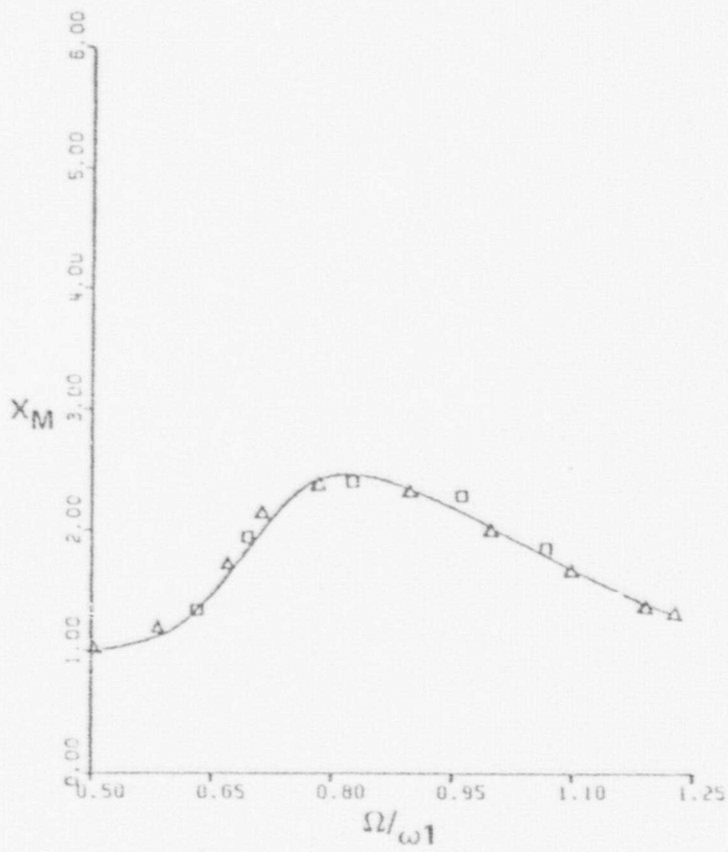

FIGURE 1.18 COMPARISON OF THEORETICAL AND EXPERIMENTAL DATA; $K2/_{K1} = 0.414$, $\zeta 1 = 0.0$, $\zeta 2 = 0.2$, $F_o/_{P_y} = 0.746$

DATA POINTS

— THEORY, MASRI [18]

△ EXPERIMENT (ID501)

□ EXPERIMENT (ID1C00)

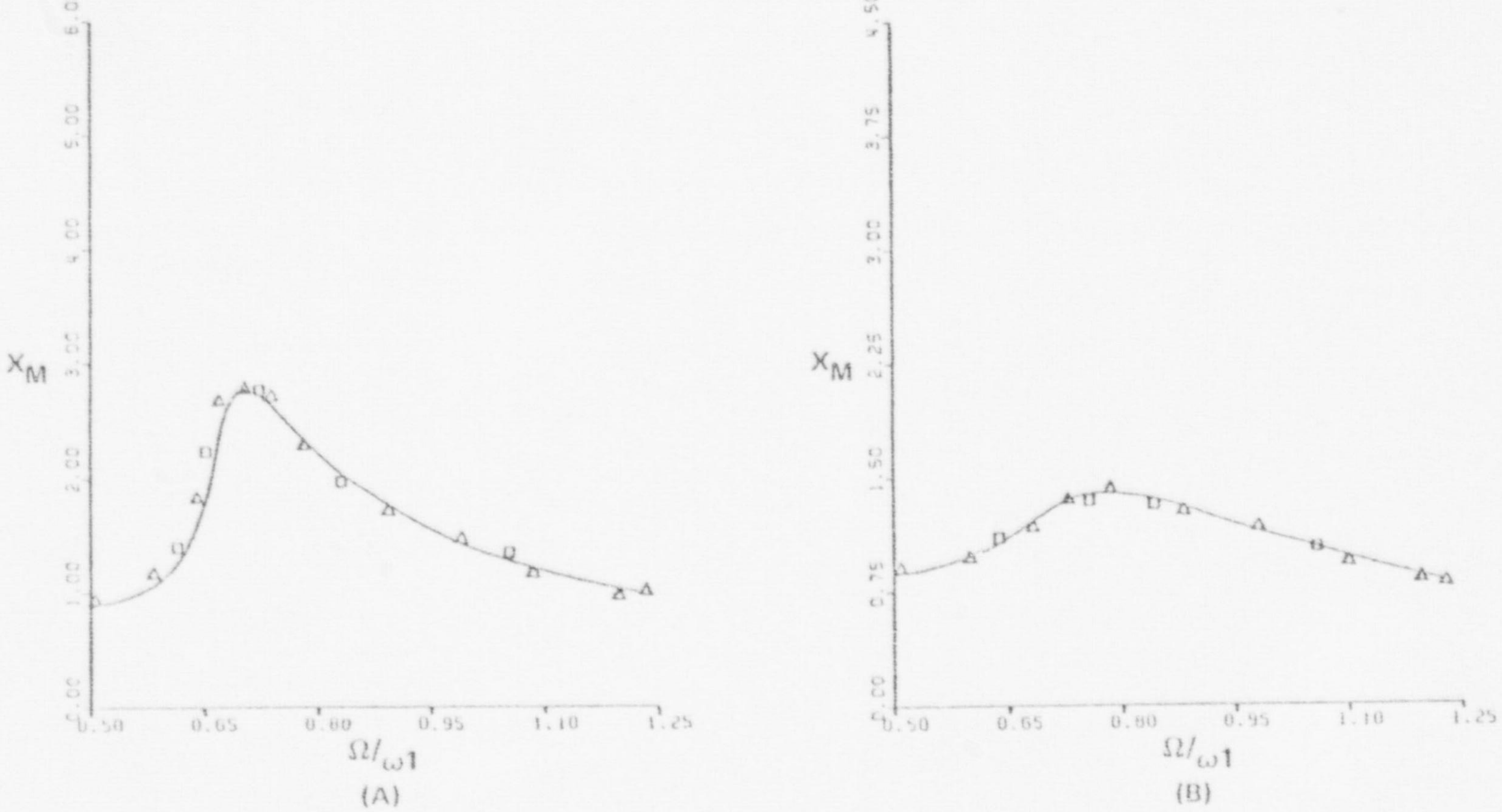

FIGURE 1.19 COMPARISON OF THEORETICAL AND EXPERIMENTAL DATA; $K2/_{K1} = 0.414$, $\zeta 2 = 0.0$, $F_o/_{P_Y} = 0.746$; (A) $\zeta 1 = 0.20$; (B) $\zeta 1 = 0.30$

DATA POINTS

—THEORY, MASRI (18)

△ EXPERIMENT (ID501)

□ EXPERIMENT (ID1000)

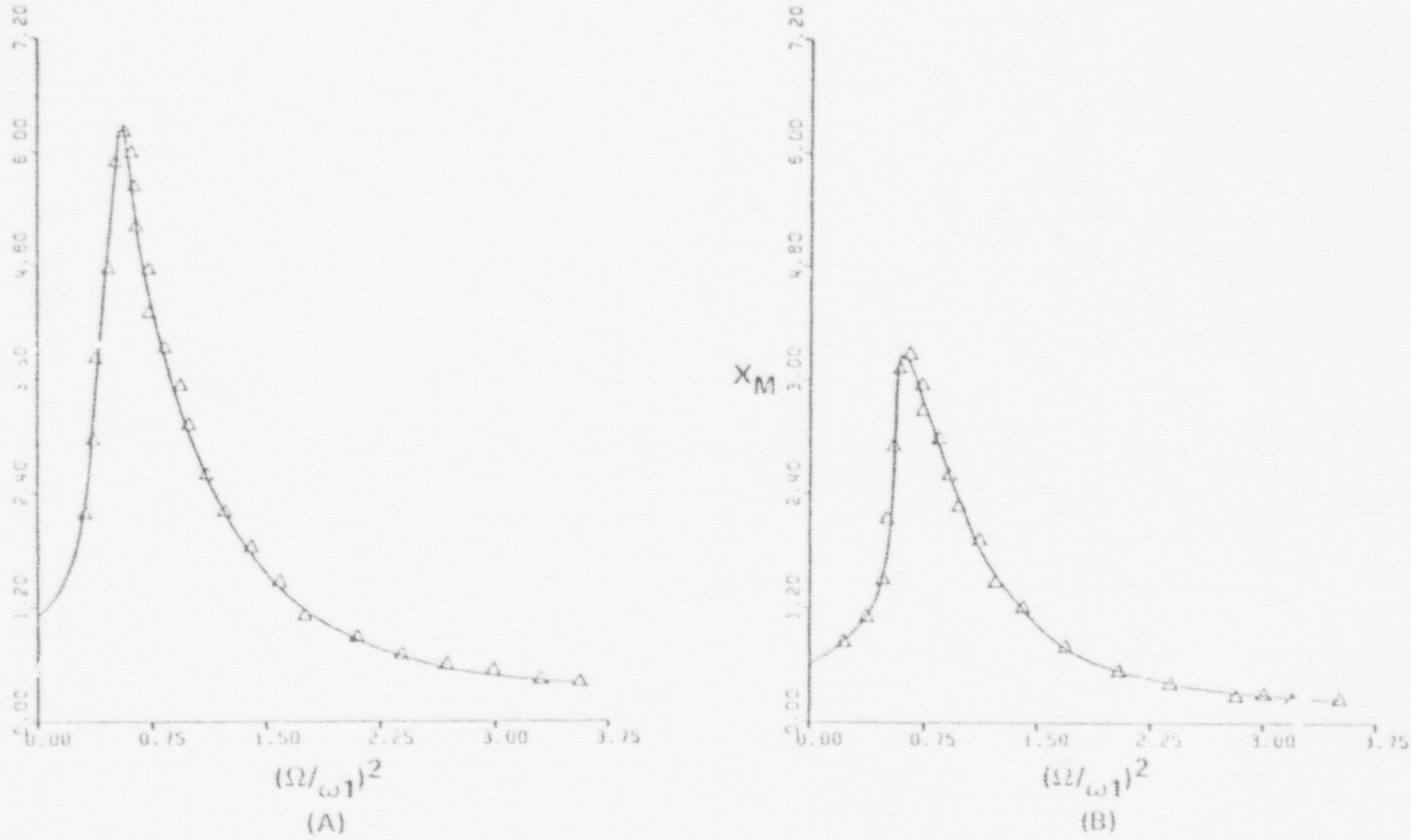

FIGURE 1.20 COMPARISON OF THEORETICAL AND EXPERIMENTAL DATA; $r = 3$, $\alpha = 0.10$; (A) $F_o/P_y = 1.0$; (B) $F_o/P_y = 0.6$

DATA POINTS

—THEORY, JENNINGS (8)

Δ EXPERIMENT (ID501)

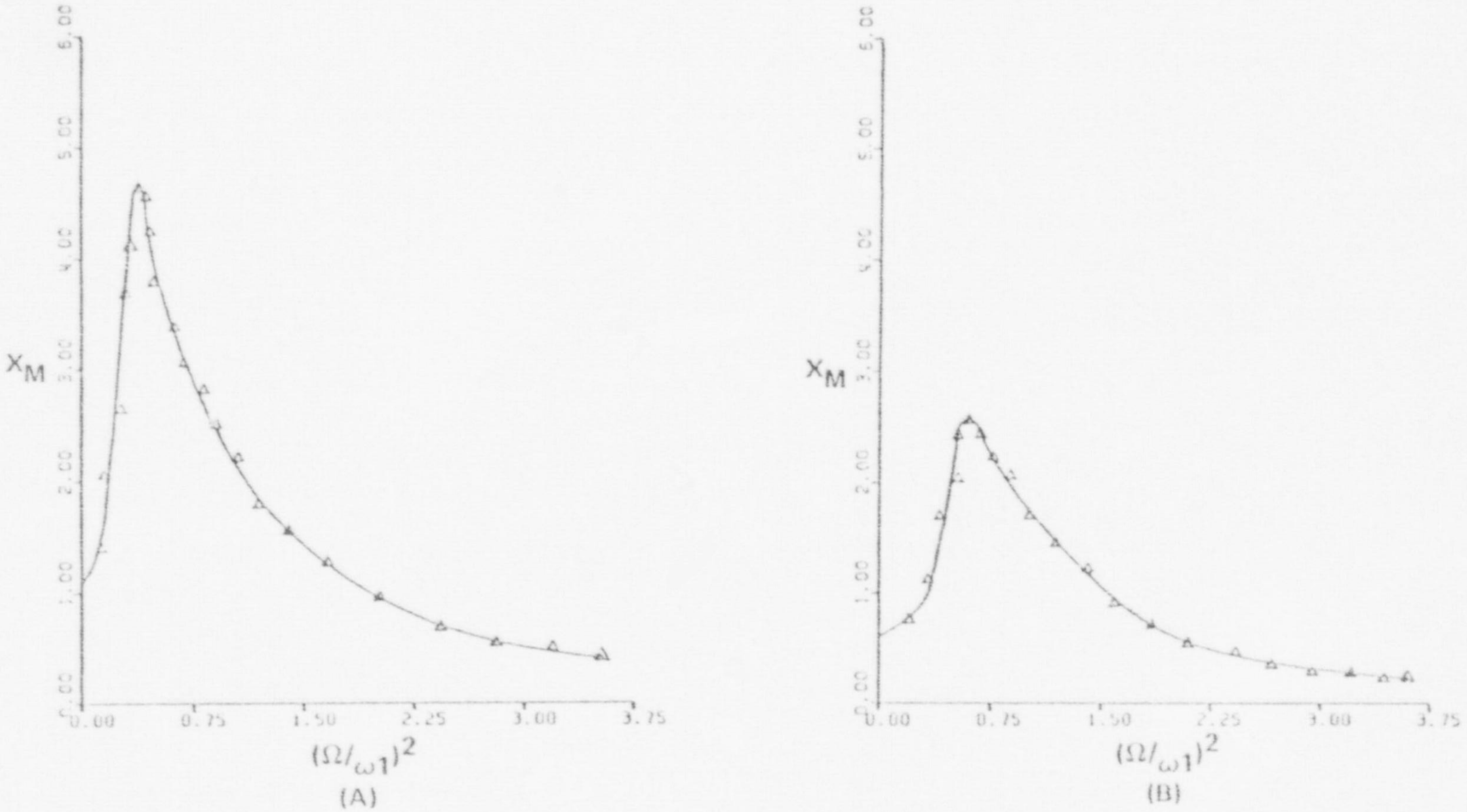

FIGURE 1.21 COMPARISON OF THEORETICAL AND EXPERIMENTAL DATA; $r = 7$, $\alpha = 0.10$; (A) $F_o/P_y = 1.0$; (B) $F_o/P_y = 0.6$

DATA POINTS
— THEORY, JENNINGS (8)
△ EXPERIMENT (ID501)

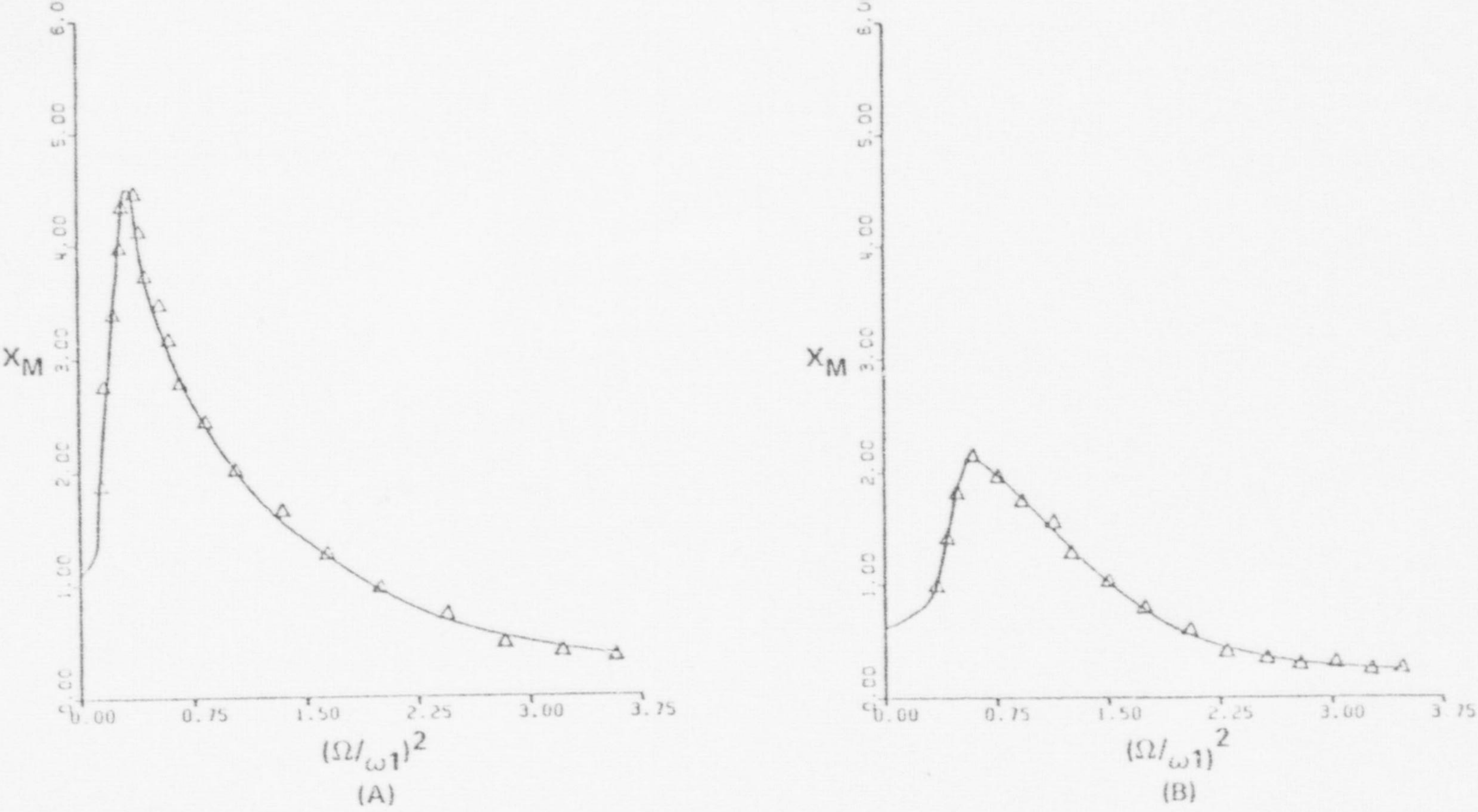

FIGURE 1.22 COMPARISON OF THEORETICAL AND EXPERIMENTAL DATA; $r = 11$, $\alpha = 0.10$; (A) $F_o/P_y = 1.0$; (B) $F_o/P_y = 0.6$

DATA POINTS

— THEORY, JENNINGS (8)

△ EXPERIMENT (ID501)

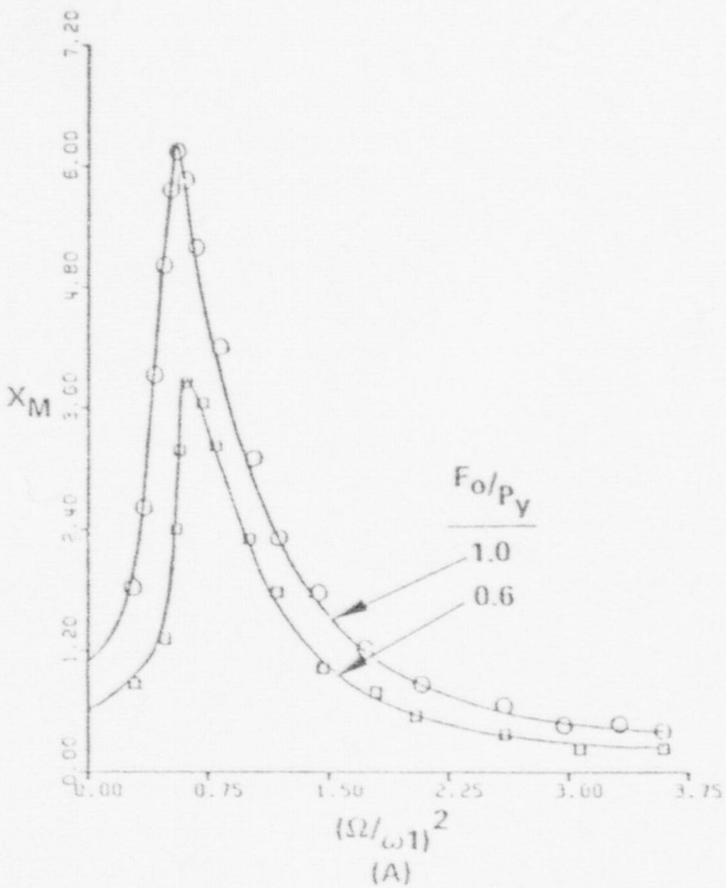

FIGURE 1.23 COMPARISON OF THEORETICAL AND EXPERIMENTAL DATA; α = 0.10; (A) r = 3; (B) r = 7

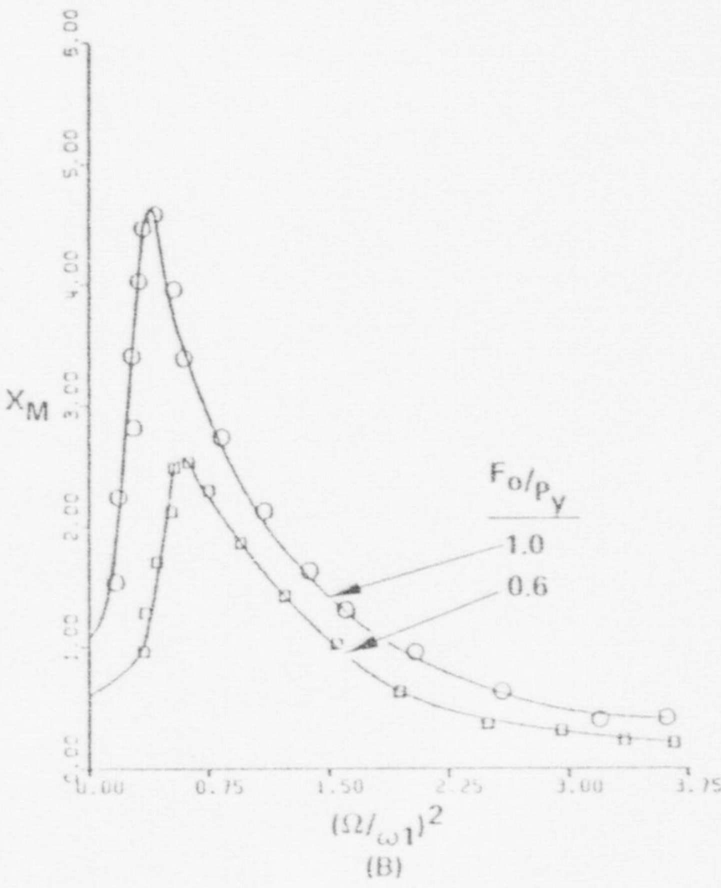

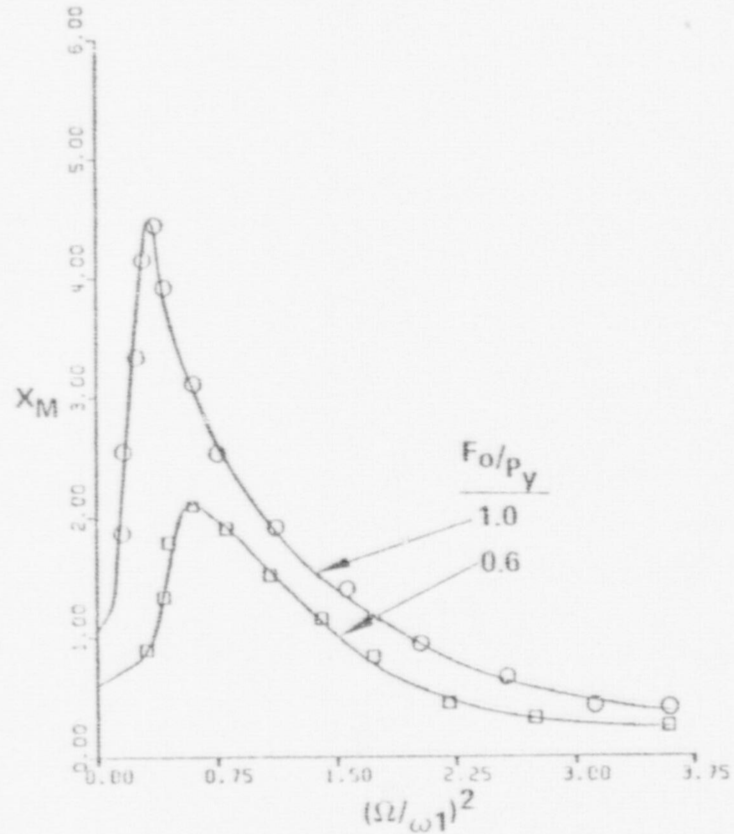

FIGURE 1.24 COMPARISON OF THEORETICAL AND EXPERIMENT DATA; $r = 11$, $\alpha = 0.10$

DATA POINTS

— THEORY, JENNINGS [8]

□ EXPERIMENT (ID1000) $F_o/P_y = 0.6$

○ EXPERIMENT (ID1000) $F_o/P_y = 1.0$

SEGMENT (i)	ξ_i	K_i/K_y	LHIST
1	0.0	8.403361D-02	0
2	0.0	1.408451D-01	0
3	0.0	2.127660D-01	0
4	0.0	3.053435D-01	0
5	0.0	3.712283D-01	0
6	0.0	4.244050D-01	0
7	0.0	4.862867D-01	0
8	0.0	5.575379D-01	0
9	0.0	6.374299D-01	0
10	0.0	7.240081D-01	0
11	0.0	8.510638D-01	1
12	0.0	9.756098D-01	1
13	0.0	8.510638D-01	1
14	0.0	7.240081D-01	0
15	0.0	6.374299D-01	0
16	0.0	5.575379D-01	0
17	0.0	4.862867D-01	0
18	0.0	4.244050D-01	0
19	0.0	3.712283D-01	0
20	0.0	3.053435D-01	0
21	0.0	2.127660D-01	0
22	0.0	1.408451D-01	0
23	0.0	8.403361D-02	0

NODE (i)	P_i/P_y	y_i/y_y
1	-7.0000000D 00	-4.1300000D 01
2	-5.0000000D 00	-1.7500000D 01
3	-4.0000000D 00	-1.0400000D 01
4	-3.0000000D 00	-5.7000000D 00
5	-2.5000000D 00	-4.0625000D 00
6	-2.2500000D 00	-3.3890600D 00
7	-2.0000000D 00	-2.8000000D 00
8	-1.7500000D 00	-2.2859000D 00
9	-1.5000000D 00	-1.8375000D 00
10	-1.2500000D 00	-1.4453000D 00
11	-1.0000000D 00	-1.1000000D 00
12	-5.0000000D-01	-5.1250000D-01
13	5.0000000D-01	5.1250000D-01
14	1.0000000D 00	1.1000000D 00
15	1.2500000D 00	1.4453000D 00
16	1.5000000D 00	1.8375000D 00
17	1.7500000D 00	2.2859000D 00
18	2.0000000D 00	2.8000000D 00
19	2.2500000D 00	3.3890600D 00
20	2.5000000D 00	4.0625000D 00
21	3.0000000D 00	5.7000000D 00
22	4.0000000D 00	1.0400000D 01
23	5.0000000D 00	1.7500000D 01
24	7.0000000D 00	4.1300000D 01

TABLE 1.1 COMPUTER APPROXIMATION FOR JENNINGS MODEL; $r = 3,\ \alpha = .10$

NOTE: LHIST IS A FLAG USED TO DEFINE THE DYNAMIC BEHAVIOR THE i-TH SEGMENT

0 = PLASTIC SEGMENT

1 = ELASTIC SEGMENT

SEGMENT (i)	ξ_i	K_i/K_y	LHIST
1	0.0	7.789861D-03	0
2	0.0	1.502223D-02	0
3	0.0	3.115847D-02	0
4	0.0	6.018054D-02	0
5	0.0	9.298001D-02	0
6	0.0	1.382315D-01	0
7	0.0	2.164915D-01	0
8	0.0	3.344661D-01	0
9	0.0	4.938759D-01	0
10	0.0	8.343067D-01	1
11	0.0	9.986020D-01	1
12	0.0	8.343067D-01	1
13	0.0	4.938759D-01	0
14	0.0	3.344661D-01	0
15	0.0	2.164915D-01	0
16	0.0	1.382315D-01	0
17	0.0	9.298001D-02	0
18	0.0	6.018054D-02	0
19	0.0	3.115847D-02	0
20	0.0	1.502223D-02	0
21	0.0	7.789861D-03	0

NODE (i)	P_i/P_y	Y_i/Y_y
1	-2.5000000D 00	-6.353500D 01
2	-2.2500000D 00	-3.144200D 01
3	-2.0000000D 00	-1.480000D 01
4	-1.7500000D 00	-6.776500D 00
5	-1.6000000D 00	-4.284000D 00
6	-1.5000000D 00	-3.208500D 00
7	-1.3750000D 00	-2.304220D 00
8	-1.2500000D 00	-1.726830D 00
9	-1.1250000D 00	-1.353100D 00
10	-1.0000000D 00	-1.100000D 00
11	-5.0000000D-01	-5.007000D-01
12	5.0000000D-01	5.007000D-01
13	1.0000000D 00	1.100000D 00
14	1.1250000D 00	1.353100D 00
15	1.2500000D 00	1.726830D 00
16	1.3750000D 00	2.304220D 00
17	1.5000000D 00	3.208500D 00
18	1.6000000D 00	4.284000D 00
19	1.7500000D 00	6.776500D 00
20	2.0000000D 00	1.480000D 01
21	2.2500000D 00	3.144200D 01
22	2.5000000D 00	6.353500D 01

TABLE 1.2 COMPUTER APPROXIMATION FOR JENNINGS MODEL;

$r = 7, \quad \alpha = .10$

NOTE: LHIST IS A FLAG USED TO DEFINE THE DYNAMIC BEHAVIOR OF THE i-TH SEGMENT

0 = PLASTIC SEGMENT
1 = ELASTIC SEGMENT

SEGMENT (i)	ζ_i	K_i/K_y	LHIST
1	0.0	6.452729D-03	0
2	0.0	2.292190D-02	0
3	0.0	5.477051D-02	0
4	0.0	1.353063D-01	0
5	0.0	3.202501D-01	0
6	0.0	8.333333D-01	1
7	0.0	1.000000D 00	1
8	0.0	8.333333D-01	1
9	0.0	3.202501D-01	0
10	0.0	1.353063D-01	0
11	0.0	5.477051D-02	0
12	0.0	2.292190D-02	0
13	0.0	6.452729D-03	0

NODE (i)	P_i/P_y	Y_i/Y_y
1	-1.750000D 00	-4.889300D 01
2	-1.500000D 00	-1.014970D 01
3	-1.375000D 00	-4.696400D 00
4	-1.250000D 00	-2.414150D 00
5	-1.125000D 00	-1.490320D 00
6	-1.000000D 00	-1.100000D 00
7	-5.000000D-01	-5.000000D-01
8	5.000000D-01	5.000000D-01
9	1.000000D 00	1.100000D 00
10	1.125000D 00	1.490320D 00
11	1.250000D 00	2.414150D 00
12	1.375000D 00	4.696400D 00
13	1.500000D 00	1.014970D 01
14	1.750000D 00	4.889300D 01

TABLE 1.3 COMPUTER APPROXIMATION FOR JENNINGS MODEL;

$r = 11,\ \alpha = .10$

NOTE: LHIST IS A USED TO DEFINE THE DYNAMIC BEHAVIOR OF THE i-TH SEGMENT

0 = PLASTIC SEGMENT
1 = ELASTIC SEGMENT

1.9 REFERENCES

1. Kumar, S., "Materials for Energy Absorption and Dissipation," AD450805, U.S. Army Research Office, 1964.

2. Vierck, R.K., *Vibration Analysis*, International Textbook, Scranton, Pennsylvania, 1969.

3. Thompson, W.T., *Vibration Theory and Application*, Prentice-Hall, New Jersey, 1965.

4. Den Hartog, J.P., *Mechanical Vibrations*, 4th ed., McGraw-Hill, New York, 1956.

5. Myklestad, N.O., *Fundamentals of Vibration Analysis*, McGraw-Hill, New York, 1956.

6. Lazan, B.J., *Damping of Materials and Members in Structural Mechanics*, Pergamon Press, New York, 1968.

7. Harris, C.M., and Crede, C.E., *Shock and Vibration Handbook*, vol. 1, McGraw-Hill, ew York, 1961, pp. 4.1-4.35.

8. Jennings, P.C., "Response of Simple Yielding Structures to Earthquake Excitation," Ph.D. thesis, California Institute of Technology, Pasadena, 1963.

9. Matveev, V.V., "Contributions to the Description of the Mechanical Hysteresis Loop," *Probl Prochn*, vol. 5, no. 8, 1973, pp. 3-9.

10. Wood, W.A., "Re-examination of Mechanical Hysteresis," Institute for the Study of Fatigue and Reliability, TR-42, Columbia University, New York, 1967.

11. Jhansale, H.R., "A New Parameter for the Hysteretic Stress-Strain Behavior of Metals," *Trans. ASME*, vol. 97, 1975, Series H, pp. 33-38.

12. Pisarenko, G.S., "Fluctuations in Mechanical Systems Due to the Imperfect Elasticity of Materials," FSTC-HT-23-515-72, U.S. Army Foreign Science and Technology Center, Charlottesville, Virginia, 1972.

13. Masing, G., "Eigenspannungen and Verfestigung beim Messing," *Proc. of the 2nd International Congress of Applied Mechanics*, Zurich, 1926, pp. 332-335.

14. Caughey, T.K., "Forced Oscillation of a Semi-Infinite Rod Exhibiting Weak Bilinear Hysteresis," *Journal of Applied Mechanics*, vol. 27, *Trans. ASME*, vol. 82, 1960, Series E. pp. 644-648.

15. Caughey, T.K. "Sinusoidal Excitation of a System with Bilinear Hysteresis," *Journal of Applied Mechanics*, vol. 27, *Trans. ASME*, vol. 82, 1960, Series E., pp. 640-643.

16. Iwan, W.D , "The Dynamic Response of Bilinear Hysteretic Systems," Ph.D. thesis, California Institute of Technology, Pasadena, 1961.

17. Iwan, W.D., "The Steady-State Response of a Two-Degree-of-Freedom Bilinear Hysteretic System," *Journal of Applied Mechanics*, vol. 32, *Trans. ASME*, vol. 87, 1965, Series E, pp. 151-156.

18. Masri, S.F., "Forced Vibration of the Damped Bilinear Hysteretic Oscillator," *Journal of the Acoustical Society of America*, vol. 57, 1975, pp. 107-112.

19. Hanson, R.D., "Post-Elastic Dynamic Response of Mild Steel Structures," Ph.D. thesis, California Institute of Technology, Pasadena, 1965.

20. Caughey, T.K. "The Existence and Stability of Ultraharmonics and Subharmonics in Forced Nonlinear Oscillations," Ph.D. thesis, California Institute of Technology, Pasadena, 1954.

21. Abramowitz, M. and Stegun, I.A., *Handbook of Mathematical Functions*, Dover Publications, New York, 1970.

CHAPTER 2

RANDOM EXCITATION OF A SINGLE-DEGREE-OF-FREEDOM BILINEAR HYSTERETIC OSCILLATOR

2.1 BACKGROUND INFORMATION

There have been in recent years numerous analytic investigations[(1-11)*] of the dynamic response of nonlinear systems (i.e., such as coolant-loop piping) that exhibit hysteretic characteristics to stationary random excitation. The bilinear hysteretic oscillator, in particular, has been investigated in detail because of its mathematical simplicity and because it approximates the behavior often displayed by many engineering systems. For an analytic investigation, the displacement response of a bilinear hysteretic system to nondeterministic (i.e., general nonstationary random) excitation is usually desired. However, a substantial knowledge about the general behavior of the system can be obtained by consideration of the stationary random excitation problem, even if it is extremely problematic that the actual excitation of the system model in a given situation approximates a stationary random signal. As mentioned in Chapter 1, the most popular method of solution for this problem class would be approximate methods, which have been investigated by several authors.[(12-22)]

2.2 INTRODUCTION

The system model is an SDOF oscillator as shown in Figure 2.1 with a "skeleton curve," which is defined as the static spring-restoring

---

*Numbers in parentheses designate references at the end of the chapter.

force versus deflection relationship, displayed in Figure 2.2. This model also has the flexibility that the critical damping ratio (ζ)* can assume a different value for the elastic or plastic segment. When subjected to a random excitation forcing function, this system has a hysteresis loop similar to that shown in Figure 2.3.

Iwan and Lutes,[2] Lutes and Shah,[3] and Caughey[1] have studied this system model in detail, using digital and analog computer simulations in conjunction with approximate analytical methods. These authors have observed that this system model under the influence of random excitation displays the following basic characteristics:

a. When σ_y/Y is very large, the system displacement response is quite similar to that of a linear system with natural frequency $\alpha^{1/2}\omega_1$ (Figure 2.4).

b. When σ_y/Y is very small, the system displacement response is quite similar to that of a linear system with natural frequency ω_1 (Figure 2.4).

c. The probability distribution function of the system response is strongly influenced by the level of the excitation and is, in general, noticeably non-Gaussian. Figure 2.5 shows that when compared to an equivalent linear Gaussian system, large σ_y/Y values have a greater probability, and small σ_y/Y values have a smaller probability, of being at large displacement values. This phenomenon is called "amplitude

---

*See List of Symbols, page xv.

limiting" and is associated with the abrupt initiation of hysteretic energy dissipation when the displacement response exceeds Y. However, when viscous damping of a sufficient magnitude is introduced into the system, this effect becomes less pronounced.

d. Yielding may either increase or decrease the system RMS displacement response. The softening spring effect of the nonlinearity always tends to increase displacement response, whereas the energy dissipation due to yielding tends to decrease the response. However, for large σ_y/Y values the softening effect dominates and the net result is an overall increase in system displacement.

e. The Krylov and Bogoliubov approximate method yields acceptable results for estimating the RMS (root-mean squared) response of a system with a small to moderate nonlinearity ($\alpha \geq 1/2$) and small finite viscous damping.

f. For small critical damping ratios (ζ), the system displays an RMS displacement that has definite minimum values for σ_y/Y between 1 and 2.

g The response of a severely nonlinear hysteretic oscillator is not contained in a narrow frequency band.

h. The primary effect of yielding on the system response PSD (Figure 2.4) is to cause a shift in peak frequencies with changing excitation level. In some cases, this shift is accompanied by a significant broadening of the response peak or even elimination of the peak entirely.

2.3 DESCRIPTION OF PROBLEM

The equation of motion for the system model displayed in Figure 2.1, which has a skeleton curve and hysteresis loop as shown in Figures 2.2 and 2.3 respectively, can be written for regions of constant restoring force (K_i) as

$$M\ddot{y} + C_i\dot{y} + P_i(y) = F(t) \qquad (2\text{-}1)$$

Let x be a normalized dimensionless parameter defined as follows:

$$x(t) = y(t)/Y \qquad (2.2)$$

$$\dot{x}(t) = \dot{y}(t)/Y \qquad (2.3)$$

$$\ddot{x}(t) = \ddot{y}(t)/Y \qquad (2.4)$$

As shown in Figure 2.3, the restoring-force function can be written for segment region 1 as

$$P_1(y) = K_1|Y| + K_2(|y_M| - |Y|) - K_1(|y_M| - y) \qquad (2.5)$$

$$= K_1y - K_1|y_M| + K_1|Y| + K_2|y_M| - K_2|Y| \qquad (2.6)$$

and for segment region 3 as

$$P_3(y) = K_1(|y_M| + y) - K_1|Y| - K_2(|y_M| - |Y|) \qquad (2.7)$$

$$= K_1y + K_1|y_M| - K_1|Y| - K_2|y_M| + K_2|Y| \qquad (2.8)$$

Notice that in segment region 1

$$\mathrm{sgn}(\dot{y}) = -1 \qquad (2.9)$$

and that in segment region 3

$$\operatorname{sgn}(\dot{y}) = +1 \tag{2.10}$$

Using Equations 2.9 and 2.10, Equations 2.8 and 2.6 can be combined into the following single relationship

$$P_1(y) = P_3(y) = K_1 y + K_1 \operatorname{sgn}(\dot{y}) \left(|y_M| - |Y|\right) - K_2\left[\operatorname{sgn}(\dot{y})\right]\left(|y_M| - |Y|\right) \tag{2.11}$$

Rewritten, this relationship becomes

$$P_1(y) = P_3(y) = P_Y\left\{\left(\frac{y}{Y}\right) + \left[\operatorname{sgn}(\dot{y})\right]\left(\left|\frac{y_M}{Y}\right| - 1\right)(1 - \alpha)\right\} \tag{2.12}$$

Likewise, the restoring-force function can be written for segment region 4 as

$$P_4(y) = K_1 Y + K_2(y - Y) \tag{2.13}$$

$$= K_2 y + (K_1 - K_2)Y \tag{2.14}$$

and for segment region 2 as

$$P_2(y) = -K_1 Y + K_2(y + Y) \tag{2.15}$$

$$= K_2 y - (K_1 - K_2)Y \tag{2.16}$$

Notice that in segment region 4

$$\operatorname{sgn}(\dot{y}) = +1 \tag{2.17}$$

and that in segment region 2

$$\mathrm{sgn}(\dot{y}) = -1 \tag{2.18}$$

Using Equations 2.17 and 2.18, Equations 2.14 and 2.16 can be combined into the following single relationship:

$$P_4(y) = P_2(y) = K_2 y + \left[\mathrm{sgn}(y)\right]\left(K_1 - K_2\right)Y \tag{2.19}$$

Rewritten, this relationship becomes

$$P_4(y) = P_2(y) = P_Y\left\{\alpha\left(\frac{y}{Y}\right) + \left[\mathrm{sgn}(\dot{y})\right]\left(1 - \alpha\right)\right\} \tag{2.20}$$

Additionally, for segment regions 1 and 3

$$C_1 = C_3 \tag{2.21}$$

$$\omega_1 = \omega_3 \tag{2.22}$$

and for segment regions 2 and 4

$$C_2 = C_4 \tag{2.23}$$

$$\omega_2 = \omega_4 \tag{2.24}$$

Rewriting Equation 2.1 in dimensionless form using Equations 2.2 through 2.4, one obtains

$$\ddot{x} + 2\zeta_i\omega_i\dot{x} + \omega_i^2\left\{x + \left[\mathrm{sgn}(\dot{x})\right] Q_i\right\} = f(t) \tag{2.25}$$

where

$$Q_i = D_i|x_M|(1 - \alpha) + E_i(1 - \alpha) \tag{2.26}$$

$$D_1 = D_3 = 1 \tag{2.27}$$

$$D_2 = D_4 = 0 \tag{2.28}$$

$$E_1 = E_3 = -1 \tag{2.29}$$

$$E_2 = E_4 = 1/\alpha \tag{2.30}$$

$$f(t) = F(t)/(MY) \tag{2.31}$$

The excitation $F(t)$ is a normally distributed, random function with a uniform PSD (power spectral density), which is discussed in Appendix A. The typical hysteresis loop for the system model when subjected to $F(t)$ is as displayed in Figure 2.3. It is important in the figure to notice the "trace-back" segment regions, IJ and CD, which are common for random excitation. The equation of motion, Equation 2.25, is valid for a random excitation hysteresis loop if CD is considered a segment region 1 with y_M defined by point C. Likewise, IJ is considered a segment region 1 with y_M defined by point I. For segment region 3, $-y_M$ is defined by point G; and in general, $-y_M$ does not equal $+y_M$.

A special case solution for this problem class is for harmonic excitation (i.e., the "trace-back" regions are absent):

$$f(t) = \frac{F_o}{MY}\sin(\omega t) \tag{2.32}$$

Masri[5] has shown that if during steady state harmonic motion the time origin is shifted so that (ωt) is equal to zero at the maximum displacement point $+y_M$, the excitation force is modified to the following form:

$$f(t) = \frac{F_o}{MY} \sin(\omega t + \alpha_o) \tag{2.33}$$

and the corresponding solution for Equations 2.25 and 2.33 for motion in the i-th segment region is

$$x(t) = \exp\left[-\left(\frac{\zeta_i}{r_i}\right)(\omega t - \phi_i)\right]\left[a_i \sin\left(\frac{\eta_i}{r_i}\right)(\omega t - \phi_i) + b_i \cos\left(\frac{\eta_i}{r_i}\right)(\omega t - \phi_i)\right] + A_i \sin(\omega t - \tau_i) + Q_i \tag{2.34}$$

$$\dot{x}(t) = \omega_i \exp\left[-\left(\frac{\zeta_i}{r_i}\right)(\omega t - \phi_i)\right]\left[-(\zeta_i a_i + \eta_i b_i) \sin\left(\frac{\eta_i}{r_i}\right)(\omega t - \phi_i) + (\eta_i a_i - \zeta_i b_i) \cos\left(\frac{\eta_i}{r_i}\right)(\omega t - \phi_i)\right] + \omega A_i \cos(\omega t + \tau_i) \tag{2.35}$$

where the constants are all defined in Reference 5. Masri[5] has also shown that for steady-state harmonic motion, $\phi_1 \equiv 0$ and $\phi_3 \equiv \pi$ and the single transcendental equation*

$$\beta_1 + \beta_2^{1/2} \beta_3 + \beta_4 = 0 \tag{2.36}$$

---

*β_1, β_2, β_3, and β_4 are functions of ϕ_2.

can be solved by iteration for the unknown ϕ_2, which leads to the complete determination of the unknowns of the system motion.

2.4 SCOPE OF RESEARCH

This chapter derives two separate analytic solutions for the displacement response of an SDOF damped bilinear hysteretic oscillator subjected to a stationary, normally distributed, random forcing function. The first of these solution methods generates response data by idealizing the system model as being piecewise linear, and uses standard numerical integration techniques (i.e., Runge-Kutta method) of the system equations of motion, while the other solution method is a hypothesized approximate analytical technique.

The bilinear hysteretic spring stiffness studied in this chapter is of the softening type defined by Masing's Hypothesis, which is detailed in Chapter 1. The random excitation function is generated by computer software and calibrated by the methods presented in Appendix A. To determine the accuracy as well as the inherent limitations of these analytic solutions, two computer methodologies obtained by using algorithms derived for both solution methods are evaluated by comparing their generated numerical data with data published by Iwan and Lutes,(2) Lutes and Shah,(3) and Caughey.(1)

This study was conducted under the following assumptions:

o. The random forcing function, which has a fixed spectral density, will yield a unique displacement response value (i.e., σ_x). This assumption has been verified by several authors(2,4) for similar system models.

b. The natural frequency of the SDOF system in its linear range (i.e., ω_1) is substantially smaller than the cutoff frequency of the generated random excitation to ensure the validity of the approximation of random "white noise" excitation. This assumption is discussed in detail in Appendix A.

c. Experimental RMS data results presented in this chapter are the statistical ensemble average ($N = 24$) of generated data, per the discussion in Appendix B.

2.5 SOLUTION OF THE PROBLEM

The response of the bilinear hysteretic system to random excitation has been shown in Section 2.4 to be represented by Equation 2.25. Basically, there are three classical methods for obtaining the solution of this system equation.

2.5.1 Digital or Analog Computer Simulations

Analog computer simulations have been presented by several authors[1,2,4] for obtaining the system response to harmonic excitation. Additionally, Lutes and Shah[3] have used a digital computer for the simulation of the system model to random excitation. However, little published information is generally available about computer simulation techniques and applications.

2.5.2 Equivalent Linearization Techniques

Equivalent linearization techniques have been studied in detail by several authors.(17-18) The most common method is the Krylov-Bogoliubov technique. In this method, two parameters, ω_{eq} and ζ_{eq}, are chosen to establish an equivalent linear system that minimizes the mean square difference between the following equations:

$$\ddot{x} + 2\zeta\omega\dot{x} + \omega^2\psi(x) = f(t) \tag{2.37}$$

$$\ddot{x} + 2\zeta_{eq}\omega_{eq}\dot{x} + \omega_{eq}^2 x = f(t) \tag{2.38}$$

Equation 2.37 is a normalized extension of Equation 2.1, with the damping coefficient C_i equal to a constant C and $\psi(x)$ representing the hysteresis spring stiffness restoring-force function. Caughey[1] has shown under the assumption of a narrow-band displacement response with a Rayleigh distribution that the following relationships apply:

$$\left(\frac{\omega_{eq}}{\omega}\right)^2 = 1 - \left[\frac{8(1-\alpha)}{\pi}\right] \int_1^{\infty} \left(z^{-3} + \lambda^{-1} z^{-1}\right)(z-1)^{1/2} \exp(-z^2/\lambda) \tag{2.39}$$

$$\zeta_{eq} = \zeta\left(\frac{\omega}{\omega_{eq}}\right) + \left(\frac{\omega}{\omega_{eq}}\right)^2 (1-\alpha)(\pi\lambda)^{-1/2} \operatorname{erfc}(\lambda^{-1/2}) \tag{2.40}$$

where

$$\lambda = 2\sigma_x^2 \tag{2.41}$$

Evaluating Equations 2.39 through 2.41 numerically, one is able to determine ω_{eq} and ζ_{eq} and thus define the "equivalent" RMS response of the system. The basic difficulties encountered using this method are that the displacement response normally is not narrow-banded nor does it have a Rayleigh distribution. Lutes[14] has proposed a modification to this method that takes into account the experimentally observed statistics of the system response. However, a detailed evaluation and error analysis of the hypothetical Lutes[14] modification has not been presented in published literature.

2.5.3 Power Balance Method

Karnopp[19-22] originally proposed this technique, which is an attempt to equate the average power, P_I, supplied to the system by the environment

$$P_I = E\left[f(t) \cdot \dot{x}(t)\right] = \frac{\pi S_o}{M} \tag{2.42}$$

with the power dissipated, P_D, by the system hysteretic effects. The basic underlying assumption of this method is that the system viscous damping (ζ) must be small ($\approx$ 1%) so that the effect of hysteresis energy dissipation is dominant. Karnopp[22] has also shown that this method has a great deal of promise for extension to multidegree-of-freedom hysteretic systems. The analytic procedure for this method consists of selecting a statistical characterization for $x(t)$, computing the average power dissipated P_D, and using Equation 2.42 to relate $x(t)$ to the input forcing level S_o. This is basically a theoretical approximation, and there are few published data to verify its accuracy. However, Takemiya and Lutes[31] recently showed that for the two basic equations of the Krylov and Bogoliubov equivalent linearization technique, Equations 2.37 and 2.38, one is identical to this power-balance method and the other can be expressed as a simple energy identity. Takemiya and Lutes[31] also showed that the accuracy of the power-balance method is dependent on how well one can equate input versus dissipated power and the validity of the approximation for the assumed response statistics.

2.6 COMPUTER SOLUTION

Included in this section is a brief description of the two digital computer logics (ID117E and ID91E) created to obtain numerical data for the analytic solutions of the system model proposed in this chapter and shown in Figures 2.1 through 2.3.

2.6.1 Computer Logic (ID91E)

The basic underlying concept of this approximate (i.e., theoretical) solution, is that it is reasonable to assume to a first order approximation that the displacement spectral density $S_x(\omega)$ of the system can be approximated by

$$S_x(\omega) = |H_d(\omega)|^2 S_f(\omega) \tag{2.43}$$

where $S_f(\omega)$ is the excitation PSD and $|H_d(\omega)|$ is the amplitude of the frequency response function of the system when subjected to a harmonic excitation function of frequency ω. This approximation is particularly valid for narrow-band processes; and, as shown in Figure 2.4, the PSD response of a bilinear hysteretic system displays a narrow-band response when (α = 1/2), but an extremely wide-band response when (α = 1/21).

The amplification factor (i.e., transfer function) $|H_d(\omega)|$ is given by

$$|H_d(\omega)| = \frac{x_{max}}{(F_o/K_1)} \tag{2.44}$$

where x_{max} is the maximum displacement from Equation 3.34 corresponding to an acceptable ϕ_2 solution of Equation 2.36.* If both ϕ_2 solutions (i.e., SOL[1] and SOL[2]) are acceptable, then

$$x_{max} = \frac{SOL(1) + SOL(2)}{2} \tag{2.45}$$

Additionally, the computer logic equates

$$x_{max} = 0 \tag{2.46}$$

if both ϕ_2 solutions are unacceptable; but prior to integration, all zero values of the transfer function are interpolated to correspond with adjacent neighboring values and thus to create a smooth transfer

---

*It should be noted that an acceptable solution of ϕ_2 must be between the limits, $0 < \phi_2 < \pi$.

function without discontinuities. The magnitude of the harmonic force F_o used to determine the transfer function is obtained from the random excitation level by the relation

$$S_o = \frac{F_o^2}{2} \tag{2.47}$$

Using $|H_d(\omega)|$ determined from Equation 2.44, the RMS displacement response σ_x is given by

$$\sigma_x^2 \equiv E[x^2] = S_o \int_{\omega=0}^{+\infty} |H_d(\omega)|^2 \, d\omega \tag{2.48}$$

where S_o is the uniform spectral density of $F(t)/(MY)$. The final theoretical response value is obtained by the numerical integration of Equation 2.48 by Simpson's rule.

2.6.2 Computer Logic ID117E

The "experimental" displacement response of the system model to random excitation was determined through the use of a digital computer methodology using Runge-Kutta techniques for the numerical integration of the governing equation of motion, Equation 3.25.

2.7 CONCLUSIONS

Two digital computer methodologies (i.e., ID117E and ID91E) have been presented for determining the dynamic response of a viscously damped bilinear hysteretic oscillator subjected to stationary, Gaussian random excitation. The basic limitations observed for these proposed computer logics are:

a. The system hysteresis loop must be a softening type defined by Masing's Hypothesis. However, similar to the program versions discussed in Chapter 1, these computer logics can be modified to predict the displacement response of a system with a hardening type of spring stiffness if the hysteresis loop geometry is defined.

b. The accuracy of computer method ID91E is comparable to the presently popular Krylov and Bogoliubov approximate method.

The approximate analytical solution (ID91E), which obtains theoretical response values by using a transfer function derived from a discrete harmonic excitation function, is shown in Figures 2.6 and 2.7 to be in good agreement with published data for (α = 1/2). However, Figures 2.8 through 2.10 show that for (α = 1/21), this method is no more accurate than the Krylov and Bogoliubov approximate method in estimating the response values published by Iwan and Lutes.[2] Since accurate overall estimates of displacement response are obtained only for (α = 1/2), it appears by inspection that the inability to obtain reasonable displacement response estimates for small α values is due primarily to observed wide-band PSD responses (Figure 2.4) rather than the effect of non-Gaussian (i.e., "amplitude limiting") displacement characteristics (Figure 2.5). For example, Figures 2.8 through 2.10 clearly show that for midrange values of σ_y/Y ($0.5 \leq \sigma_y/Y \leq 30$), which correspond in Figure 2.4(A) to wide-band PSD responses, the approximate method tends to yield less accurate response estimates.

This inaccuracy of the approximate method (ID91E) is not totally unexpected, since it is impossible for a discrete harmonic excitation function to generate a transfer function that approximates the actual frequency response relationships of a system with wide-band characteristics. It was originally anticipated that the ID91E approximate method would be more accurate than the Krylov and Bogoliubov approximate method, but this investigation clearly shows that there is no appreciable difference in the accuracy of either method.

The "experimental" solution (ID117E), which obtains displacement response by numerical integration of the system model equation of motion, is shown in Figures 2.11 through 2.15 to be in good agreement both qualitatively and quantitatively with published data for the parameter ranges displayed. It is important to remember that (α = 1/2) represents a moderate bilinear hysteretic system and (α = 1/21) closely approximates the elastoplastic problem. Figures 2.11 through 2.16 validate the accuracy of this proposed digital methodology. They also demonstrate that as the system damping ratio (ζ) is increased, the effect of hysteresis is decreased.

2.8 ILLUSTRATIONS

Included in this section are all the figures associated with Chapter 2. They appear in the order in which they are referenced in the text. The following special notes apply to Chater 2 figures and tables:

a. All parameters used in the figures are defined in the List of Symbols, page

b. The Iwan and Lutes[2] data presented in Figures 2.6 through 2.15 are identical to the system displacement response data published by Lutes and Shah[3] and Caughey.[1]

c. The Krylov and Bogoliubov data obtained from Iwan and Lutes[2] and displayed in Figures 2.6 through 2.15 are representative of displacement response estimates obtained with this approximate method.

d. The ID117E ("experimental") data displayed in Figures 2.11 through 2.16 are, per the discussion in Appendix B, the statistical ensemble average of (N = 24) data samples.

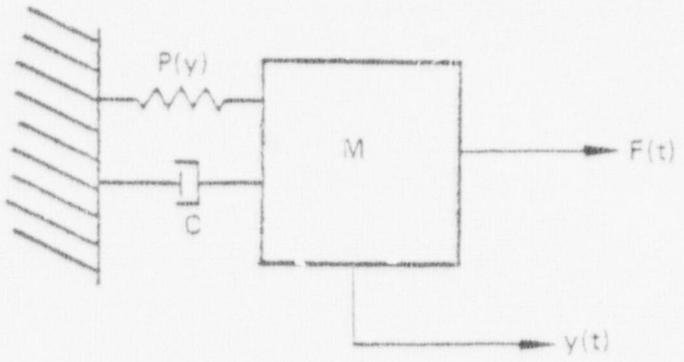

FIGURE 2.1 SYSTEM MODEL

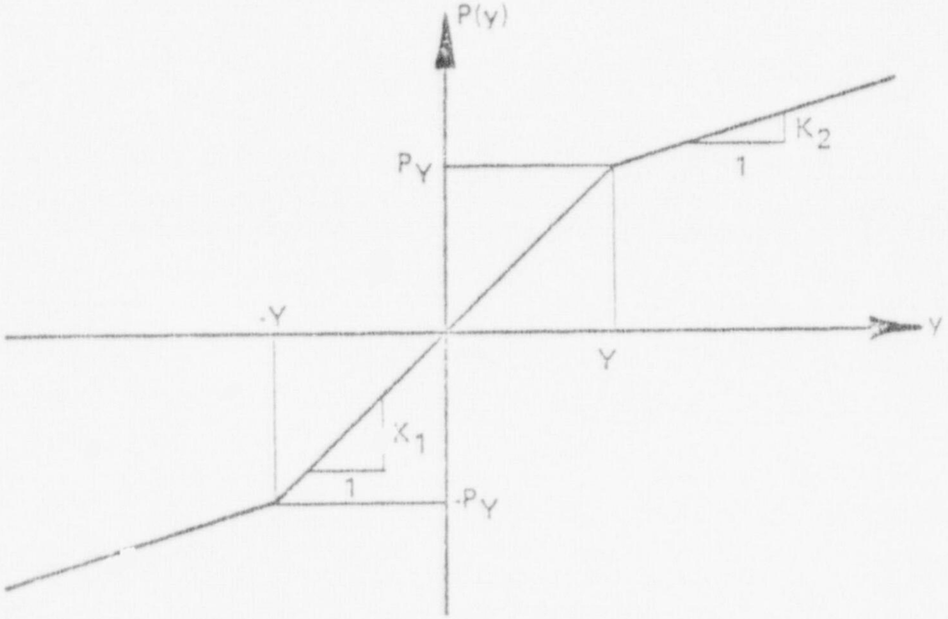

FIGURE 2.2

RESTORING FORCE VERSUS DEFLECTION RELATIONSHIP FOR BILINEAR SPRING

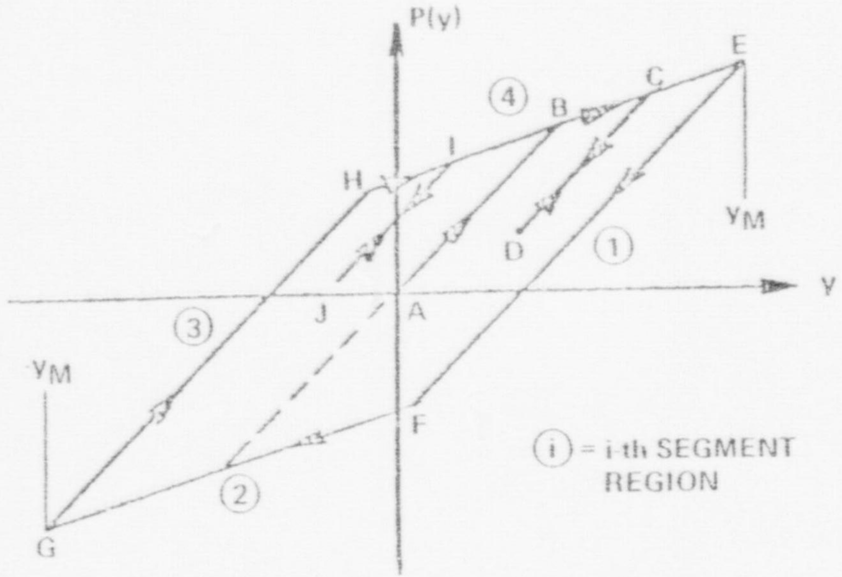

FIGURE 2.3
HYSTERESIS LOOP FOR RANDOM EXCITATION

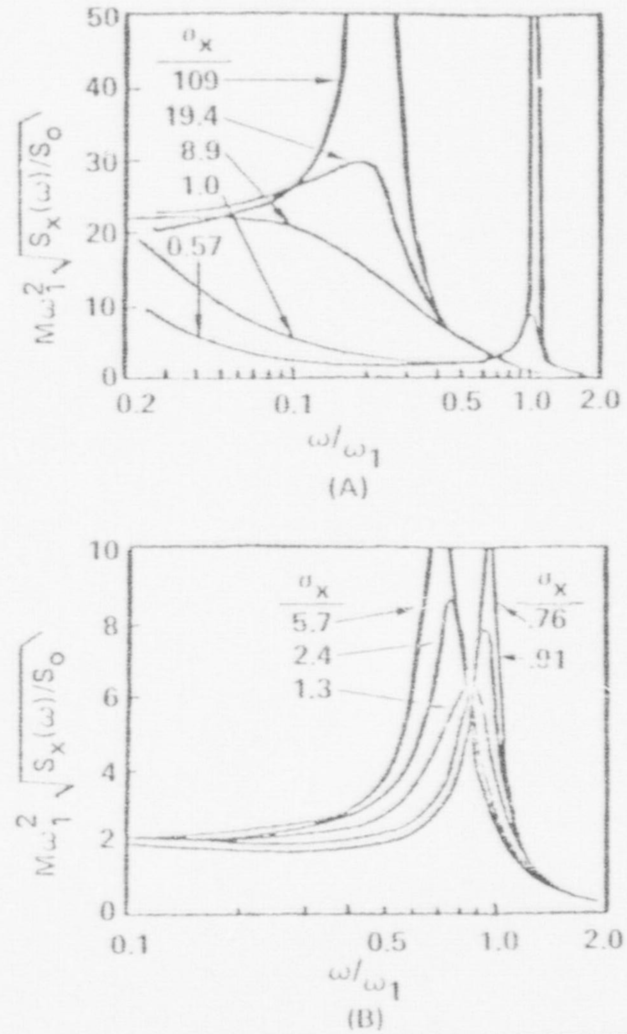

FIGURE 2.4 TYPICAL PSD RESPONSE FOR BILINEAR HYSTERETIC SYSTEM; (A) $\zeta_1 = \zeta_2 = 0.0$, $a = 1/21$, (B) $\zeta_1 = \zeta_2 = 0.0$, $a = 1/2$

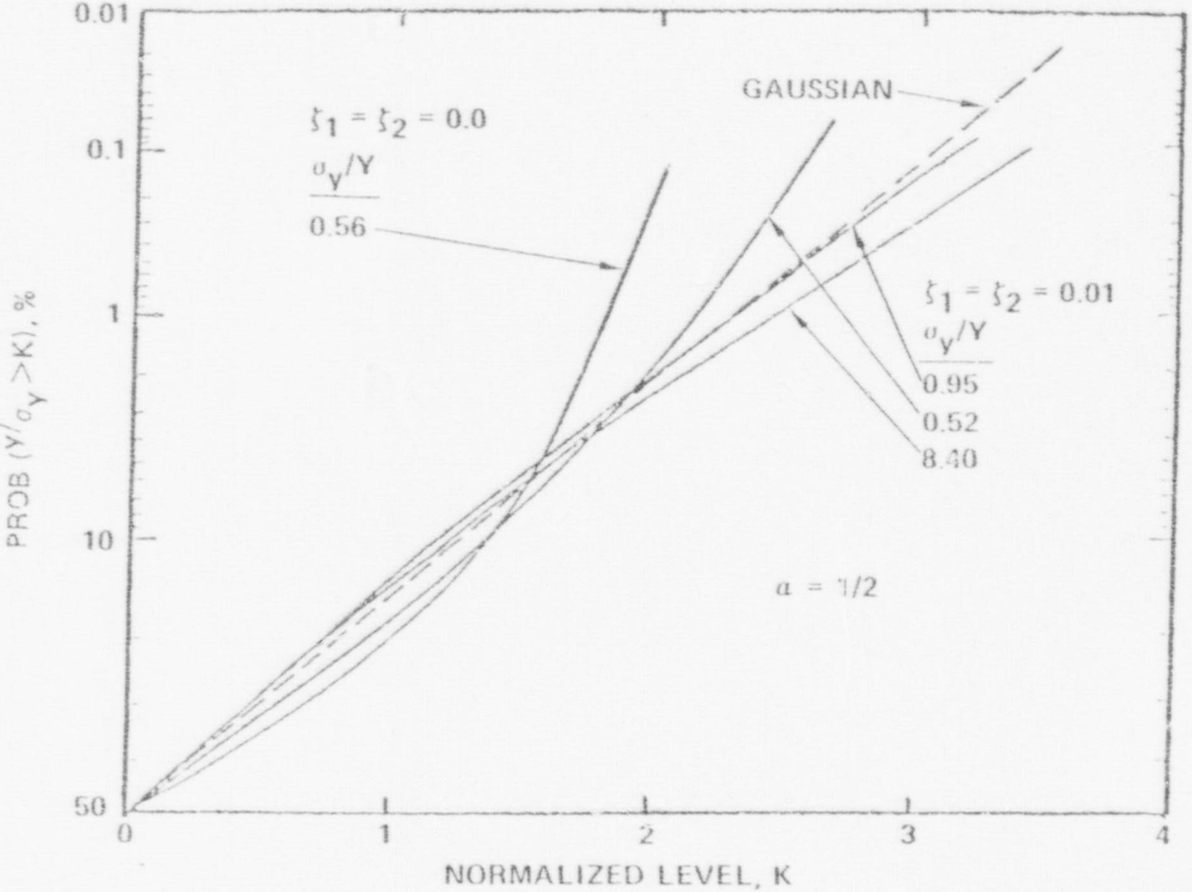

FIGURE 2.5 RESPONSE PROBABILITY FOR BILINEAR HYSTERETIC SYSTEM

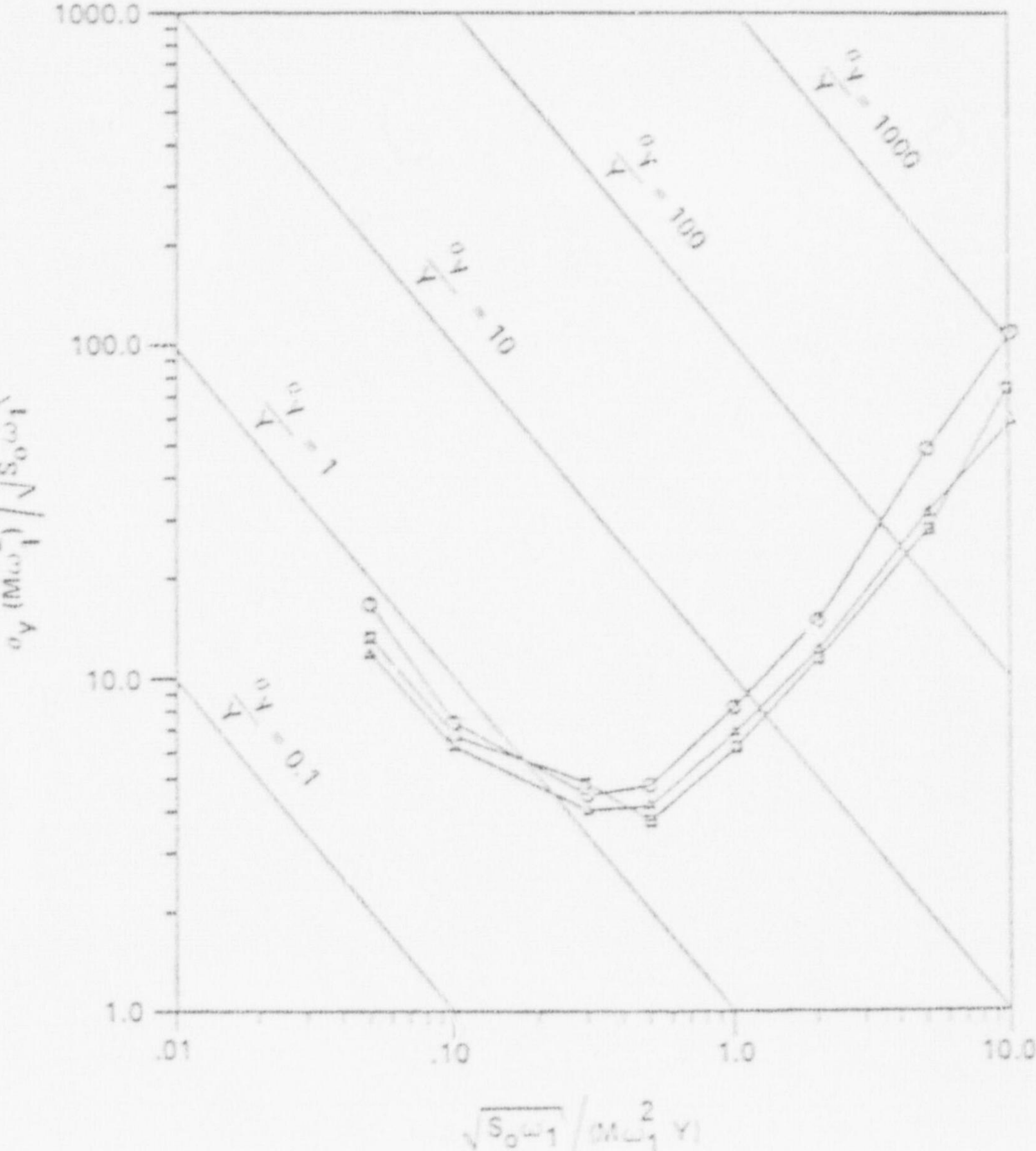

FIGURE 2.6 COMPARISON OF DATA; α = 1/2, ζ_1 = 0.0, ζ_2 = 0.0

<u>DATA POINTS</u>

○ THEORY (IWAN AND LUTES[2])

△ THEORY (KRYLOV AND BOGOLIUBOV[2])

□ THEORY (ID91E)

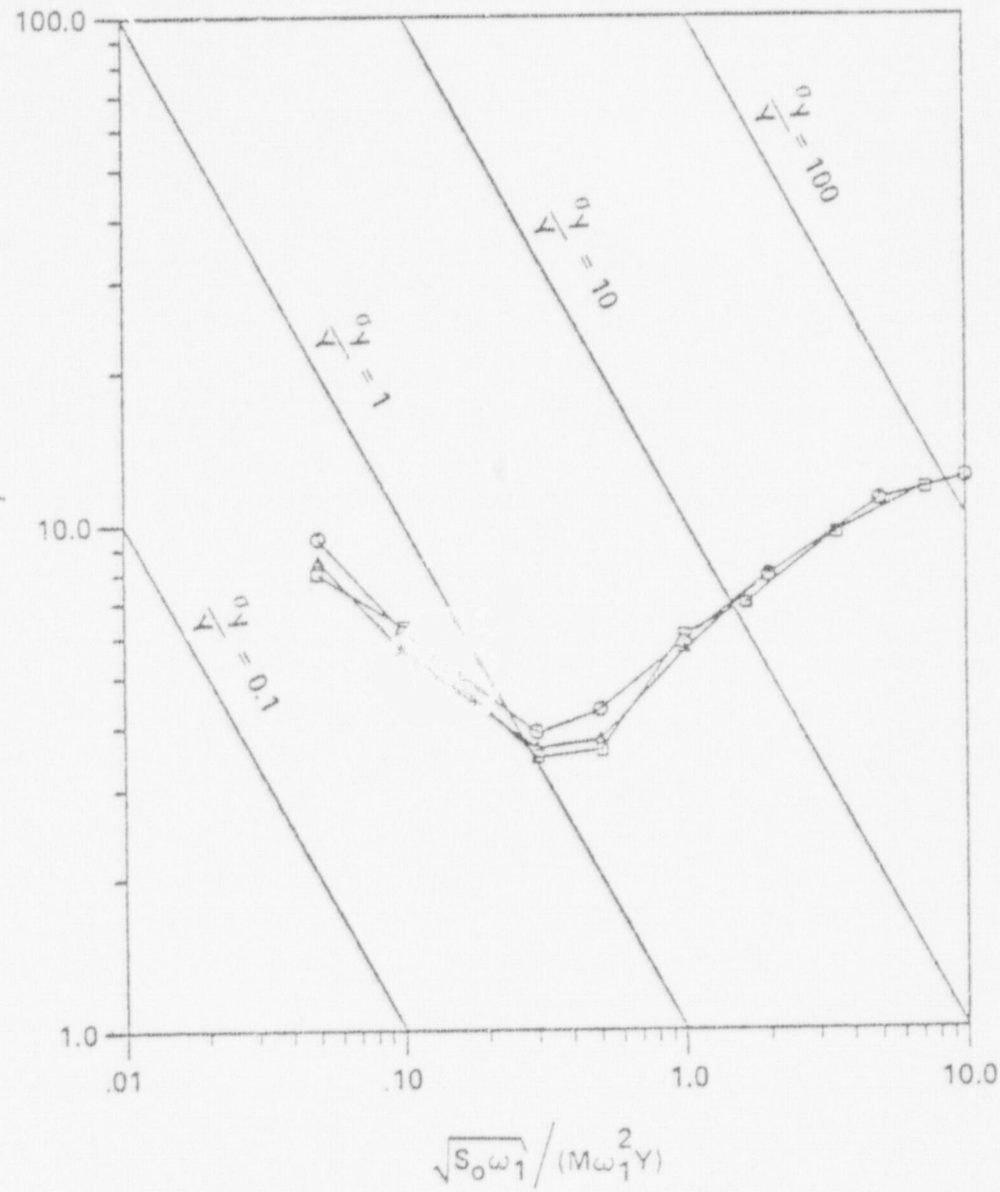

FIGURE 2.7 COMPARISON OF DATA; $a = 1/2$, $\zeta_1 = 0.01$, $\zeta_2 = 0.014$

DATA POINTS
○ THEORY (IWAN AND LUTES[(2)])
△ THEORY (KRYLOV AND BOGOLIUBOV[(2)])
□ THEORY (ID91E)

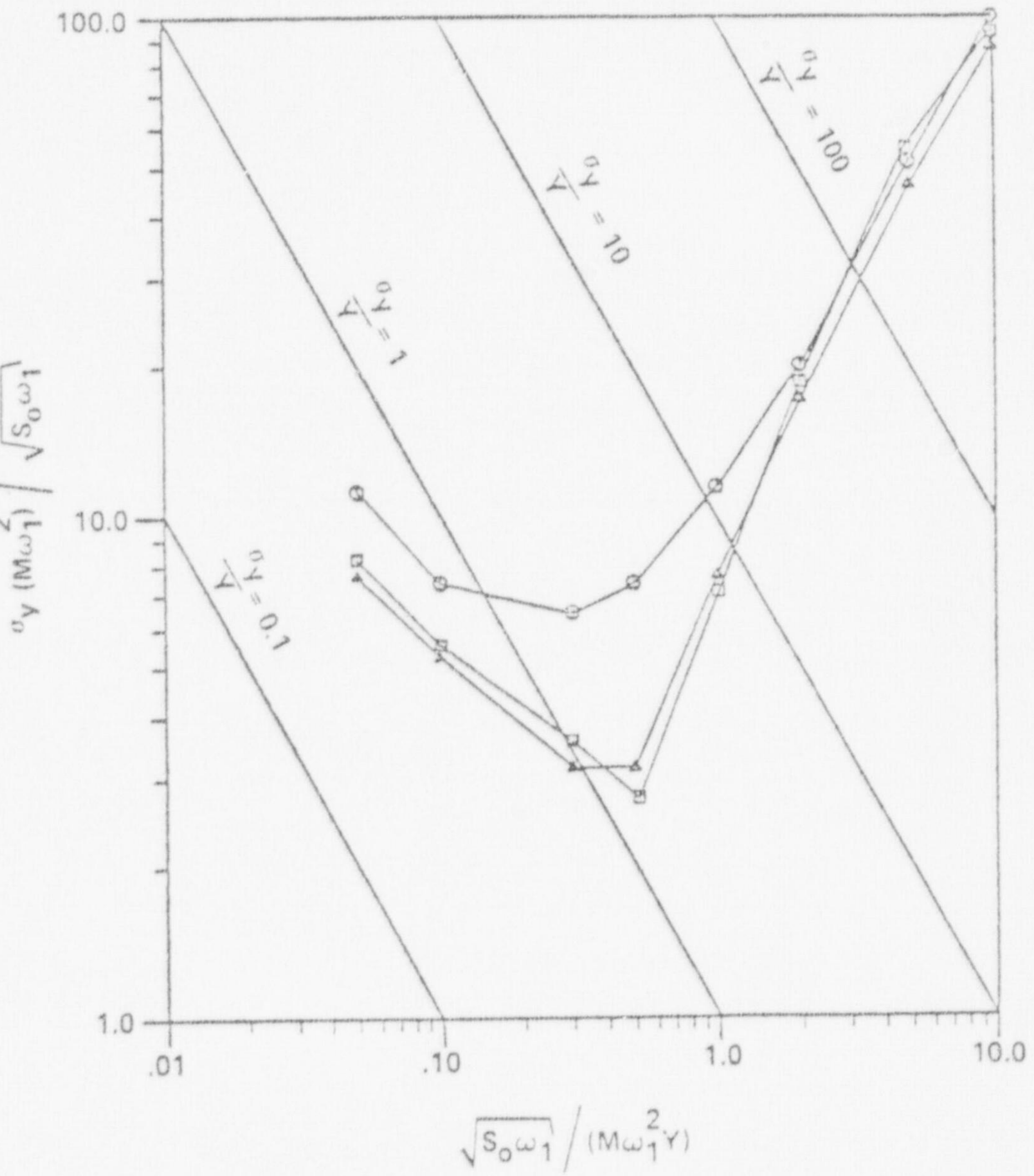

FIGURE 2.8 COMPARISON OF DATA; $\alpha = 1/21$, $\zeta_1 = 0.0$, $\zeta_2 = 0.0$

DATA POINTS

○ THEORY (IWAN AND LUTES[2])

△ THEORY (KRYLOV AND BOGOLIUBOV[2])

□ THEORY (ID91E)

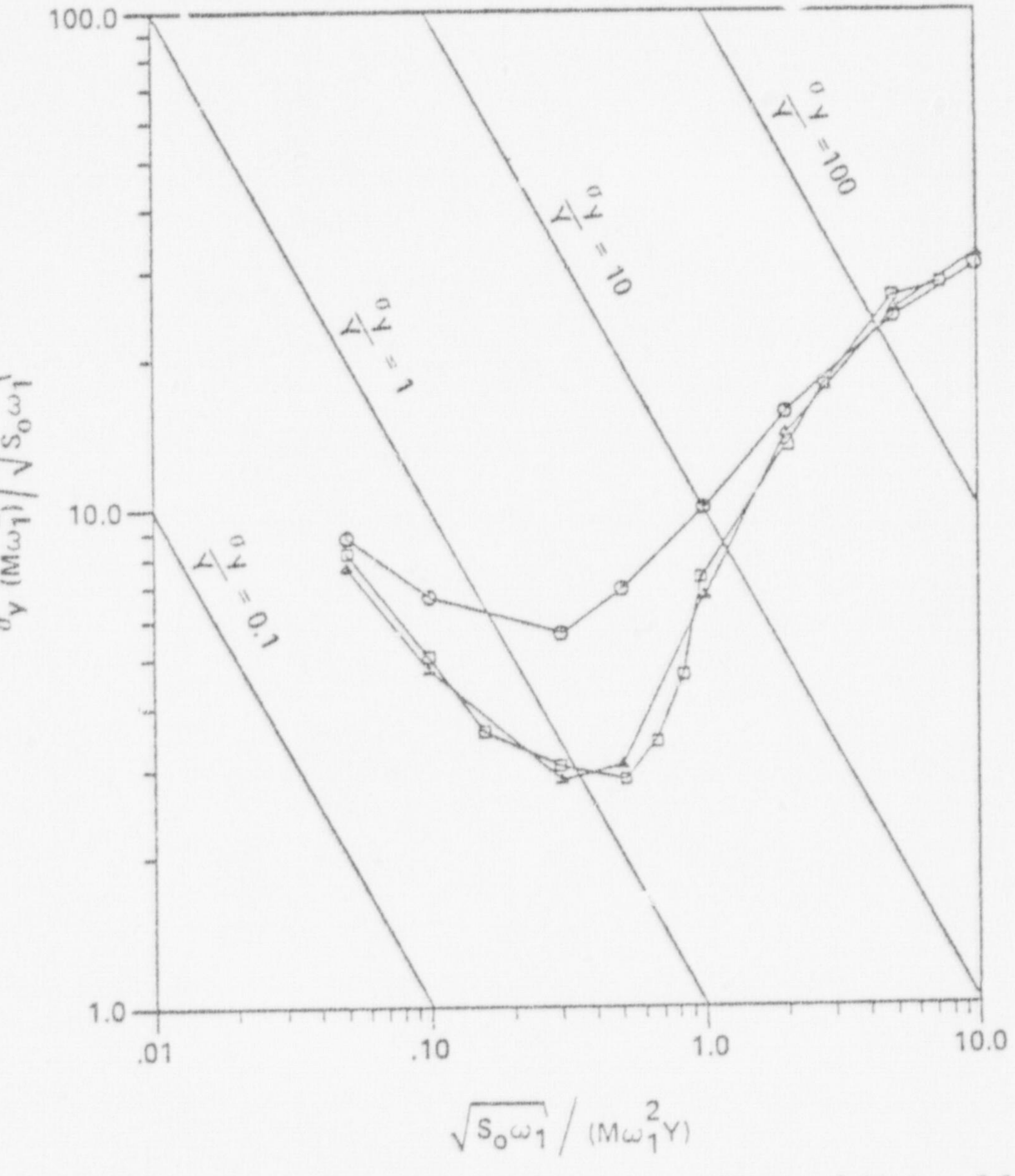

FIGURE 2.9 COMPARISON OF DATA; α = 1/21, ζ_1 = 0.01, ζ_2 = 0.046

DATA POINTS

○ THEORY (IWAN AND LUTES[(2)])

△ THEORY (KRYLOV AND BOGOLIUBOV[(2)])

□ THEORY (ID91E)

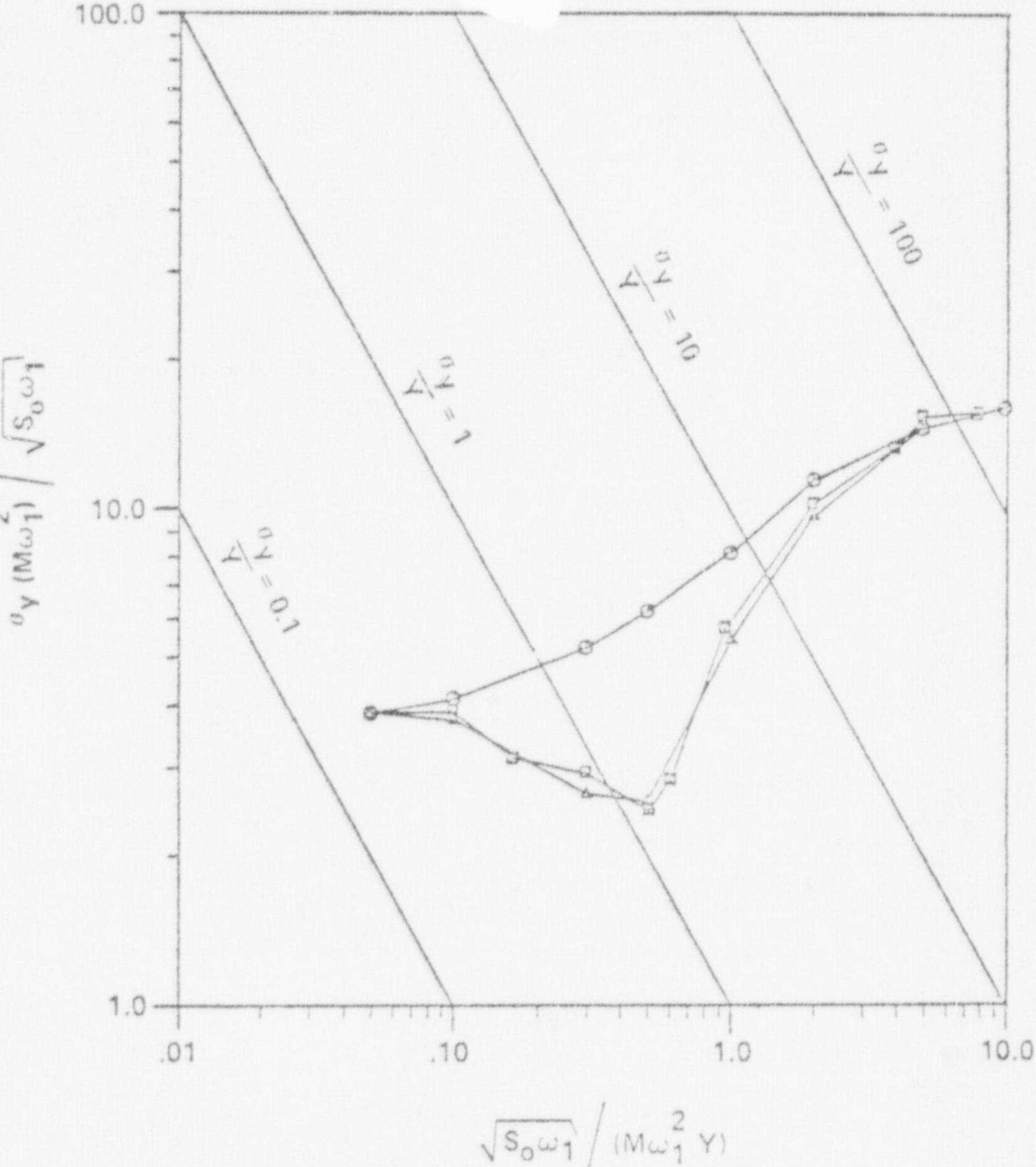

FIGURE 2.10 COMPARISON OF DATA; a = 1/21, ζ_1 = 0.05, ζ_2 = 0.23

DATA POINTS

○ THEORY (IWAN AND LUTES[2])

△ THEORY (KRYLOV AND BOGOLIUBOV[2])

□ THEORY (ID91E)

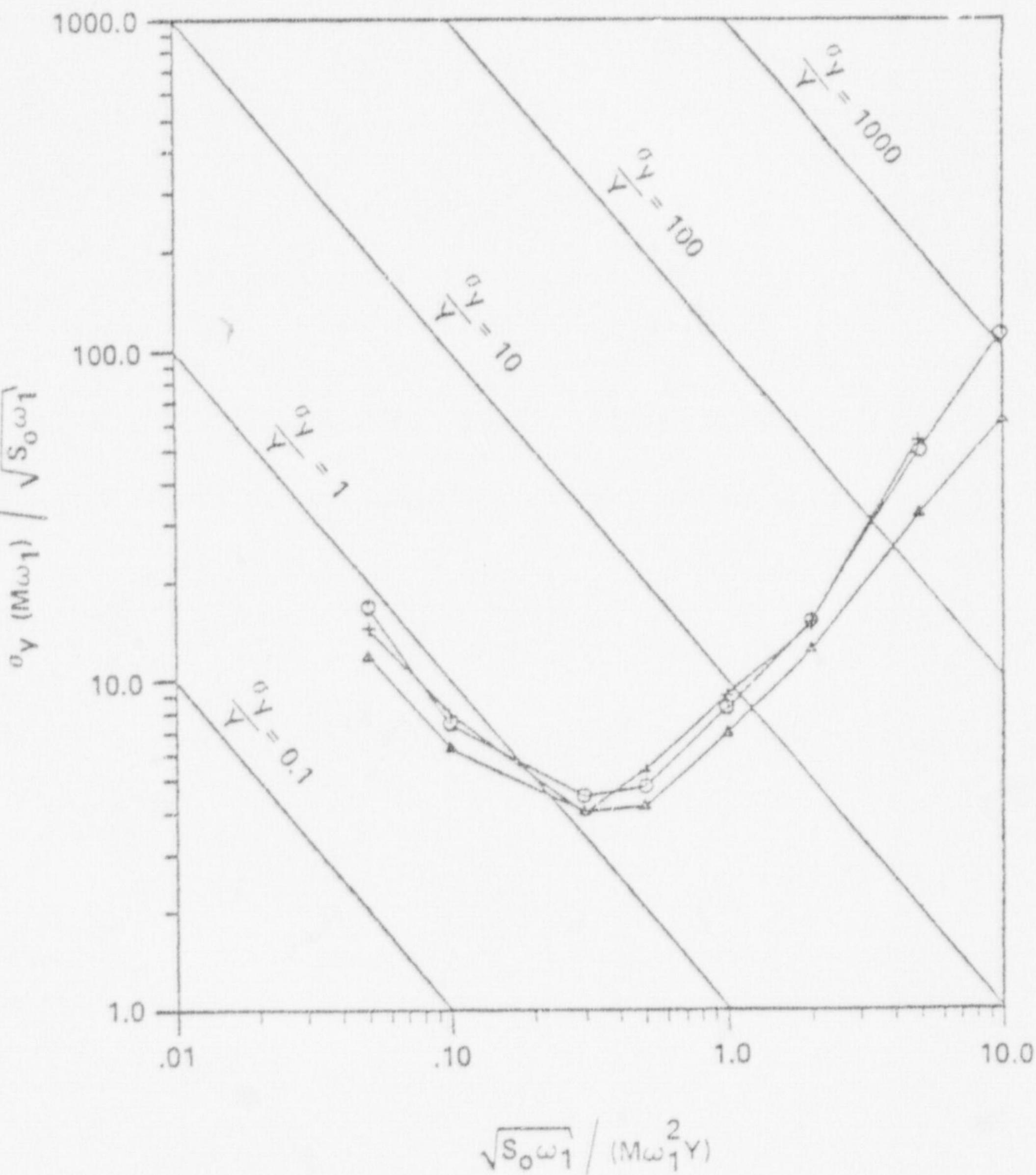

FIGURE 2.11 COMPARISON OF DATA; $a = 1/2$, $\zeta_1 = 0.0$, $\zeta_2 = 0.0$

DATA POINTS

○ THEORY (IWAN AND LUTES[2])

△ THEORY (KRYLOV AND BOGOLIUBOV[2])

+ EXPERIMENT (ID117E)

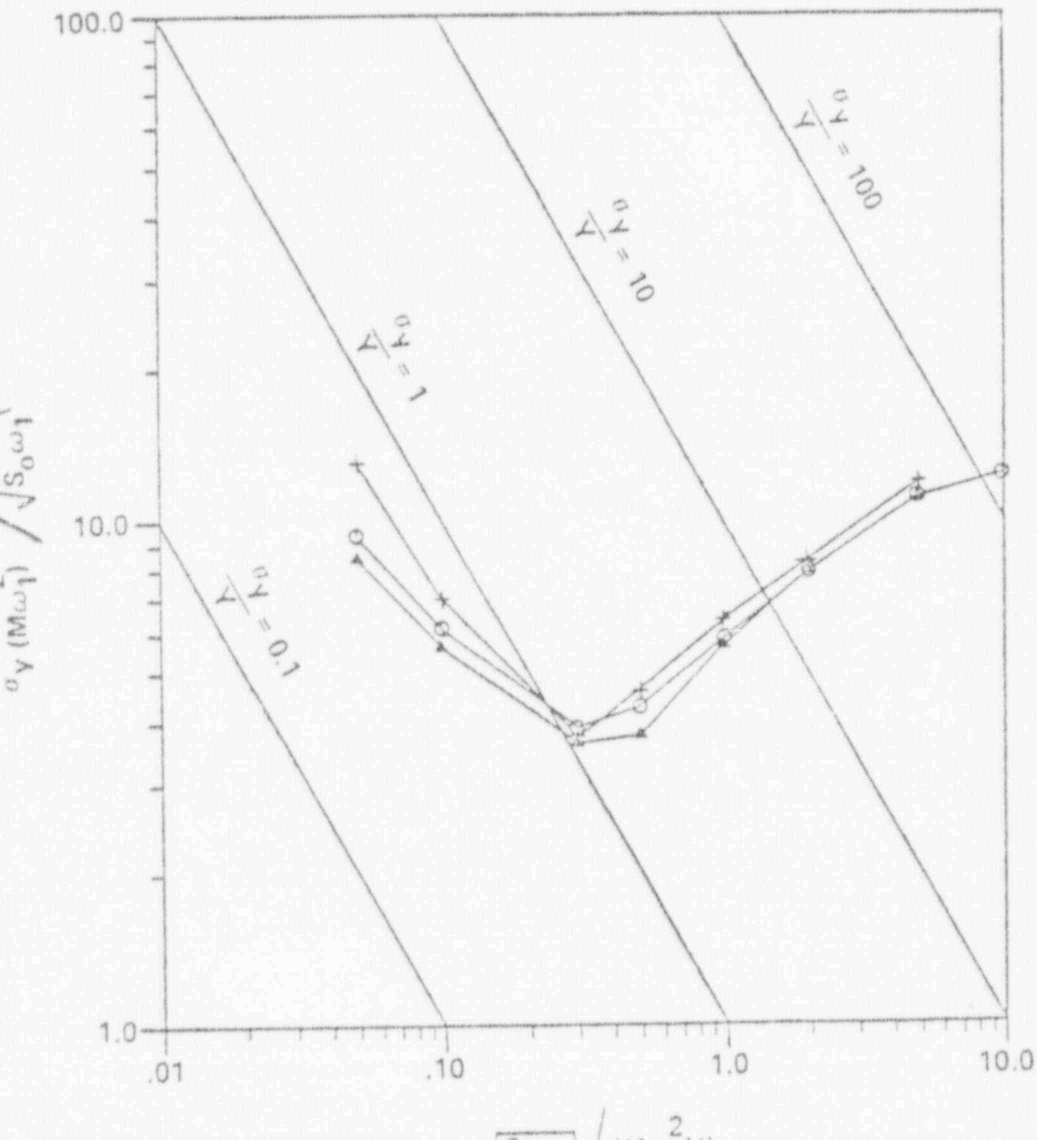

FIGURE 2.12 COMPARISON OF DATA; a = 1/2, ζ_1 = 0.01, ζ_2 = 0.014

DATA POINTS

○ THEORY (IWAN AND LUTES(2))

△ THEORY (KRYLOV AND BOGOLIUBOV(2))

\+ EXPERIMENT (ID117E)

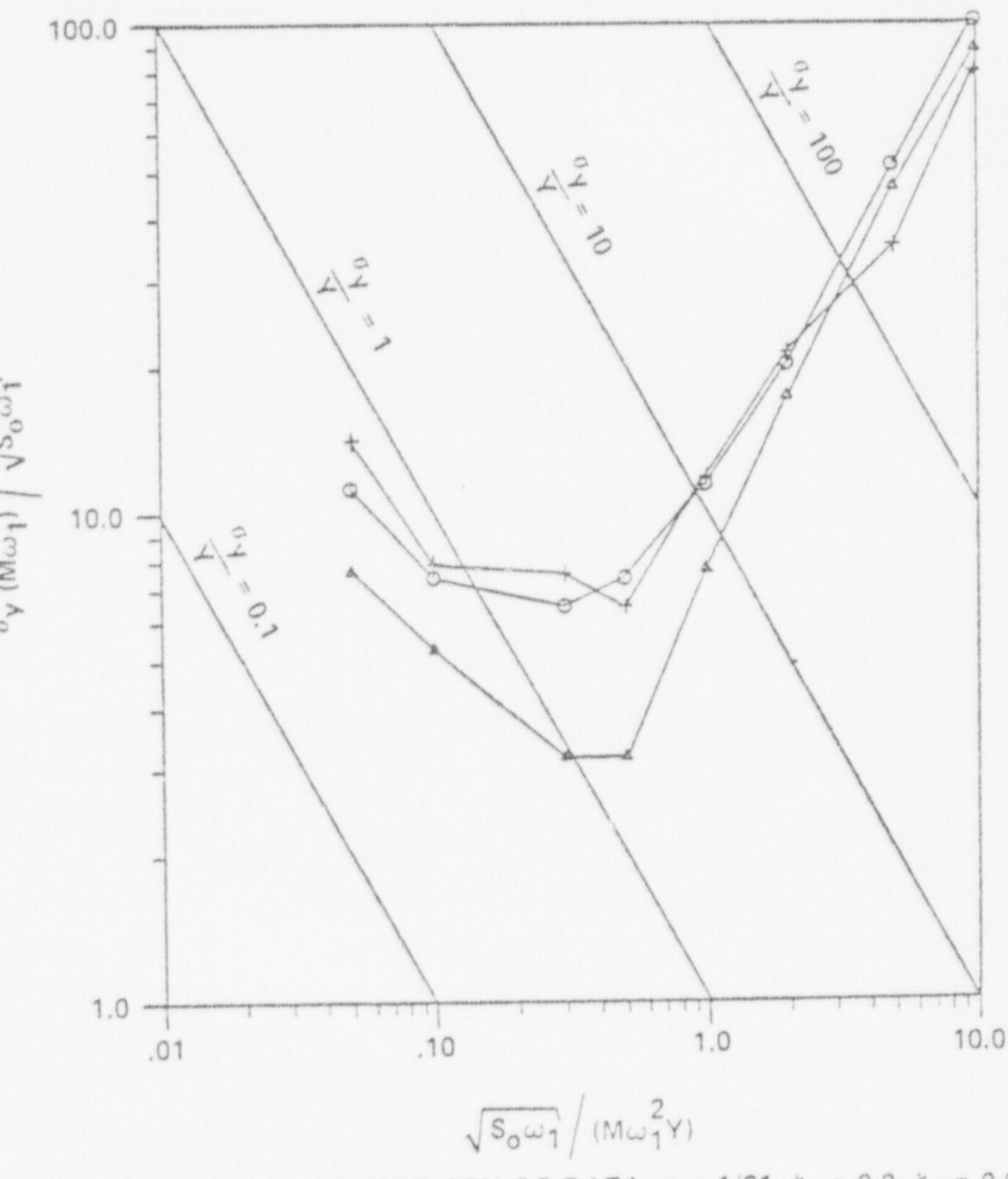

FIGURE 2.13 COMPARISON OF DATA; α = 1/21, ζ_1 = 0.0, ζ_2 = 0.0

DATA POINTS

○ THEORY (IWAN AND LUTES[2])

△ THEORY (KRYLOV AND BOGOLIUBOV[2])

+ EXPERIMENT (ID117E)

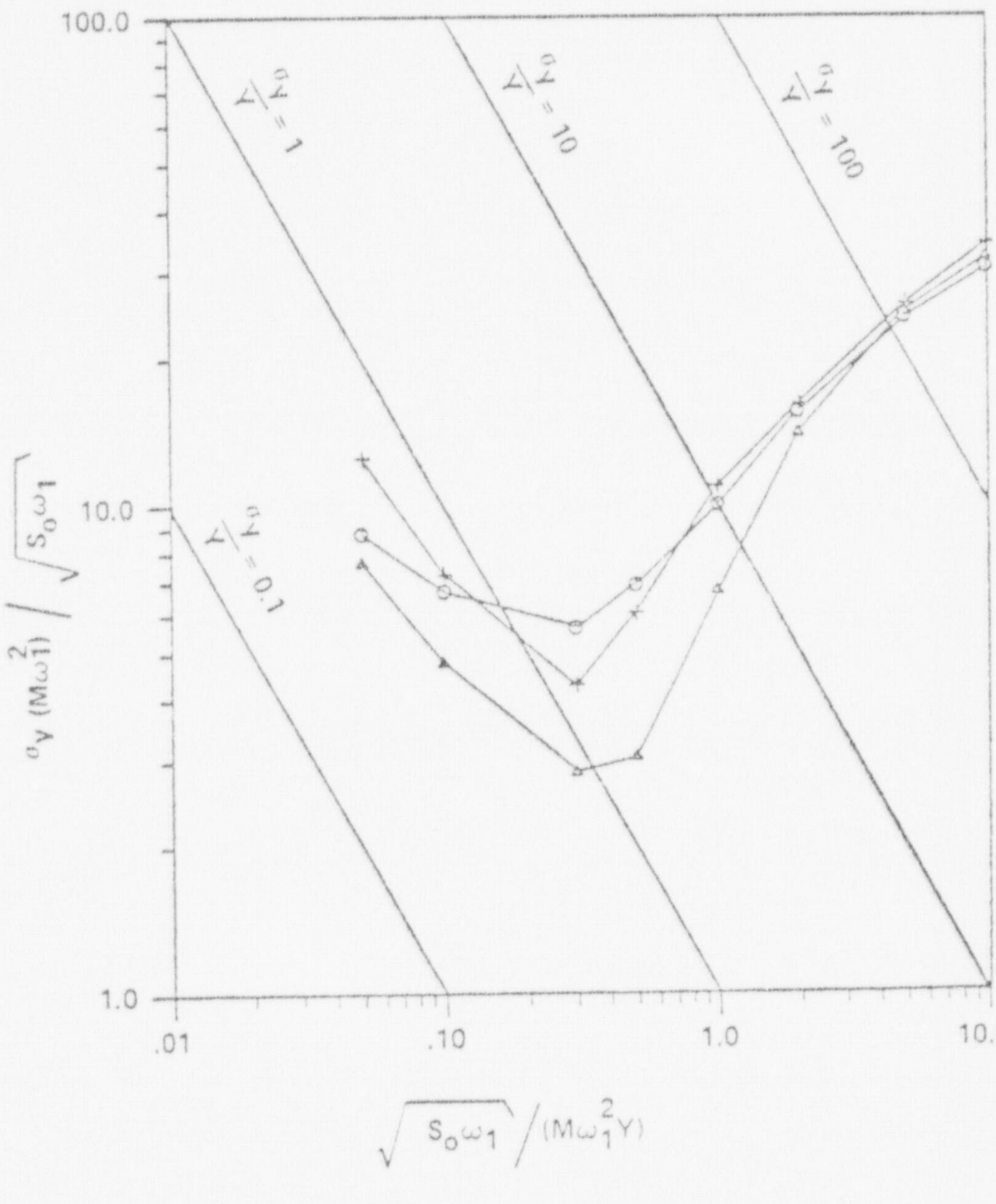

FIGURE 2.14 COMPARISON OF DATA; $\alpha = 1/21$, $\zeta_1 = 0.01$, $\zeta_2 = 0.046$

DATA POINTS

○ THEORY (IWAN AND LUTES[2])

△ THEORY (KRYLOV AND BOGOLIUBOV[2])

+ EXPERIMENT (ID117E)

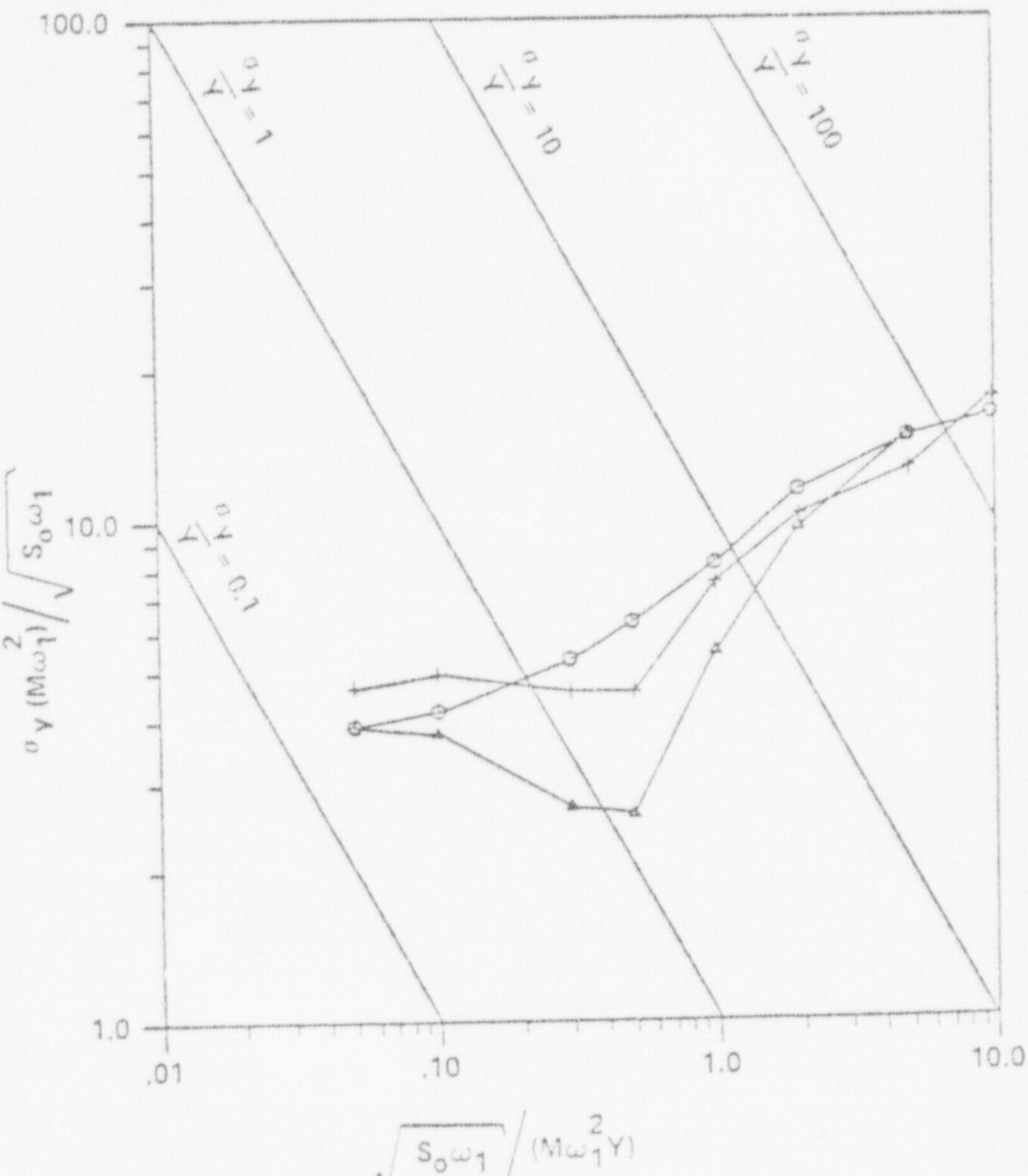

FIGURE 2.15 COMPARISON OF DATA; α = 1/21, ζ_1 = 0.05, ζ_2 = 0.23

DATA POINTS

○ THEORY (IWAN AND LUTES[(2)])

△ THEORY (KRYLOV AND BOGOLIUBOV[(2)])

+ EXPERIMENT (ID117E)

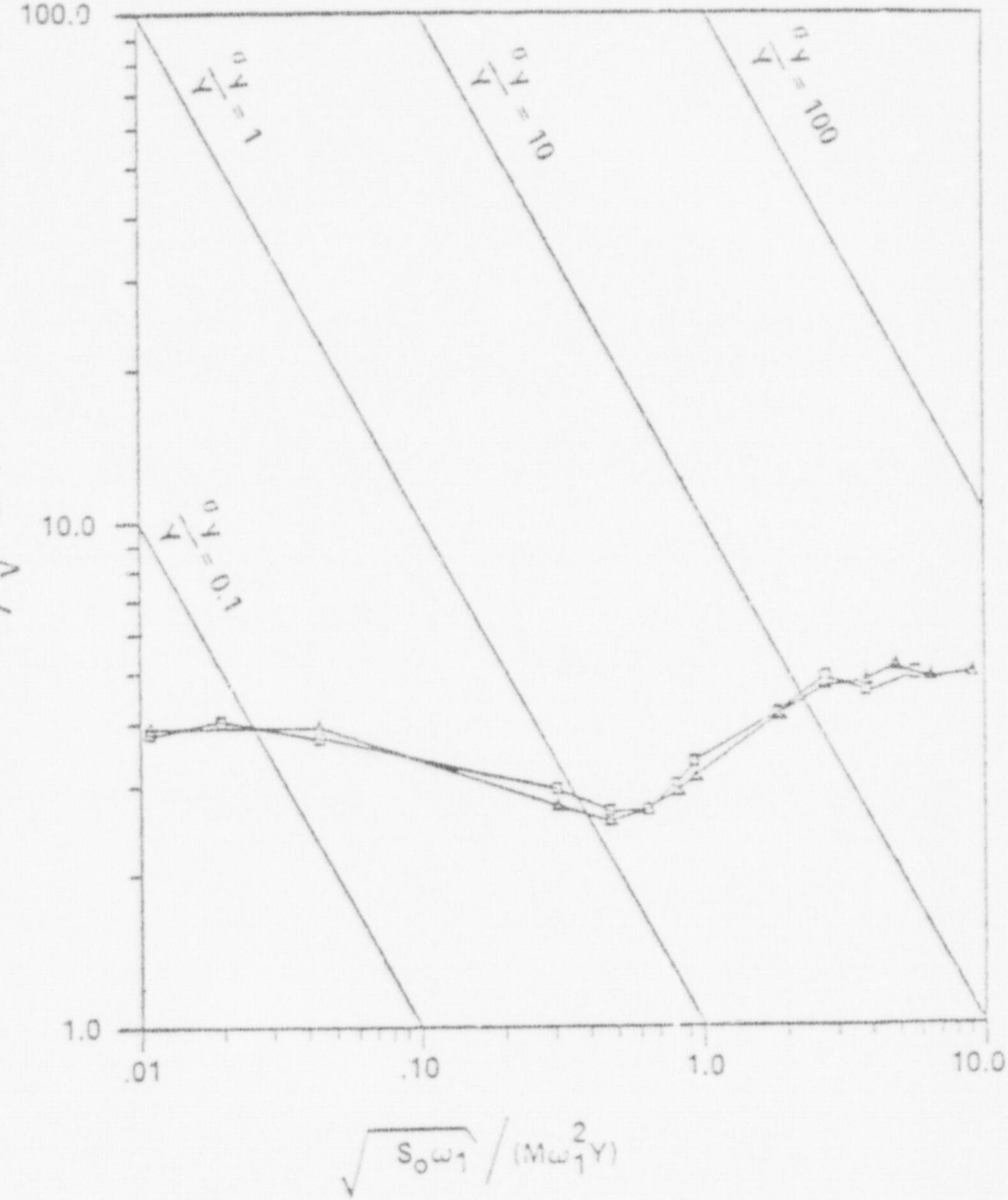

FIGURE 2.16 COMPARISON OF DATA; $\alpha = 1/2$, $\zeta_1 = 0.05$, $\zeta_2 = 0.07$

DATA POINTS

△ THEORY (ID91E)

□ EXPERIMENT (ID117E)

2.9 REFERENCES

1. Caughey, T.K., "Random Excitation of a System with Bilinear Hysteresis," *Journal of Applied Mechanics*, vol. 82, 1960, Series E, pp. 649-652.

2. Iwan, W.D. and Lutes, L.D., "Response of the Bilinear Hysteretic System to Stationary Random Excitation," *Journal of the Acoustical Society of America*, vol. 43, 1968, pp. 545-552.

3. Lutes, L.D. and Shah, V.S., "Transient Random Response of Bilinear Oscillators," Report No. 17, Department of Civil Engineering, Rice University, Houston, 1972.

4. Lyon, R.H.; Heckl, M.; and Hazelgrove, C.B., "Response of Hard-Spring Oscillator to Narrow Band Excitation," *Journal of the Acoustical Society of America*, vol. 33, 1961, pp. 1404-1411.

5. Masri, S.F., "Forced Vibration of the Damped Bilinear Hysteretic Oscillator," *Journal of the Acoustical Society of America*, vol. 57, 1975, pp. 106-112.

6. Caughey, T.K. and Vijayaraghavan, A., "Free and Forced Oscillations of a Dynamic System with 'Linear Hysteretic Damping' (Non-Linear Theory)," *International Journal of Non-Linear Mechanics*, vol. 5, 1970, pp. 533-555.

7. Iwan, W.D., "A Distributed-Element Model for Hysteresis and Its Steady-State Dynamic Response," *Journal of Applied Mechanics*, vol. 33, *Trans. ASME*, vol. 88, 1966, Series E, pp. 893-900.

8. Jennings, P.C., "Periodic Response of a General Yielding Structure," *Journal of the Engineering Mechanics Division, ASCE*, vol. 90, 1964, pp. 131-166.

9. Lutes, L.D. and Takemiya, H., "Random Vibration of Yielding Oscillator," *Journal of the Engineering Mechanics Division, ASCE*, vol. 100, 1974, pp. 343-358.

10. Kaul, M., "Stochastic Inelastic Response of Offshore Towers to Strong Motion Earthquakes," Report No. 72-4, University of California, Berkeley, 1972.

11. Takemiya, H., "Stochastic Seismic Response Analysis of Hysteretic Multidegree-of-Freedom Structures," *Proceedings of the Japan Society of Civil Engineers*, no. 245, 1976, pp. 101-110.

12. Crandall, S.H., "Perturbation Techniques for Vibration of Nonlinear Systems," *Journal of the Acoustical Society of America*, vol. 35, 1963, pp. 1700-1705.

13. Caughey, T.K., "Equivalent Linearization Techniques," *Journal of the Acoustical Society of America*, vol. 35, 1963, pp. 1706-[illegible].

14. Lutes, L.D., "An Approximate Technique for Treating Random Vibration of Hysteretic Systems," Report No. 4, Department of Civil Engineering, Rice University, Houston, 1969.

15. Hudson, D.E., "Equivalent Viscous Friction for Hysteretic Systems with Earthquake-like Excitation," *Proceedings of the Third World Conference on Earthquake Engineering*, Auckland and Wellington, New Zealand, 1965, pp. 185-201.

16. Lutes, L.D., "Equivalent Linearization for Random Vibrations," *Journal of the Engineering Mechanics Division, ASCE*, vol. 96, 1970, pp. 227-242.

17. Takemiya, H., "Equivalent Linearization for Randomly Excited Bilinear Oscillator," *Proceedings of the Japan Society of Civil Engineers*, no. 219, 1973, pp. 1-13.

18. Iwan, W.D. and Yang, I.M., "Application of Statistical Linearization Techniques to Nonlinear Multidegree-of-Freedom Systems," *Trans. ASME*, vol. 39, 1972, Series E, pp. 545-550.

19. Karnopp, D., "Power Balance Method for Nonlinear Random Vibration," *Trans. ASME*, vol. 34, 1967, Series E, pp. 213-224.

20. Karnopp, D. and Scharton, T.D., "Plastic Deformation in Random Vibration," *Journal of the Acoustical Society of America*, vol. 39, 1966, pp. 1154-1161.

21. Karnopp, D., "Inelastic Effects in Random Vibration," AFOSR 65-1915, Air Force Office of Scientific Research, 1965.

22. Karnopp, D. and Brown, R.N., "Random Vibration of Multidegree-of-Freedom Hysteretic Structures," *Journal of the Acoustical Society of America*, vol. 42, 1967, pp. 54-59.

23. Bendat, J.S. and Piersol, A.G., *Random Data: Analysis and Measurement Procedures*, John Wiley & Sons, New York, 1971.

24. Otnes, R.K. and Enochson, L., *Digital Time Series Analysis*, John Wiley & Sons, New York, 1972.

25. Lin, Y.K., *Probabilistic Theory of Structural Dynamics*, McGraw-Hill, New York, 1967.

26. Minorsky, N., *Nonlinear Oscillations*, D, Van Nostrand, New York, 1962.

27. Crandall, S.H. and Mark, W.D., *Random Vibration in Mechanical Systems*, Academic Press, New York, 1963.

28. Blackman, R. B. and Tukey, J.W., *The Measurement of Power Spectra*, Dover Publications, New York, 1958.

29. Papoulis, A., *Probability, Random Variables, and Stochastic Processes*, McGraw-Hill, New York, 1965.

30. Bendat, J.S., *Principles and Applications of Random Noise Theory*, John Wiley & Sons, New York, 1958.

31. Takemiya, H. and Lutes, L.D., "Stationary Random Vibration of Hysteretic Systems," *Journal of the Engineering Mechanics Division, ASCE*, vol. 103, 1977, pp. 673-678.

APPENDIX A

PSD CALIBRATION OF RANDOM FORCING FUNCTION EXCITATION

The random input forcing function used for system excitation in program ID117E is generated with computer software routines GAUSS and RANDU, which are part of the IBM 360 Scientific Subroutine Package. These routines use a uniformly distributed random number generator in conjunction with the Central Limit Theorem to generate a normally distributed random variable (F) with a specified mean ($\overline{F}$) and standard deviation (σ_F). Since the time spacing between these generated random variables (DT) is also specified, it is important to be able to calibrate the PSD (i.e., power spectral density) magnitude (S_o) of the input excitation as a function of DT, $\overline{F}$, and σ_F.

The standard analytic procedures used in time series analysis require at least two data samples per cycle to identify a frequency component within real-time-based data. Hence, the highest frequency component that can be observed by sampling or generating data values at a rate of 1/DT samples per second is 1/(2DT) hertz. Therefore, the PSD of the normally distributed random excitation force will be band limited as shown in Figure A 1, with a cutoff frequency ω_2 defined as

$$\omega_2 = \frac{1}{2DT} \text{ hertz} = \frac{\pi}{DT} \text{ radians} \tag{A.1}$$

A review of the basic definitions of statistics yields the following:

$$E[F] = \int_{-\infty}^{+\infty} F\ p(F)dF = \text{mean or expected value } (\overline{F}) \tag{A.2}$$

$$E[F^2] = \int_{-\infty}^{+\infty} F^2\, p(F)dF = \text{mean square value } (\overline{F^2}) \tag{A.3}$$

$$\sqrt{E[F^2]} = \text{root mean square (RMS) value} \tag{A.4}$$

$$E[(F - \overline{F})^2] = \text{variance } (\sigma_F^2) \tag{A.5}$$

Using Definitions A.2 and A.3, Definition A.5 can be written as

$$\sigma_F^2 = \int_{-\infty}^{+\infty} (F - \overline{F})^2\, p(F)dF \tag{A.6}$$

Expanding Definition A.6, one obtains

$$\sigma_F^2 = \int_{-\infty}^{+\infty} F^2\, p(F)dF - 2E[F] \int_{-\infty}^{+\infty} Fp(F)dF + E[F]^2 \tag{A.7}$$

$$\sigma_F^2 = \overline{F^2} - \overline{F}^2 \tag{A.8}$$

For the special case of the mean equal to zero (i.e., $\overline{F} = 0$),

$$\sigma_F^2 = E[F^2] = \overline{F^2} \tag{A.9}$$

The autocorrelation function is defined as

$$R_F(\tau) = E[F(t) \cdot F(t + \tau)] \tag{A.10}$$

When τ is equal to zero, Definition A.10 is written as

$$R_F(0) = E[F(t) \cdot F(t)] = E[F^2(t)] = \overline{F^2} \tag{A.11}$$

Thus the autocorrelation function evaluated at zero is equal to the mean square value. Using Definitions A.8 and A.11, the following relationship is obtained:

$$R_F(0) = \overline{F^2} = \sigma_F^2 + (\overline{F})^2 \tag{A.12}$$

For the special case of the mean equal to zero (i.e., $\overline{F} = 0$),

$$R_F(0) = \sigma_F^2 \tag{A.13}$$

Definition A.13 establishes the important property that a random variable with zero mean has an autocorrelation function that, when evaluated at zero, is equal to its variance.

A normally distributed, band-limited excitation forcing function with a PSD as displayed in Figure A2 will have an autocorrelation function as displayed in Figure A3; the following relationship is established if the forcing excitation has a zero mean:

$$R_F(0) = 2\ S_o(\omega_2 - \omega_1) = \sigma_F^2 \tag{A.14}$$

However, because of the nature of the excitation forcing function generated by GAUSS and RANDU, ω_1 is equal to zero. Using Definitions A.1 and A.14, one obtains

$$R_F(0) = 2\ S_o\ \omega_2 = \frac{2\pi S_o}{DT} \tag{A.15}$$

Combining Definitions A.13 and A.15, one obtains

$$\sigma_F^2 = \frac{2\pi S_o}{DT} \tag{A.16}$$

Therefore, when the mean is zero (i.e., $\overline{F} = 0$), the following relationship will calibrate the excitation PSD:

$$S_o = \frac{\sigma_F^2 \, DT}{2\pi} \tag{A.17}$$

The variable (1/BIGDT1) is an arbitrary normalization factor that is defined as the number of data points generated in the natural period of the primary system (i.e., $2\pi/\omega$). Therefore, DT can be written as

$$DT = \frac{2\pi}{\omega} \text{ BIGDT1} \tag{A.18}$$

Thus, Definitions A.1 and A.17 can be rewritten in normalized form as

$$S_o = \frac{\sigma_F^2 \text{ BIGDT1}}{\omega} \tag{A.19}$$

$$\omega_2 = \frac{\omega}{2.0 \text{ (BIGDT1)}} \tag{A.20}$$

It should be noted that although our computer-generated excitation is band limited, it can for theoretical purposes be considered "white noise" excitation, since ω_2 is much greater than any fundamental frequencies present in the system. Both of the following examples, which represent the parameters used in all instances for the data values generated in this report, show that

$$\omega_2 = 10.0\ \omega \tag{A.21}$$

where ω is the natural frequency of the primary system. In general, the system models studied in this report have response functions that display peak values between zero and 2ω. Thus the "white noise" excitation assumption is valid.

Example No. 1

Input Parameters:

$\overline{F}$ = mean value of excitation function = 0.0

ω = 1 radian/unit time

Period = $2\pi/\omega = 2\pi$

BIGDT1 = 0.05

Calculated Parameters:

$$DT = \frac{2\pi}{\omega}\ \text{BIGDT1} = 0.314$$

$$\omega_2 = \frac{\omega}{2.0\ \text{BIGDT1}} = \frac{\pi}{0.314} = 10 \text{ radians/unit time}$$

Relationship between σ_F, σ_F^2 and S_o:

σ_F Standard Deviation of Excitation	σ_F^2 Variance of Excitation	S_o PSD: One-sided	S_o PSD: Two-sided
0.158113	0.024999	0.0025	0.00125
0.316227	0.09999	0.01	0.005
0.948683	0.89999	0.09	0.045
1.581	2.499	0.25	0.125
3.16227	9.99	1.0	0.50
6.3245	39.999	4.0	2.0
15.8113	249.997	25.0	12.5
31.6227	999.995	100.0	50.0

Example No. 2

Input Parameters:

$\overline{F}$ = mean value of excitation function = 0.0

ω = 2π radians/unit time

Period = 1

BIGDT1 = 0.05

Calculated Parameters

$$DT = \frac{2\pi}{\omega} \text{ BIGDT1} = 0.05$$

$$\omega_2 = \frac{\omega}{2.0 \text{ BIGDT1}} = 62.83 \frac{\text{radians}}{\text{unit time}} = 10\ (2\pi) \frac{\text{radians}}{\text{unit time}}$$

Relationship between σ_F, σ_F^2 and S_o:

σ_F Standard Deviation of Excitation	σ_F^2 Variance of Excitation	S_o PSD: One-sided	S_o PSD: Two-sided
0.158113	0.024999	0.000397	0.000198
0.316227	0.09999	0.00159	0.000795
0.948683	0.89999	0.01432	0.007161
1.581	2.499	0.0397	0.019886
3.16227	9.99	0.1589	0.07949
6.3245	39.999	0.63646	0.31823
15.8113	249.997	3.9788	1.989
31.6227	999.995	15.915	7.957

Let the vector A as shown in Figure A4 represent the forcing function, which is a sequence of discrete independent random variables with a normal distribution, specified standard deviation, and zero mean. The time history of this forcing function (i.e., F[t]) is written as

$$F(t) = A_K \quad \text{for} \quad (K)\,DT \leq t < (K+1)\,DT \tag{A.22}$$

The autocorrelation function of this process is written as

$$E[F(t_1) \cdot F(t_2)] = E[A_K^2] \tag{A.23}$$

if t_1 and t_2 are in the same time increment (i.e., $(K)DT \leq t_1, t_2 < (K+1)DT$), or as

$$E[F(t_1) \cdot F(t_2)] = 0 \qquad (A.24)$$

if t_1 and t_2 are not in the same time increment. This generating forcing function can be considered as an approximation to true band-limited "white noise" excitation, which has an autocorrelation function defined as

$$E[F(t_1) \cdot F(t_2)] = E\,[A^2]\ DT \left[\delta(t_1 - t_2)\right]^*$$

if the response of the system being studied has a characteristic time (i.e., a fundamental period equal to $2\pi/\omega$) that is large compared to DT. In this report the fundamental period of the system model was set equal to 20 DT, which was verified by experimental investigation to be sufficiently large to assure that the input forcing function did in fact approximate true band-limited "white noise" excitation.

---

*$\delta(t_1 - t_2)$ is the Dirac delta function.

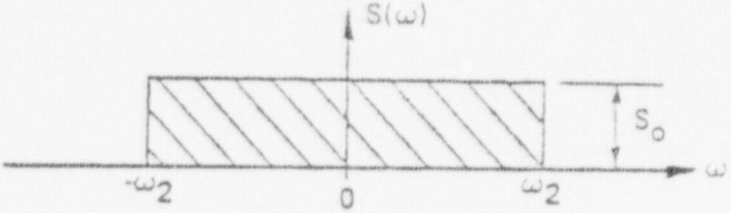

FIGURE A1

PSD OF THE FORCING EXCITATION GENERATED USING SUBROUTINES GAUSS AND RANDU

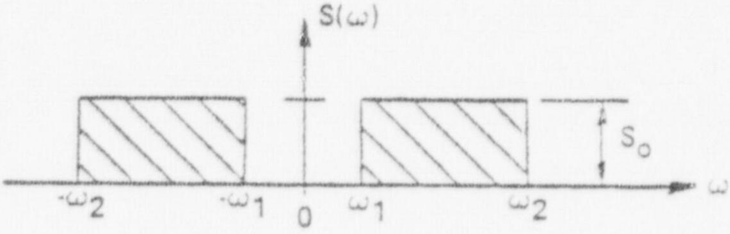

FIGURE A2

PSD OF BAND LIMITED FORCING EXCITATION

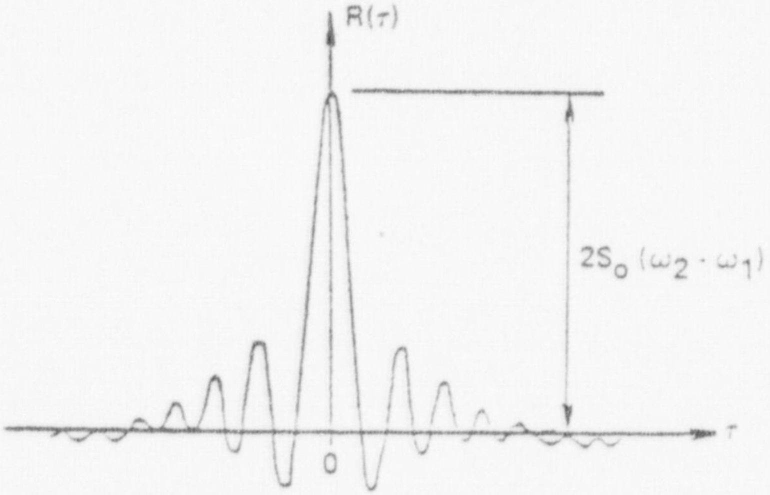

FIGURE A3

AUTOCORRELATION FUNCTION FOR BAND LIMITED FORCING EXCITATION

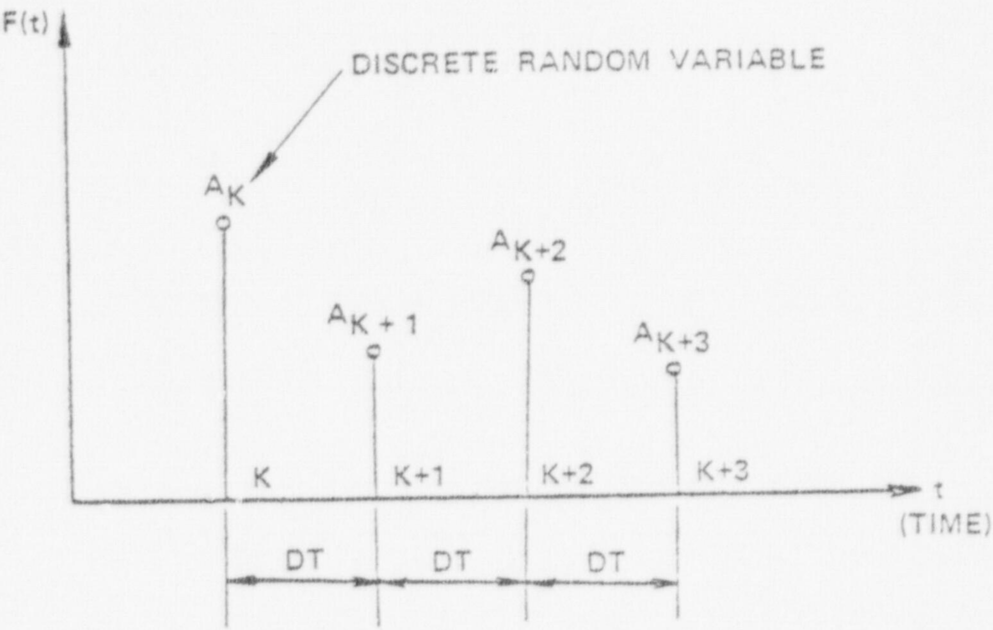

FIGURE A4
TIME HISTORY OF COMPUTER GENERATED FORCING FUNCTION

APPENDIX B

STATISTICAL DISCUSSION OF EXPERIMENTAL RESULTS

The data values presented in this report represent an empirical "Monte Carlo" investigation, are ensemble averages of N generated time-history responses. Each of the time-history responses, which represent the numerical integration of the system model equations of motion, were obtained by using the appropriate computer program logic with an arbitrary sample of $F(t)$ (i.e., normally distributed random forcing function with a specified mean and variance) as excitation. Initial conditions (i.e., displacement and velocity) were set equal to zero for all data samples.

Let $\langle x \rangle$ denote a simple ensemble average over an ensemble size N for a random variable x. It is statistically known that the variance of $\langle x \rangle$ is given by

$$\sigma^2_{\langle x \rangle} = \frac{\sigma_x^2}{N} \tag{B.1}$$

where σ_x^2 is the variance of the random variable x. From fundamental statistics the following definitions are presented:

$$E[x] = \text{mean value } (\overline{x}) = \int_{-\infty}^{+\infty} x\, p(x)dx \tag{B.2}$$

$$E[(x - \overline{x})^2] = \text{variance } (\sigma_x^2) = \int_{-\infty}^{+\infty} (x - \overline{x})^2\, p(x)dx \tag{B.3}$$

$$E[x^2] = \text{mean square value } (\overline{x^2}) = \int_{-\infty}^{+\infty} x^2\, p(x)dx \tag{B.4}$$

$$\int_{-\infty}^{+\infty} p(x)dx = 1 \tag{B.5}$$

$$\sigma_x^2 = \overline{x^2} - \bar{x}^2 \tag{B.6}$$

The variance of the mean square is written as

$$\sigma_{x^2}^2 = E\left[\left(x^2 - E[x^2]\right)^2\right] = \int_{-\infty}^{+\infty} \left(x^2 - E[x^2]\right)^2 p(x)dx \tag{B.7}$$

From Definition B.6 with the mean (i.e., $\bar{x}$) set equal to zero one obtains the following relationship

$$E[x^2] = \overline{x^2} = \sigma_x^2 \tag{B.8}$$

Using Definition B.8, Definition B.7 can be rewritten as

$$\sigma_{x^2}^2 = \int_{-\infty}^{+\infty} x^4 p(x)dx - 2\sigma_x^2 \int_{-\infty}^{+\infty} x^2 p(x)dx + \sigma_x^4 \int_{-\infty}^{+\infty} p(x)dx \tag{B.9}$$

$$\sigma_{x^2}^2 = E[x^4] - \sigma_x^4 \tag{B.10}$$

Studies of $E[x^4]$ or $\sigma_{x^2}^2$ were not performed for the response data obtained in this report. However, one can obtain some useful information about the variance of $\langle x^2 \rangle$ by assuming the response x is

Gaussian even though it has been shown by Lutes* that this assumption is not always valid, especially for hysteretic or nonlinear systems. If x is a normally distributed random variable (i.e., Gaussian) with zero mean, the following relationship is useful

$$E[x^D] = \begin{cases} 1 \cdot 3 \ldots (D-1)\, \sigma_x^D & \text{for } D = \text{even} \\ 0 & \text{for } D = \text{odd} \end{cases} \tag{B.11}$$

Evaluating Definition B.11 for D equal to 4,

$$E[x^4] = 3\sigma_x^4 \tag{B.12}$$

Combining Definitions B.12 and B.10 one obtains

$$\sigma_{x^2}^2 = 2\sigma_x^4 \tag{B.13}$$

Using Definition B.1 as an example, the ensemble variance of the mean square value is expressed as

$$\sigma^2_{\langle x^2 \rangle} = \frac{\sigma^2_{x^2}}{N} \tag{B.14}$$

Substituting Definition B.13 into Definition B.14 yields

$$\sigma_{\langle x^2 \rangle} = \sqrt{\frac{2\sigma_x^4}{N}} = \sigma_x^2 \left(\frac{2}{N}\right)^{1/2} \tag{B.15}$$

*Lutes, L.D., "An Approximate Technique for Treating Random Vibration of Hysteretic Systems," Report No. 4, Department of Civil Engineering, Rice University, Houston, 1969.

Definition B.15 expresses the relationship between the standard deviation of the mean square ensemble average $\langle x^2 \rangle$ of a Gaussian process with variance σ_x^2 and the number of averages N in the ensemble. This equation applies equally well to displacement or velocity. Table B.1 presents some typical numerical examples.

TABLE B.1. STATISTICAL RELATIONSHIP AS ENSEMBLE LENGTH N VARIES

N	$(2/N)^{1/2}$	$\sigma_{\langle x^2 \rangle}$
10	0.4472	0.4472 σ_x^2
20	0.3162	0.3162 σ_x^2
24	0.2887	0.2887 σ_x^2
40	0.2236	0.2236 σ_x^2
48	0.2041	0.241 σ_x^2
60	0.1826	0.1826 σ_x^2
80	0.1581	0.1581 σ_x^2
160	0.1118	0.1118 σ_x^2

For this study, N was set equal to 24. It should be noted that doubling the ensemble size, which would consequently double the computer costs, would have reduced the standard deviation of $\langle x^2 \rangle$ by only 29%. The numerical "scatter" observed in the data values presented in this report can be associated directly with the limited number of ensemble averages generated. The primary constraint on the number of ensemble averages used in this investigation was a financial one dictated by computer costs. The number of ensemble averages chosen (i.e., N = 24) was not an unreasonably small number. However, Lutes and Shah* used as many as 80 ensemble averages in their study of the transient response of hysteretic systems.

---

*Lutes, L.D. and Shah, V.S., "Transient Random Response of Bilinear Oscillators," Report No. 17, Department of Civil Engineering, Rice University, Houston, 1970.

NRC FORM 335 (7-77) U.S. NUCLEAR REGULATORY COMMISSION **BIBLIOGRAPHIC DATA SHEET**	1. REPORT NUMBER (Assigned by DDC) NUREG/CR-0362
4. TITLE AND SUBTITLE (Add Volume No., if appropriate) Dynamic Excitation of a Single-Degree-of-Freedom Hysteretic System	2. (Leave blank)
	3. RECIPIENT'S ACCESSION NO.
7. AUTHOR(S) S. J. Stott and S. F. Masri	5. DATE REPORT COMPLETED MONTH May YEAR 1978
9. PERFORMING ORGANIZATION NAME AND MAILING ADDRESS (Include Zip Code) Civil Engineering Department University of Southern California Los Angeles, California 90007	DATE REPORT ISSUED MONTH August YEAR 1978
	6. (Leave blank)
	8. (Leave blank)
12. SPONSORING ORGANIZATION NAME AND MAILING ADDRESS (Include Zip Code) General Reactor Safety Research Nuclear Regulatory Research Nuclear Regulatory Commission Washington, D.C. 20555	10. PROJECT/TASK/WORK UNIT NO.
	11. CONTRACT NO. NRC-04-76-262
13. TYPE OF REPORT Topical	PERIOD COVERED (Inclusive dates) 10/1/77 - 9/30/78
15. SUPPLEMENTARY NOTES	14. (Leave blank)

16. ABSTRACT (200 words or less)

An analytical investigation is made of the dynamic response of two special classes of nonlinear hysteretic oscillators that model some of the basic phenomena involved in the response of complex nuclear power plant systems which are subjected to dynamic environments.

Numerical studies as well as approximate analytical solutions for the response of the nonlinear oscillators under (a) harmonic and (b) random excitation are presented. The effects of various system parameters are evaluated and the range of validity of the approximate solutions is determined.

17. KEY WORDS AND DOCUMENT ANALYSIS	17a. DESCRIPTORS
Two-Degree-of-Freedom Random Vibration Dynamics, Analog, Nonlinear, Dampers	Parametric Evaluation, Dynamic Response, Computer Model, Structure/Equipment Interaction
17b. IDENTIFIERS/OPEN-ENDED TERMS	

18. AVAILABILITY STATEMENT	19. SECURITY CLASS (This report)	21. NO. OF PAGES
Unlimited	20. SECURITY CLASS (This page)	22. PRICE $

UNITED STATES
NUCLEAR REGULATORY COMMISSION
WASHINGTON, D. C. 20555

OFFICIAL BUSINESS
PENALTY FOR PRIVATE USE, $300

POSTAGE AND FEES PAID
U.S. NUCLEAR REGULATORY
COMMISSION

U.S. MAIL

120555003927 1 R5RAAN
US NRC
SECY PUBLIC DOCUMENT ROOM
BRANCH CHIEF
HST LOBBY
WASHINGTON DC 20555